

UAB-FT-397  
July, 1996  
hep-ph/9607485

## QUANTUM EFFECTS ON $t \rightarrow H^+ b$ IN THE MSSM: A WINDOW TO “VIRTUAL” SUPERSYMMETRY?

J.A. COARASA, David GARCIA, Jaume GUASCH,  
Ricardo A. JIMÉNEZ, Joan SOLÀ

Grup de Física Teòrica  
and  
Institut de Física d’Altes Energies  
Universitat Autònoma de Barcelona  
08193 Bellaterra (Barcelona), Catalonia, Spain

### ABSTRACT

We analyze the one-loop effects (strong and electroweak) on the unconventional top quark decay mode  $t \rightarrow H^+ b$  within the MSSM. The results are presented in the on-shell renormalization scheme with a physically well motivated definition of  $\tan\beta$ . The study of this process at the quantum level is useful to unravel the potential supersymmetric nature of the charged Higgs emerging from that decay. As compared with the standard mode  $t \rightarrow W^+ b$ , the corrections to  $t \rightarrow H^+ b$  are large, slowly decoupling and persist at a sizeable level even for all sparticle masses well above the LEP 200 discovery range. Therefore, if the charged Higgs decay of the top quark is kinematically allowed – a possibility which is not excluded by the recent measurements of the branching ratio  $BR(t \rightarrow W^+ b)$  at the Tevatron – it could be an invaluable laboratory to search for “virtual” supersymmetry. As a matter of fact, the potential size of the SUSY effects, which amount to corrections of several ten percent, could counterbalance the standard QCD corrections and even make them to appear with the “wrong” sign. While a first significant test of these effects could possibly be performed at the upgraded Tevatron, a more precise verification would most likely be carried out in future experiments at the LHC.

# 1. Introduction

Recently, the Standard Model (SM) of the strong and electroweak interactions has been crowned with the discovery of the penultimate building block of its theoretical structure: the top quark,  $t$  [1]. At present the best determination of the top-quark mass at the Tevatron reads as follows [2]:

$$m_t = 175 \pm 9 \text{ GeV}. \quad (1)$$

While the SM has been a most successful framework to describe the phenomenology of the strong and electroweak interactions for the last thirty years, the top quark itself stood, at a purely theoretical level –namely, on the grounds of requiring internal consistency, such as gauge invariance and renormalizability–as a firm prediction of the SM since the very confirmation of the existence of the bottom quark and the measurement of its weak isospin quantum numbers [3]. With the finding of the top quark, the matter content of the SM has been fully accounted for by experiment. Still, the last building block of the SM, namely the fundamental Higgs scalar, has not been found yet, which means that in spite of the great significance of the top quark discovery the theoretical mechanism by which all particles acquire their masses in the SM remains experimentally unconfirmed. Thus, it is not clear at present whether the SM will remain as the last word in the phenomenology of the strong and electroweak interactions around the Fermi’s scale or whether it will be eventually subsumed within a larger and more fundamental theory. The search for physics beyond the SM, therefore, far from being accomplished, must continue with redoubled efforts. Fortunately, the peculiar nature of the top quark (in particular its large mass–in fact, perhaps the heaviest particle in the SM!– and its characteristic interactions with the scalar particles) may help decisively to unearth any vestige of physics beyond the SM.

We envisage at least four wide avenues of interesting new physics potentially conveyed to us by top quark dynamics and which could offer the clue to solving the nature of the spontaneous symmetry breaking (SSB) mechanism, namely: i) The “Top Mode” realization(s) of the SSB mechanism, i.e. SSB without fundamental Higgs scalars, but rather through the existence of  $t\bar{t}$  condensates [4]; ii) The extended Technicolour Models; also without Higgs particles, and giving rise to residual non-oblique interactions of the top quark with the weak gauge bosons [5]; iii) The non-linear (chiral Lagrangian) realization of the  $SU(2)_L \times U(1)_Y$  gauge symmetry [6], which may either accommodate or dispense with the Higgs scalars. It can also generate additional (i.e. non-standard) non-oblique interactions of the top quark with the weak gauge bosons [7]; and iv) The supersymmetric (SUSY) realization of the SM, such as the Minimal Supersymmetric Standard Model (MSSM) [8], where also a lot of potential new phenomenology might be creeping in here and there. Vestiges of this new phenomenology may show up either in the form of direct

or virtual effects from supersymmetric Higgs particles or from the “sparticles” themselves (i.e. the  $R$ -odd partners of the SM particles), in particular from the top-squark (stop) which is the SUSY counterpart of the top quark. Due to the huge mass of the latter, one expects that the top-stop system is the most preferential chiral supermultiplet to which the Higgs sector should couple. Therefore, top quark dynamics is deemed to be the ideal environment for Higgs phenomenology and the most suitable SUSY trigger, if SUSY is there at all.

In this paper, we shall focus our attention on the fourth large avenue of hypothetical physics beyond the SM, i.e. on the (minimal) SUSY extension of the SM, the MSSM, which is at present the most predictive framework for physics beyond the SM and, in contradistinction to all other approaches, it has the virtue of being a fully-fledged Quantum Field Theory. Most important, on the experimental side the global fit analyses to all indirect precision data within the MSSM are at least as good as in the SM; in particular, the MSSM analysis implies that  $m_t = 170 \pm 7$  [9], a result which is compatible with the above mentioned experimental determinations of  $m_t$ . In the MSSM the spectrum of Higgs-like particles and of Yukawa couplings is far and away richer than in the SM. In this respect, a crucial fact affecting the results of our work is that in such a framework the bottom-quark Yukawa coupling may counterbalance the smallness of the bottom mass,  $m_b \simeq 5 \text{ GeV}$ , at the expense of a large value of  $\tan \beta$  – the ratio of the vacuum expectation values (VEV’s) of the two Higgs doublets – the upshot being that the top-quark and bottom-quark Yukawa couplings (normalized with respect to the  $SU(2)$  gauge coupling) as they stand in the superpotential, viz.

$$\lambda_t \equiv \frac{h_t}{g} = \frac{m_t}{\sqrt{2} M_W \sin \beta} \quad , \quad \lambda_b \equiv \frac{h_b}{g} = \frac{m_b}{\sqrt{2} M_W \cos \beta} , \quad (2)$$

can be of the same order of magnitude, perhaps even showing up in “inverse hierarchy”:  $h_t < h_b$  for  $\tan \beta > m_t/m_b$ . Notice that due to the perturbative bound  $\tan \beta \lesssim 70$  one never reaches a situation where  $h_t \ll h_b$ . In a sense,  $h_t \sim h_b$  could be judged as a natural relation in the MSSM; it can even be a necessary relation in specific SUSY-GUT models, e.g. those based on  $t, b$  and  $\tau$  Yukawa coupling unification [10], at least at the unification point.

Since the Higgs sector of the MSSM doubles that of the SM, and it comes associated with the fermionic SUSY partners –the so-called higgsinos–, one expects that in the limit  $h_t \sim h_b$  there should occur a very stimulating top-stop-higgsino, bottom-sbottom-higgsino and stop-sbottom-Higgs dynamics. A particularly brilliant form of this dynamics, on which we shall focus our attention, is revealed through the study of the quantum corrections to the non-standard top quark decay into a charged Higgs:  $t \rightarrow H^+ b$ . This decay is not at all excluded by the recent measurements (at the Tevatron) of the branching

ratio of the standard top quark decay,  $t \rightarrow W^+ b$ , as will be discussed in more detail in Section 2. The quantum effects on  $t \rightarrow H^+ b$ , which we wish to compute in the framework of the MSSM at one-loop, can be both strong and electroweak like. Of these the strong conventional (QCD) corrections mediated by gluons have already been treated in detail [11]. Also the subset of strong supersymmetric corrections mediated by gluinos, stop and sbottom squarks, i.e. the SUSY-QCD corrections, have been discussed in Ref.[12]. Here, therefore, we will come to grips with the remaining part –as a matter of fact, the largest and most difficult part – of the MSSM corrections: namely, the multifarious electroweak supersymmetric corrections produced by squarks, sleptons charginos, neutralinos and supersymmetric Higgs bosons, which we shall combine with the total strong (QCD +SUSY-QCD) corrections to obtain the leading MSSM correction.

In the present study<sup>1</sup>, we will closely follow the systematic pathway adopted in our previous treatment of the supersymmetric quantum corrections to the canonical decay  $t \rightarrow W^+ b$  [14, 15]. However, because of the Higgs particle in the final state, we have to incorporate the details of the renormalization of the Higgs sector of the MSSM, which substantially alter the counterterm structure of the  $t b H^\pm$ -vertex as compared to the conventional  $t b W^\pm$ -vertex. This also has dramatical consequences on the quantitative side, as we shall see. Furthermore, we have to include the quantum corrections from the supersymmetric higgses themselves. In spite of their negligible effect on the width of the standard decay  $t \rightarrow W^+ b$  [16] – a fact which was not obvious a priori since there are potentially large non-oblique Higgs interactions originating from the Yukawa couplings (2) – their impact on the alternative decay  $t \rightarrow H^+ b$  must also be carefully evaluated. In certain circumstances, they can be comparable to the virtual effects from the genuine supersymmetric particles (sparticles).

It is worth mentioning that the one-loop analysis of the unconventional top quark decay  $t \rightarrow H^+ b$  is motivated not only by its obvious interest on its own as a laboratory to test the spontaneous symmetry breaking mechanism beyond the SM, but also as a way to characterize the SUSY nature of the charged Higgs emerging from that decay [13]. In fact, we shall see that important ( $\sim 50\%$ ) SUSY radiative corrections can be obtained in certain regions of the MSSM parameter space. In one of these regions,  $\tan \beta \sim m_t/m_b$  is large enough such that  $h_b \sim h_t$ . Incidentally, we note these are the typical values of  $\tan \beta$  characterizing one of the possible regions of the MSSM parameter space highlighted in the literature [17] in order to alleviate some formerly claimed “anomalies” observed in the decay modes of the  $Z$  into  $b\bar{b}$  and  $c\bar{c}$ . Other regions have also been claimed [18]-[19]. However, since all the fuss about the  $Z$ -boson “anomalies” seems to be declining [20], our analysis will not be too conditioned by the MSSM results on  $Z$ -boson observables.

---

<sup>1</sup>A preliminary presentation of these results was already given in Ref.[13].

Rather, we wish to quest for generic regions of the parameter space where the decay rate of  $t \rightarrow H^+ b$  is maximized and at the same time the SUSY quantum effects become sizeable enough. Thus, for definiteness, in this paper we will take the point of view that the study of the decay  $t \rightarrow H^+ b$  is worthwhile provided that its branching ratio is comparable to the branching ratio of the standard decay  $t \rightarrow W^+ b$ , i.e. we typically require  $BR(t \rightarrow H^+ b) \geq 10\%$ , a condition which is not excluded by present Tevatron data (see Section 2) and, from the theoretical point of view, is fully guaranteed provided that  $\tan \beta$  is large enough ( $\gtrsim 20$ ). In these conditions, the one-loop corrections themselves induced by the supersymmetric Yukawa couplings  $h_t$  and  $h_b$  can be rather large (10–50%) and so they are liable to being measured in future experiments at the Tevatron and/or at the LHC.

The paper is organized as follows. In Section 2 the lowest order relations concerning the Higgs sector and the top quark decay are given. We also discuss the status of the charged Higgs decay of the top quark in the light of the recent data, and the prospects for its detection. Section 3 discusses the renormalization of the  $t b H^\pm$ -vertex in the on-shell scheme. In Section 4 we present the full analytical formulae for the one-loop corrected partial width  $\Gamma(t \rightarrow H^+ b)$  in the MSSM. The numerical analysis and discussion, as well as the conclusions, are delivered in Section 5, where we also comment on the feasibility of measuring the computed quantum effects in hadron colliders. Finally, we devote three appendices, respectively on SUSY Lagrangians, renormalization details and one-loop functions, in order to make the paper as self-contained as possible.

## 2. Lowest order relations and $BR(t \rightarrow H^+ b)$ from experiment

In this paper we wish to emphasize the possibility that a charged pseudoscalar involved in a possible unconventional decay of the top-quark be the charged Higgs of the MSSM:  $t \rightarrow H^+ b$ <sup>2</sup>. A charged Higgs is necessary in the MSSM since we need two Higgs  $SU(2)_L$ -doublets with opposite weak-hypercharges to give masses to matter and gauge fields:

$$\begin{pmatrix} H_1^0 \\ H_1^- \end{pmatrix} \quad (Y = -1), \quad \begin{pmatrix} H_2^+ \\ H_2^0 \end{pmatrix} \quad (Y = +1). \quad (3)$$

After SSB, the physical content of the Higgs sector consists of one CP-odd (“pseudoscalar”) neutral Higgs,  $A^0$ , two CP-even neutral Higgs bosons,  $h^0, H^0$ , and a charged Higgs boson,  $H^\pm$ . Because of the SUSY constraints on the structure of the Higgs potential, the masses of these particles are determined in terms of just three parameters,

---

<sup>2</sup>In the MSSM there are several additional, more exotic, 2-body decays of the top quark and also a host of 3-body final states worth studying [21].

which can be chosen to be the two vacuum expectation values (VEV's)  $\langle H_2^0 \rangle = v_2$ ,  $\langle H_1^0 \rangle = v_1$ , giving masses to the top and bottom quarks respectively, and one physical Higgs mass. However, due to the SSB constraint

$$v^2 \equiv v_1^2 + v_2^2 = 2M_W^2/g^2 = 2^{-3/2}G_F^{-1} \simeq (174 \text{ GeV})^2, \quad (4)$$

where  $G_F$  is Fermi's constant in  $\mu$ -decay, in the end only two parameters suffice to completely specify the MSSM Higgs masses at the tree-level. Moreover, since we are interested in the decay process  $t \rightarrow H^+ b$ , it is natural to take  $M_{H^\pm}$  as the physical input mass rather than  $M_{A^0}$ , as frequently done in other contexts. As the second independent parameter, one can take the ratio of the two VEV's:  $\tan \beta = v_2/v_1$ . Then, in lowest order, we have the relations [22]

$$\begin{aligned} M_{A^0}^2 &= M_{H^\pm}^2 - M_W^2, \\ M_{H^0, h^0}^2 &= \frac{1}{2} \left( M_{A^0}^2 + M_Z^2 \pm \sqrt{(M_{A^0}^2 + M_Z^2)^2 - 4M_Z^2 M_{A^0}^2 \cos^2 2\beta} \right). \end{aligned} \quad (5)$$

It is well-known [23] that these formulas become modified at one-loop. In our case, once  $M_{H^\pm}$  is fixed, the other Higgs masses enter the decay rate of  $t \rightarrow H^+ b$  only through virtual corrections. Moreover, the renormalization of the masses also induces a renormalization of the CP-even mixing angle. Although these one-loop effects are necessary to guarantee a Higgs spectrum fully compatible with the phenomenological bounds near the  $\tan \beta \simeq 1$  region, one expects that a one-loop shift in the masses and couplings just entails a small two-loop order correction to the decay rate. We have explicitly checked this fact.

The charged Higgs can be, as noted above, very sensitive to bottom-quark interactions. Specifically, after expressing the two-doublet Higgs fields of the MSSM in terms of the corresponding mass-eigenstates, the interaction Lagrangian describing the  $t b H^\pm$ -vertex reads as follows [22]:

$$\mathcal{L}_{Hbt} = \frac{g V_{tb}}{\sqrt{2} M_W} H^- \bar{b} [m_t \cot \beta P_R + m_b \tan \beta P_L] t + \text{h.c.}, \quad (6)$$

where  $V_{tb}$  is the corresponding Cabibbo-Kobayashi-Maskawa matrix element, and  $P_{L,R} = (1/2)(1 \mp \gamma_5)$  are the projection operators on LH and RH fermions. On the phenomenological side, one should not dismiss the possibility that the bottom-quark Yukawa coupling could play a momentous role in the physics of the top quark, to the extend of drastically changing standard expectations on top-quark observables, particularly on the top-quark width. Of course, this is possible because of the potential  $\tan \beta$ -enhancement of that Yukawa coupling.

In the “ $\alpha$ -parametrization”, where the input parameters are  $(\alpha, M_W, M_Z, M_H, m_f, \dots)$ , the coupling  $g$  on eq.(6) stands for  $e/s_W$ , where  $\alpha \equiv \alpha_{\text{e.m.}}(q^2 = 0) = e^2/4\pi$  and  $s_W^2 \equiv$

$1 - c_W^2 \equiv 1 - M_W^2/M_Z^2$ . An alternative framework (“ $G_F$ -parametrization”) based on the set of inputs ( $G_F, M_W, M_Z, M_H, m_f, \dots$ ) is also useful, especially at higher orders in perturbation theory (Cf. Section 3). At the tree-level, the relation between the two parametrizations is trivial:

$$\frac{G_F}{\sqrt{2}} = \frac{\pi\alpha}{2M_W^2 s_W^2}. \quad (7)$$

From the Lagrangian (6), the tree-level width of the unconventional top quark decay into a charged Higgs boson in the  $G_F$ -parametrization reads:

$$\begin{aligned} \Gamma^{(0)}(t \rightarrow H^+ b) = & \left( \frac{G_F}{8\pi\sqrt{2}} \right) \frac{|V_{tb}|^2}{m_t} \lambda^{1/2}(1, \frac{m_b^2}{m_t^2}, \frac{M_{H^\pm}^2}{m_t^2}) \\ & \times [(m_t^2 + m_b^2 - M_{H^\pm}^2)(m_t^2 \cot^2 \beta + m_b^2 \tan^2 \beta) + 4m_t^2 m_b^2], \end{aligned} \quad (8)$$

where

$$\lambda^{1/2}(1, x^2, y^2) \equiv \sqrt{[1 - (x + y)^2][1 - (x - y)^2]}. \quad (9)$$

It is useful to compare eq.(8) with the tree-level width of the canonical top quark decay in the SM:

$$\begin{aligned} \Gamma^{(0)}(t \rightarrow W^+ b) = & \left( \frac{G_F}{8\pi\sqrt{2}} \right) \frac{|V_{tb}|^2}{m_t} \lambda^{1/2}(1, \frac{m_b^2}{m_t^2}, \frac{M_W^2}{m_t^2}) \\ & \times [M_W^2(m_t^2 + m_b^2) + (m_t^2 - m_b^2)^2 - 2M_W^4]. \end{aligned} \quad (10)$$

The ratio between the two partial widths becomes more transparent upon neglecting the kinematical bottom mass contributions, while retaining all the Yukawa coupling effects:

$$\frac{\Gamma^{(0)}(t \rightarrow H^+ b)}{\Gamma^{(0)}(t \rightarrow W^+ b)} = \frac{\left(1 - \frac{M_{H^\pm}^2}{m_t^2}\right)^2 \left[\frac{m_b^2}{m_t^2} \tan^2 \beta + \cot^2 \beta\right]}{\left(1 - \frac{M_W^2}{m_t^2}\right)^2 \left(1 + 2\frac{M_W^2}{m_t^2}\right)}. \quad (11)$$

We see from it that, if  $M_{H^\pm} \gtrsim M_W$ , there are two regimes of  $\tan \beta$  where the unconventional top quark decay becomes of the same order as (or larger than) the conventional decay: namely, i) for  $\tan \beta \leq 1$ , and ii) for  $\tan \beta \geq m_t/m_b \sim 35$ . The critical regime of the decay  $t \rightarrow H^+ b$  occurs at the intermediate value  $\tan \beta = \sqrt{m_t/m_b} \sim 6$ , where the partial width has a pronounced dip. Around this value, the canonical decay  $t \rightarrow W^+ b$  is dominant over the charged Higgs decay. There is an interval, say  $1 \lesssim \tan \beta \lesssim 10$  where the decay rate of the mode  $t \rightarrow H^+ b$  is basically irrelevant as compared to the standard mode:  $BR(t \rightarrow H^+ b) \ll 10\%$ . Therefore, as already advanced in Section 1, a detailed study of the quantum effects within that interval is of no practical interest. While the approximate perturbative regime for  $\tan \beta$  extends over the wide range

$$0.5 \lesssim \tan \beta \lesssim 70, \quad (12)$$

we shall only explore the phenomenologically interesting high  $\tan\beta$  regime (typically  $20 \lesssim \tan\beta \lesssim 70$ ), and also to some extent the low  $\tan\beta$  end ( $0.5 \lesssim \tan\beta \lesssim 1$ ) in spite of being generally less appealing from the theoretical point of view. As mentioned in Section 1, we do have some theoretical motivation to contend that at least one of the two regimes i) or ii) may apply, most conspicuously the large  $\tan\beta$  regime. Therefore, it is justified to focus our attention on  $t \rightarrow H^+ b$ , not only as a possibility on its own, but also because there may be realistic situations where it could have a non-negligible branching ratio.

As a matter of fact, despite naive expectations, the non-SM branching ratio  $BR(t \rightarrow H^+ b)$  is not constrained at all by the recent measurements of the standard branching ratio  $BR(t \rightarrow W^+ b)$  at the Tevatron. To assess this fact, notice that the frequently quoted result in the literature,  $BR(t \rightarrow W^+ b) \gtrsim 70\%$  [2], strictly applies only under the assumption that the only source of top quarks in  $p\bar{p}$  collisions is the standard Drell-Yan pair production mechanism  $q\bar{q} \rightarrow t\bar{t}$  [24]. Now, the observed cross-section is equal to the Drell-Yan production cross-section convoluted over the parton distributions times the squared branching ratio. Schematically,

$$\sigma_{\text{obs.}} = \int dq d\bar{q} \sigma(q\bar{q} \rightarrow t\bar{t}) \times |BR(t \rightarrow W^+ b)|^2. \quad (13)$$

However, in the framework of the MSSM, we rather expect a generalization of this formula in the following way:

$$\begin{aligned} \sigma_{\text{obs.}} = & \int dq d\bar{q} \sigma(q\bar{q} \rightarrow t\bar{t}) \times |BR(t \rightarrow W^+ b)|^2 \\ & + \int dq d\bar{q} \sigma(q\bar{q} \rightarrow \tilde{g}\tilde{g}) \times |BR(\tilde{g} \rightarrow t\tilde{t}_1)|^2 \times |BR(t \rightarrow W^+ b)|^2 \\ & + \int dq d\bar{q} \sigma(q\bar{q} \rightarrow \tilde{b}_a\tilde{b}_a) \times |BR(\tilde{b}_a \rightarrow t\chi_1^-)|^2 \times |BR(t \rightarrow W^+ b)|^2 + \dots, \end{aligned} \quad (14)$$

where  $\tilde{g}$  stand for the gluinos,  $\tilde{t}_1$  for the lightest stop and  $\tilde{b}_a (a = 1, 2)$  for the sbottom quarks. One should also include electroweak and QCD radiative corrections to all these production cross-sections within the MSSM. For some of these processes calculations already exist in the literature showing that one-loop effects can be important [25].

It should be clear that the observed cross-section on eq.(14) refers not only to the standard  $bWbW$  events, but to all kind of final states that can simulate them. Thus, effectively, we should substitute  $BR(t \rightarrow W^+ b)$  in these formulas by  $\sum_X BR(t \rightarrow X b)$ , where  $X$  is any state that leads to a pattern of leptons and jets similar to those resulting from  $W$ -decay. In particular,  $X = H^\pm$  would contribute (see below) to the  $\tau$  signature if  $\tan\beta$  is large enough, and there are many other top quark decays into SUSY particles that could mimic the SM decay of the top quark [21]. Therefore, from eq.(14) it is clear that at present one cannot effectively derive any stringent upper bound on  $BR(t \rightarrow W^+ b)$ , the only restriction being an approximate lower bound  $BR(t \rightarrow W^+ b) \gtrsim 50$

in order to guarantee the observed top quark decay data at the Tevatron. Thus, from these considerations it should be clear that the non-SM branching ratio of the top quark,  $BR(t \rightarrow \text{"new"})$ , could be as big as the SM one, i.e.  $\sim 50\%$ .

A first step to improve this situation would be to compute some of the additional top quark production cross-sections in the MSSM under given hypotheses on the SUSY spectrum. Recently, the inclusion of the  $q\bar{q} \rightarrow \tilde{g}\bar{\tilde{g}}$  mechanism followed by the  $\tilde{g} \rightarrow t\bar{t}_1$  decay has been considered in Ref.[26], where it is claimed that  $BR(t \rightarrow \tilde{t}_1 \chi_1^0) \simeq 50\%$ . By the same token, one cannot restrict  $BR(t \rightarrow H^+ b)$  from the present FNAL data. In particular, if  $\tan \beta$  is large and there exists a relatively light chargino, the third mechanism suggested on eq.(14), namely  $q\bar{q} \rightarrow \tilde{b}_a \bar{\tilde{b}}_a$  followed by  $\tilde{b}_a \rightarrow t \chi_1^-$ , could also be a rather efficient non-SM source of top quarks. Moreover, if  $100 \text{ GeV} \lesssim M_{H^+} \lesssim m_t$ , then a large portion of the top quarks would decay into a charged Higgs (Cf. eq.(11)). Thus, one may equally argue that a large branching ratio  $BR(t \rightarrow H^+ b) \simeq 50\%$  is not incompatible with the present measurement of the top quark cross-sections [1].

Finally, it is worth mentioning that the decay mode  $t \rightarrow H^+ b$  has a distinctive signature which could greatly help in its detection, viz. the fact that at large  $\tan \beta$  the emergent charged Higgs would seldom decay into a pair of quark jets, but rather into a  $\tau$ -lepton and associated neutrino. This follows from inspecting the ratio

$$\begin{aligned} \frac{\Gamma(H^+ \rightarrow \tau^+ \nu_\tau)}{\Gamma(H^+ \rightarrow c\bar{s})} &= \frac{1}{3} \left( \frac{m_\tau}{m_c} \right)^2 \frac{\tan^2 \beta}{(m_s^2/m_c^2) \tan^2 \beta + \cot^2 \beta} \\ &\rightarrow \frac{1}{3} \left( \frac{m_\tau}{m_s} \right)^2 > 10 \quad (\text{for } \tan \beta > \sqrt{m_c/m_s} \gtrsim 2), \end{aligned} \quad (15)$$

where we see that the identification of the charged Higgs decay of the top quark could be a matter of measuring a departure from the universality prediction between all lepton channels. In practice,  $\tau$ -identification is possible at Tevatron [27, 28]; and the feasibility of tagging the excess of events with one isolated  $\tau$ -lepton as compared to events with an additional lepton has been substantiated by studies of the LHC collaborations [29]. A recent study in this direction has been able to exclude basically the whole region of the  $(\tan \beta, M_{H^+})$ -plane characterized by  $\tan \beta > 60$  [30], thus improving the perturbative bound already mentioned, eq.(12). Therefore, although we shall present our results in most of the original range (12), it should be clear that, for our purposes, the phenomenologically interesting  $\tan \beta$  segment, allowed by experiment, is the following:

$$20 \lesssim \tan \beta \lesssim 60, \quad (16)$$

To round off this business, it has recently been shown that it should be fairly easy to discriminate between the  $W$ -daughter  $\tau$ 's and the  $H^\pm$ -daughter  $\tau$ 's by just taking advantage of the opposite states of  $\tau$  polarization resulting from the  $W^\pm$  and  $H^\pm$  decays;

the two polarization states can be distinguished by measuring the charged and neutral contributions to the 1-prong  $\tau$ -jet energy (even without identifying the individual meson states) [31, 32]. In short, there are good prospects of detecting the decay  $t \rightarrow H^+ b$ . Unfortunately, on the sole basis of computing tree-level effects we cannot find out whether the charged Higgs emerging from that decay is supersymmetric or not. Quantum effects, however, can.

### 3. Renormalization of the $t b H^+$ -vertex

Proceeding closely in parallel with our approach [14, 15] to the conventional decay  $t \rightarrow W^+ b$ , we shall address the calculation of the one-loop corrections to the partial width of  $t \rightarrow H^+ b$  in the MSSM within the context of the on-shell renormalization framework [33, 34]<sup>3</sup>. Again we may use both the  $\alpha$  or the  $G_F$  parametrizations. At one-loop order, we shall call the former the “ $\alpha$ -scheme”, where the fine structure constant  $\alpha \equiv \alpha_{\text{em}}(q^2 = 0)$  and the masses of the gauge bosons, fermions and scalars are the renormalized parameters:  $(\alpha, M_W, M_Z, M_H, m_f, M_{\text{SUSY}}, \dots) - M_{\text{SUSY}}$  standing for the collection of renormalized sparticle masses. Similarly, the “ $G_F$ -scheme” is characterized by the set of inputs  $(G_F, M_W, M_Z, M_H, m_f, M_{\text{SUSY}}, \dots)$ . Beyond lowest order, the relation between the two on-shell schemes is no longer given by eq.(7) but by

$$\frac{G_F}{\sqrt{2}} = \frac{\pi\alpha}{2M_W^2 s_W^2} (1 + \Delta r^{\text{MSSM}}), \quad (17)$$

where  $\Delta r^{\text{MSSM}}$  is the prediction of the parameter  $\Delta r$  [35] in the MSSM<sup>4</sup>.

Let us sketch the renormalization procedure affecting the parameters and fields related to the  $t b H^\pm$ -vertex, whose interaction Lagrangian was given on eq.(6). In general, the renormalized MSSM Lagrangian  $\mathcal{L} \rightarrow \mathcal{L} + \delta\mathcal{L}$  is obtained following a similar pattern as in the SM, i.e. by attaching multiplicative renormalization constants to each free parameter and field:  $g_i \rightarrow (1 + \delta g_i/g_i)g_i \equiv Z_{g_i}g_i$ ;  $\Phi_i \rightarrow Z_{\Phi_i}^{1/2}\Phi_i$ . As a matter of fact, field renormalization (and so Green’s functions renormalization) is unessential and can be either omitted [34] or be carried out in many different ways without altering physical ( $S$ -matrix) amplitudes. In our case, in the line of Refs.[14, 15] we shall use minimal field renormalization, i.e. one renormalization constant per gauge symmetry multiplet [36]. In this way the counterterm Lagrangian,  $\delta\mathcal{L}$ , as well as the various Green’s functions are automatically gauge-invariant. Specifically, for the quark fields under consideration, we

---

<sup>3</sup>For a comprehensive exposition, see e.g. Refs.[35]-[37].

<sup>4</sup>A dedicated study of  $\Delta r^{\text{MSSM}}$  has been presented in Ref[38].

have

$$\begin{aligned} \begin{pmatrix} t_L \\ b_L \end{pmatrix} &\rightarrow Z_L^{1/2} \begin{pmatrix} t_L \\ b_L \end{pmatrix} \rightarrow \begin{pmatrix} (Z_L^t)^{1/2} t_L \\ (Z_L^b)^{1/2} b_L \end{pmatrix}, \\ b_R &\rightarrow (Z_R^b)^{1/2} b_R, \quad t_R \rightarrow (Z_R^t)^{1/2} t_R. \end{aligned} \quad (18)$$

Here  $Z_i = 1 + \delta Z_i$  are the doublet ( $Z_L$ ) and singlet ( $Z_R^{t,b}$ ) field renormalization constants for the top and bottom quarks, with  $Z_L^b = Z_L$ , but  $Z_L^t \neq Z_L$  due to an additional *finite* renormalization effect [36]. To fix all these constants one starts from the usual on-shell mass renormalization condition for fermions,  $f$ , together with the “residue = 1” condition on the renormalized propagator. These are completely standard procedures, and in this way one obtains <sup>5</sup>

$$\frac{\delta m_f}{m_f} = - \left[ \frac{\Sigma_L^f(m_f^2) + \Sigma_R^f(m_f^2)}{2} + \Sigma_S^f(m_f^2) \right] \quad (19)$$

and

$$\delta Z_{L,R}^f = \Sigma_{L,R}^f(m_f^2) + m_f^2 [\Sigma_L^{f'}(m_f^2) + \Sigma_R^{f'}(m_f^2) + 2\Sigma_S^{f'}(m_f^2)], \quad (20)$$

where we have decomposed the (real part of the) fermion self-energy according to

$$\Sigma^f(p) = \Sigma_L^f(p^2) \not{p} P_L + \Sigma_R^f(p^2) \not{p} P_R + m_f \Sigma_S^f(p^2), \quad (21)$$

and used the notation  $\Sigma'(p) \equiv \partial \Sigma(p) / \partial p^2$ .

One also assigns doublet renormalization constants to the two Higgs doublets (3) of the MSSM:

$$\begin{pmatrix} H_1^0 \\ H_1^- \end{pmatrix} \rightarrow Z_{H_1}^{1/2} \begin{pmatrix} H_1^0 \\ H_1^- \end{pmatrix}, \quad \begin{pmatrix} H_2^+ \\ H_2^0 \end{pmatrix} \rightarrow Z_{H_2}^{1/2} \begin{pmatrix} H_2^+ \\ H_2^0 \end{pmatrix}. \quad (22)$$

The renormalization of the gauge sector is related to that of the Higgs sector. In particular, we point out the presence in our decay process  $t \rightarrow H^+ b$  of the (one-loop induced) mixing term  $H^\pm - W^\pm$  for the bare fields (Cf. Appendix B), which must be renormalized away for the physical fields  $H^\pm$  and  $W^\pm$ . In order to generate the corresponding Lagrangian counterterm we write

$$W_\mu^\pm \rightarrow (Z_2^W)^{1/2} W_\mu^\pm \pm i \frac{\delta Z_{HW}}{M_W} \partial_\mu H^\pm. \quad (23)$$

Therefore, from

$$\mathcal{L}_{Wbt} = \frac{g}{\sqrt{2}} W_\mu^- \bar{b} \gamma^\mu P_L t + \text{h.c.} \quad (24)$$

---

<sup>5</sup>We follow the notation of Ref.[14], which is close enough to that of Ref.[36], but differs from it in several respects, in particular in the sign conventions on the self-energy functions.

we obtain

$$\begin{aligned}\delta\mathcal{L}_{HW} &= -i\delta Z_{HW}\frac{g}{\sqrt{2}M_W}\partial_\mu H^-\bar{b}\gamma^\mu P_L t + \text{h.c.} \\ &\rightarrow \delta Z_{HW}\frac{g}{\sqrt{2}M_W}H^-\left[m_t\bar{b}P_R t - m_b\bar{b}P_L t\right] + \text{h.c.},\end{aligned}\quad (25)$$

and in this way it adopts the form of the original vertex (6). In the above expression,  $Z_2^W$  is the usual  $SU(2)_L$  gauge triplet renormalization constant whose explicit expression is [14]

$$\delta Z_2^W = \frac{\Sigma^\gamma(k^2)}{k^2}\Big|_{k^2=0} - 2\frac{c_W}{s_W}\frac{\Sigma^{\gamma Z}(0)}{M_Z^2} + \frac{c_W^2}{s_W^2}\left(\frac{\delta M_Z^2}{M_Z^2} - \frac{\delta M_W^2}{M_W^2}\right), \quad (26)$$

and

$$\delta M_W^2 = -Re\Sigma^W(k^2 = M_W^2), \quad \delta M_Z^2 = -Re\Sigma^Z(k^2 = M_Z^2) \quad (27)$$

are the gauge boson mass counterterms enforced by the usual on-shell mass renormalization conditions. Furthermore,  $\delta Z_{HW}$  on eqs.(23)-(25) is a dimensionless constant associated to the wave-function renormalization mixing among the bare  $H^\pm$  and  $W^\pm$  fields. Its relation with the doublet renormalization constants on eq.(22) is the following:

$$\delta Z_{HW} = \sin\beta\cos\beta(\delta Z_{H_2} - \delta Z_{H_1}) - \frac{\delta\tan\beta}{\tan\beta}, \quad (28)$$

where  $\delta\tan\beta$  is a counterterm associated to the renormalization of  $\tan\beta$  (see below).

In practice, the most straightforward way to compute  $\delta Z_{HW}$  is from the unrenormalized mixed self-energy  $\Sigma_{HW}(k^2)$  in the unitary gauge, where it takes on the simplest form:

$$\delta Z_{HW} = \frac{\Sigma_{HW}(M_{H^\pm}^2)}{M_W^2}. \quad (29)$$

However, since we shall perform the rest of the calculation in the Feynman gauge, it is worth considering the computation of  $\delta Z_{HW}$  in that gauge (see Appendix B), where the discussion is slightly more complicated due to the presence of Goldstone bosons ( $G^\pm$ ) leading to additional  $(H^\pm - G^\pm)$  mixing terms among the bare fields. However, the corresponding expression for  $\delta Z_{HW}$  is formally identical in both gauges.

For the  $SU(2)_L$  gauge coupling constant, we have

$$g \rightarrow (1 + \frac{\delta g}{g})g = (Z_1^W)(Z_2^W)^{-3/2}g, \quad (30)$$

where  $Z_1^W$  refers to the renormalization constant associated to the triple vector boson vertex. Therefore, from charge renormalization and the bare relation  $\alpha = g^2 s_W^2/4\pi \rightarrow \alpha + \delta\alpha = (g^2 + \delta g^2)(s_W^2 + \delta s_W^2)/4\pi$ , one gets for the relevant counterterms:

$$\begin{aligned}\frac{\delta\alpha}{\alpha} &= -\frac{\Sigma^\gamma(k^2)}{k^2}\Big|_{k^2=0} - 2\frac{s_W}{c_W}\frac{\Sigma^{\gamma Z}(0)}{M_Z^2}, \\ \frac{\delta g^2}{g^2} &= \frac{\delta\alpha}{\alpha} - \frac{c_W^2}{s_W^2}\left(\frac{\delta M_Z^2}{M_Z^2} - \frac{\delta M_W^2}{M_W^2}\right),\end{aligned}\quad (31)$$

and as a by-product

$$\delta Z_1^W = \frac{1}{2} \frac{\delta g^2}{g^2} + \frac{3}{2} \delta Z_2^W. \quad (32)$$

Let us now outline the renormalization of the Higgs sector of the MSSM[23]<sup>6</sup>. For the neutral Higgs sector of the MSSM, the renormalization procedure naturally adopts the CP-odd state  $A^0$  as the basic field on which to set the mass and wave-function renormalization conditions. In the present work, however, since the external Higgs particle is charged, we rather take  $H^\pm$  as the basic field. Its mass and field renormalization constants are defined by

$$M_{H^\pm}^2 \rightarrow M_{H^\pm}^2 + \delta M_{H^\pm}^2, \quad H^\pm \rightarrow Z_{H^\pm}^{1/2} H^\pm. \quad (33)$$

We remark, in passing, that the field renormalization constant  $Z_{H^\pm} = 1 + \delta Z_{H^\pm}$  is related to the doublet renormalization constants  $Z_{H_i} = 1 + \delta Z_{H_i}$  introduced on eq.(22) as follows:

$$\delta Z_{H^\pm} = \sin^2 \beta \delta Z_{H_1} + \cos^2 \beta \delta Z_{H_2}. \quad (34)$$

The structure of the renormalized self-energy is

$$\hat{\Sigma}_{H^\pm}(k^2) = \Sigma_{H^\pm}(k^2) + \delta M_{H^\pm}^2 - (k^2 - M_{H^\pm}^2) \delta Z_{H^\pm}. \quad (35)$$

where  $\Sigma_{H^\pm}(k^2)$  is the corresponding unrenormalized self-energy. In order to determine the counterterms, we impose the following renormalization conditions:

i) On-shell mass renormalization condition:

$$\text{Re} \hat{\Sigma}_{H^\pm}(M_{H^\pm}^2) = 0 \quad (36)$$

ii) “Residue = 1” condition for the renormalized propagator at the mass pole:

$$\text{Re} \frac{\partial \hat{\Sigma}_{H^\pm}(k^2)}{\partial k^2} \bigg|_{k^2=M_{H^\pm}^2} \equiv \hat{\Sigma}'_{H^\pm}(M_{H^\pm}^2) = 0. \quad (37)$$

From these conditions one derives

$$\begin{aligned} \delta M_{H^\pm}^2 &= -\text{Re} \Sigma_{H^\pm}(M_{H^\pm}^2), \\ \delta Z_{H^\pm} &= +\text{Re} \Sigma'_{H^\pm}(M_{H^\pm}^2). \end{aligned} \quad (38)$$

Although not needed in our calculation, it is clear that with these settings the neutral Higgs fields will undergo an additional finite wave function renormalization.

Consider next the renormalization of the Higgs potential in the MSSM[23]. After expanding the fields  $H_1^0$  and  $H_2^0$  around their VEV’s  $v_1$  and  $v_2$ , the one-point functions

---

<sup>6</sup>A detailed account placing much emphasis on phenomenological applications to neutral Higgs boson decays can be found e.g.in Ref. [39].

of the resulting CP-even fields are required to vanish, i.e. the tadpole counterterms are constrained to exactly cancel the tadpole diagrams, so that the renormalized tadpoles are zero and the quantities  $v_{1,2}$  remain as the VEV's of the renormalized Higgs potential. Notwithstanding, at this stage a prescription to renormalize  $\tan \beta = v_2/v_1$

$$\tan \beta \rightarrow \tan \beta + \delta \tan \beta, \quad (39)$$

is still called for. There are many possible strategies. The ambiguity is related to the fact that this parameter is just a Lagrangian parameter and as such it is not a physical observable. Its value beyond the tree-level is renormalization scheme dependent. (The situation is similar to the definition of the weak mixing angle  $\theta_W$ , or equivalently of  $\sin^2 \theta_W$ .) However, even within a given scheme, e.g. the on-shell renormalization scheme, there are some ambiguities that must be fixed. For example, we may wish to define  $\tan \beta = v_2/v_1$  as a direct external input giving the ratio between the true VEV's after renormalization of the Higgs potential. In this case we would require  $\delta \tan \beta = 0$ , or equivalently  $\delta v_1/v_1 = \delta v_2/v_2$ . Combining this condition with the renormalization of the VEV's  $v_{1,2}$  in the Higgs potential of the MSSM one determines  $\delta v_{1,2}$ . Nevertheless, one may eventually like to fix the on-shell renormalization condition on  $\tan \beta$  in a more physical way, i.e. by relating it to some concrete physical observable, so that it is the measured value of this observable that is taken as an input rather than the VEV's of the Higgs potential. Following this practical attitude, we choose as a physical observable the decay width of the charged Higgs boson into  $\tau$ -lepton and associated neutrino:  $H^+ \rightarrow \tau^+ \nu_\tau$ . As it has been argued in Section 2, this should be a good choice, because: i) When  $t \rightarrow H^+ b$  is allowed, the decay  $H^+ \rightarrow \tau^+ \nu_\tau$  is the dominant decay of  $H^\pm$  for the whole range  $\tan \beta \gtrsim 2$ ; ii) From the experimental point of view there is a well-defined method (Cf, Section 2) to separate the final state  $\tau$ 's from the ones coming out of the conventional decay  $W^+ \rightarrow \tau^+ \nu_\tau$ , and iii) At high  $\tan \beta$ , the charged Higgs decay of the top quark has a sizeable branching ratio.

The interaction Lagrangian describing the decay  $H^+ \rightarrow \tau^+ \nu_\tau$  is directly proportional to  $\tan \beta$ ,

$$\mathcal{L}_{H\tau\nu} = \frac{g m_\tau \tan \beta}{\sqrt{2} M_W} H^- \bar{\tau} P_L \nu_\tau + \text{h.c.}, \quad (40)$$

and the relevant decay width is proportional to  $\tan^2 \beta$ . Whether in the  $\alpha$ -scheme or in the  $G_F$ -scheme, it reads:

$$\Gamma(H^+ \rightarrow \tau^+ \nu_\tau) = \frac{\alpha m_{\tau^+}^2 M_{H^+}}{8 M_W^2 s_W^2} \tan^2 \beta = \frac{G_F m_{\tau^+}^2 M_{H^+}}{4\pi\sqrt{2}} \tan^2 \beta (1 - \Delta r^{MSSM}), \quad (41)$$

where we have used the relation (17). By measuring this width one obtains a physical definition of  $\tan \beta$ . A combined measurement of  $M_{H^\pm}$  and  $\tan \beta$  defined through charged

Higgs decaying into  $\tau$  in a hadron collider has been described in the literature [40, 29] by comparing the size of the various signals for charged Higgs boson production, such as the multijet channels accompanied by a  $\tau$ -jet or a large missing  $p_T$  and the two  $\tau$ -jet channel. At the upgraded Tevatron, the conventional mechanisms  $gg(q\bar{q}) \rightarrow t\bar{t}$  followed by  $t \rightarrow H^+ b$  has been studied and compared with the usual  $t \rightarrow W^+ b$ , and the result is that for  $M_{H^\pm} \simeq 100 \text{ GeV}$ , the charged Higgs production is at least as large as the  $W^\pm$  production, apart from a gap around  $\tan \beta \gtrsim 5 - 6$  [40].

Insofar as the determination of the counterterm  $\delta \tan \beta$ , it can be fixed unambiguously from our Lagrangian definition of  $\tan \beta$  on eq.(40) and the renormalization procedure described above. It is straightforward to find:

$$\frac{\delta \tan \beta}{\tan \beta} = \frac{\delta v}{v} - \frac{1}{2} \delta Z_{H^+} + \cot \beta \delta Z_{HW} + \Delta_\tau, \quad (42)$$

Notice the appearance of the counterterm

$$\frac{\delta v}{v} = \frac{1}{2} \frac{\delta v^2}{v^2} = \frac{1}{2} \frac{\delta M_W^2}{M_W^2} - \frac{1}{2} \frac{\delta g^2}{g^2}, \quad (43)$$

which is associated to  $v^2 = v_1^2 + v_2^2$ , and whose structure is fixed from eq.(4). The last term on eq.(42),

$$\Delta_\tau = -\frac{\delta m_\tau}{m_\tau} - \frac{1}{2} \delta Z_L^{\nu\tau} - \frac{1}{2} \delta Z_R^\tau - F_\tau \quad (44)$$

is the (finite) process-dependent part of the counterterm. Here  $\delta m_\tau/m_\tau$ ,  $\delta Z_L^{\nu\tau}$  and  $\delta Z_R^\tau$  are obtained from eqs. (19) and (20) (with  $m_{\nu_\tau} = 0$ ); i.e. they represent the contribution from the mass and wave-function renormalization of the  $(\nu_\tau, \tau)$ -doublet, including the finite renormalization of the neutrino leg. Finally,  $F_\tau$  on eq.(44) is the form factor describing the vertex corrections to the amplitude of  $H^+ \rightarrow \tau^+ \nu_\tau$ .

In practice, process-dependent terms are inevitable, irrespective of the definition of  $\tan \beta$ . For instance, the aforementioned alternative definition of  $\tan \beta$  where  $\delta v_1/v_1 = \delta v_2/v_2$  will also develop process-dependent contributions, as can be seen by relating the value of  $\tan \beta$  in this scheme with a value directly read off some physical observable [41]. For example, if  $M_{A^0}$  is heavy enough, one may define  $\tan \beta$  as follows:

$$\begin{aligned} \frac{\Gamma(A^0 \rightarrow b\bar{b})}{\Gamma(A^0 \rightarrow t\bar{t})} &= \tan^4 \beta \frac{m_b^2}{m_t^2} \left(1 - \frac{4m_t^2}{M_{A^0}^2}\right)^{-1/2} \left[ 1 + 4 \left( \frac{\delta v_2}{v_2} - \frac{\delta v_1}{v_1} \right) \right. \\ &\quad \left. + 2 \left( \frac{\delta m_b}{m_b} + \frac{1}{2} \delta Z_L^b + \frac{1}{2} \delta Z_R^b - \frac{\delta m_t}{m_t} - \frac{1}{2} \delta Z_L^t - \frac{1}{2} \delta Z_R^t \right) + \delta V \right], \end{aligned} \quad (45)$$

where we have neglected  $m_b^2 \ll M_{A^0}^2$ , and  $\delta V$  stands for the vertex corrections to both processes  $A^0 \rightarrow b\bar{b}$  and  $A^0 \rightarrow t\bar{t}$ . Since the sum of the mass and wave-function renormalization terms along with the vertex corrections is UV-finite, one can consistently choose

$\delta v_1/v_1 = \delta v_2/v_2$  and derive  $\tan \beta$  from eq.(45), thus incorporating the process-dependent contributions. Any definition of  $\tan \beta$  is in principle as good as any other; and although the corrections themselves may show some dependence on the choice of the particular definition, the physical observables should not depend on that choice. However, it can be a practical matter what definition to use in a given situation. For example, our definition of  $\tan \beta$  given on eq.(41) should be adequate for  $M_{H^\pm} < m_t - m_b$  and large  $\tan \beta$ , since then  $H^+ \rightarrow \tau^+ \nu_\tau$  is the dominant decay of  $H^+$ , whereas the definition based on eq.(16) requires, in order to be operative, a much heavier charged Higgs boson since  $M_{H^\pm} \simeq M_{A^0}$  when the decay  $A \rightarrow t\bar{t}$  is kinematically open in the MSSM.

Within our context, we may use Eq.(42) to compute the one-loop corrections to any other process, and in particular to our decay  $t \rightarrow H^+ b$ . Putting all the pieces together, the counterterm Lagrangian for the vertex  $t b H^\pm$  follows right away from the bare Lagrangian (6) after re-expressing everything in terms of renormalized parameters and fields in the on-shell scheme. It takes on the form :

$$\delta\mathcal{L}_{Hbt} = \frac{g}{\sqrt{2} M_W} H^- \bar{b} [\delta C_R m_t \cot \beta P_R + \delta C_L m_b \tan \beta P_L] t + \text{h.c.}, \quad (46)$$

with

$$\begin{aligned} \delta C_R &= \frac{\delta m_t}{m_t} - \frac{\delta v}{v} + \frac{1}{2} \delta Z_{H^+} + \frac{1}{2} \delta Z_L^b + \frac{1}{2} \delta Z_R^t - \frac{\delta \tan \beta}{\tan \beta} + \delta Z_{HW} \tan \beta, \\ \delta C_L &= \frac{\delta m_b}{m_b} - \frac{\delta v}{v} + \frac{1}{2} \delta Z_{H^+} + \frac{1}{2} \delta Z_L^t + \frac{1}{2} \delta Z_R^b + \frac{\delta \tan \beta}{\tan \beta} - \delta Z_{HW} \cot \beta, \end{aligned} \quad (47)$$

and where we have set  $V_{tb} = 1$  ( $V_{tb} = 0.999$  within  $\pm 0.1\%$ , from unitarity of the CKM-matrix under the assumption of three generations).

## 4. One-loop Corrected $\Gamma(t \rightarrow H^+ b)$ in the MSSM

As stated in the beginning, the study of the decay  $t \rightarrow H^+ b$  is worthwhile only in the high  $\tan \beta$  region, where its branching ratio is comparable to the branching ratio of the standard decay  $t \rightarrow W^+ b$ . And it is precisely in this region where there may be significant quantum corrections, if we set aside for the moment the theoretically unfavoured interval  $\tan \beta < 1$ . On the electroweak side, the origin of the large quantum corrections lies in the possibility of having enhanced Yukawa couplings of the type (2). Since the large quantum effects at high  $\tan \beta$  are basically of supersymmetric origin, one may safely neglect the non-enhanced  $\mathcal{O}(g^2)$  corrections from transversal gauge bosons in the Feynman gauge. These effects could be comparable to the Yukawa coupling corrections only in the uninteresting  $\tan \beta$  range,  $1 \lesssim \tan \beta \lesssim 10$ , where the branching ratio of the charged Higgs mode is too small to speak of. However, as already mentioned, the truly relevant  $\tan \beta$  range for our decay is given by eq.(16).

In the following we will describe the relevant electroweak one-loop supersymmetric diagrams entering the amplitude of  $\Gamma(t \rightarrow H^+ b)$  in the MSSM. At the tree-level, the only Feynman diagram is the one in Fig.1. At the one-loop, we have the diagrams exhibited in Figs.2-6. The computation of the one-loop diagrams requires to use the full structure of the MSSM Lagrangian. The explicit form of the most relevant pieces of this Lagrangian, together with the necessary SUSY notation, is provided in Appendix A.

Specifically, Fig.2 shows the electroweak SUSY vertices involving squarks, charginos and neutralinos. In all these diagrams a sum over all indices is taken for granted. The supersymmetric Higgs particles of the MSSM and Goldstone bosons (in the Feynman gauge) contribute a host of one-loop vertices as well (see Fig.3). As for the various self-energies, they will be treated as counterterms to the (renormalized) vertices. Their structure is dictated by the Lagrangian (46). Thus, Fig.4 displays the counterterms  $C_{b1} - C_{t4}$  generated from the external bottom and top quark lines; they include contributions from supersymmetric particles, higgses and Goldstone bosons. Similarly, Fig.5 contains the counterterms  $C_{H1} - C_{H4}$  associated to the self-energy of the external charged Higgs line. A variant of the latter contribution is the mixed  $W^+ - H^+$  self-energy counterterms  $C_{M1} - C_{M3}$  shown in Fig.6.

Although we have displayed only the process dependent diagrams, the full analysis should also include the SUSY and Higgs contributions to the universal vacuum polarization effects associated to the counterterms in eqs.(26), (27), (31); however, the calculation of all these pieces has already been discussed in detail long ago in the literature [42, 43] and thus the lengthy formulae accounting for these results will not be explicitly quoted here. Their contribution is  $\mathcal{O}(g^2)$  and therefore is not important. Nonetheless, since we wish to compute the full supersymmetric contribution in the relevant regions of the MSSM parameter space, that contribution will be included in our numerical analysis. On the other hand, the smaller –though numerically relevant –subset of strong supersymmetric one-loop graphs are displayed in Fig.2 of Ref.[12]. We use the formulae from the latter reference in the present analysis to produce the total (electroweak+strong) MSSM correction to our process.

Let us next explicitly compute the various vertex diagrams and counterterms in the on-shell renormalization scheme. The generic structure of any renormalized vertex function,  $\Lambda$ , in Figs.2-3 is composed of two form factors  $F_L, F_R$  plus the counterterms. Therefore, on making use of the formulae of Section 3, one immediately finds:

$$\Lambda = \frac{i g}{\sqrt{2} M_W} (m_t \cot \beta (1 + \Lambda_R) P_R + m_b \tan \beta (1 + \Lambda_L) P_L) , \quad (48)$$

where

$$\Lambda_R = F_R + \frac{\delta m_t}{m_t} + \frac{1}{2} \delta Z_L^b + \frac{1}{2} \delta Z_R^t - \Delta_\tau$$

$$\begin{aligned}
& - \frac{\delta v^2}{v^2} + \delta Z_{H+} + (\tan \beta - \cot \beta) \delta Z_{HW}, \\
\Lambda_L & = F_L + \frac{\delta m_b}{m_b} + \frac{1}{2} \delta Z_L^t + \frac{1}{2} \delta Z_R^b + \Delta_\tau.
\end{aligned} \tag{49}$$

The explicit analytical contributions to the vertex form factors and counterterms will be specified diagram by diagram.

## 4.1 SUSY vertex diagrams

In this section we will make intensive use of the definitions and formulae of Appendix A. We refer the reader there for questions about notation and conventions. Following the labelling of Feynman graphs in Fig.2 we write down the terms coming from virtual SUSY particles.

- Diagram ( $V_{S1}$ ): Making use of the coupling matrices of eqs. (A.16),(A.21) we may introduce the shorthands

$$A_\pm \equiv A_{\pm ai}^{(t)} \quad \text{and} \quad A_\pm^{(0)} \equiv A_{\pm a\alpha}^{(t)}, \tag{50}$$

and define the combinations (omitting indices also for  $Q_{\alpha i}^L, Q_{\alpha i}^R$ )

$$\begin{aligned}
A^{(1)} & = \cos \beta A_+^* Q^L A_-^{(0)}, & E^{(1)} & = \cos \beta A_-^* Q^L A_-^{(0)}, \\
B^{(1)} & = \cos \beta A_+^* Q^L A_+^{(0)}, & F^{(1)} & = \cos \beta A_-^* Q^L A_+^{(0)}, \\
C^{(1)} & = \sin \beta A_+^* Q^R A_-^{(0)}, & G^{(1)} & = \sin \beta A_-^* Q^R A_-^{(0)}, \\
D^{(1)} & = \sin \beta A_+^* Q^R A_+^{(0)}, & H^{(1)} & = \sin \beta A_-^* Q^R A_+^{(0)}.
\end{aligned} \tag{51}$$

The contribution from diagram ( $V_{S1}$ ) to the form factors  $F_L$  and  $F_R$  is then

$$\begin{aligned}
F_L & = M_L \left[ H^{(1)} \tilde{C}_0 + \right. \\
& + m_b \left( m_t A^{(1)} + M_\alpha^0 B^{(1)} + m_b H^{(1)} + M_i D^{(1)} \right) C_{12} \\
& + m_t \left( m_t H^{(1)} + M_\alpha^0 G^{(1)} + m_b A^{(1)} + M_i E^{(1)} \right) (C_{11} - C_{12}) \\
& \left. + \left( m_t m_b A^{(1)} + m_t M_i E^{(1)} + M_\alpha^0 m_b B^{(1)} + M_i M_\alpha^0 F^{(1)} \right) C_0 \right], \\
F_R & = M_R \left[ A^{(1)} \tilde{C}_0 + \right. \\
& + m_b \left( m_t H^{(1)} + M_\alpha^0 G^{(1)} + m_b A^{(1)} + M_i E^{(1)} \right) C_{12} \\
& + m_t \left( m_t A^{(1)} + M_\alpha^0 B^{(1)} + m_b H^{(1)} + M_i D^{(1)} \right) (C_{11} - C_{12}) \\
& \left. + \left( m_t m_b H^{(1)} + m_t M_i D^{(1)} + M_\alpha^0 m_b G^{(1)} + M_i M_\alpha^0 C^{(1)} \right) C_0 \right], \tag{52}
\end{aligned}$$

where the overall factors  $M_L$  and  $M_R$  are the following:

$$M_L = -\frac{ig^2 M_W}{m_b \tan \beta} \quad M_R = -\frac{ig^2 M_W}{m_t \cot \beta}. \tag{53}$$

The notation for the various 3-point functions is summarized in Appendix A. In eq. (52) they must be evaluated with arguments:

$$C_* = C_* (p, p', m_{\tilde{t}_a}, M_\alpha^0, M_i) . \quad (54)$$

- Diagram  $(V_{S2})$ : As for diagram  $(V_{S1})$ , with the help of the matrices of eqs. (A.16), (A.18), we use the shorthands

$$A_\pm^{(b)} \equiv A_{\pm b\alpha}^{(b)} \quad \text{and} \quad A_\pm^{(t)} \equiv A_{\pm a\alpha}^{(t)} , \quad (55)$$

to define the products of coupling matrices

$$\begin{aligned} A^{(2)} &= G_{ba} A_+^{(b)*} A_-^{(t)}, & C^{(2)} &= G_{ba} A_-^{(b)*} A_-^{(t)}, \\ B^{(2)} &= G_{ba} A_+^{(b)*} A_+^{(t)}, & D^{(2)} &= G_{ba} A_-^{(b)*} A_+^{(t)}. \end{aligned} \quad (56)$$

The contribution to the form factors  $F_L$  and  $F_R$  from this diagram is

$$\begin{aligned} F_L &= \frac{M_L}{2M_W} \left[ m_b B^{(2)} C_{12} + m_t C^{(2)} (C_{11} - C_{12}) - M_\alpha^0 D^{(2)} C_0 \right], \\ F_R &= \frac{M_R}{2M_W} \left[ m_b C^{(2)} C_{12} + m_t B^{(2)} (C_{11} - C_{12}) - M_\alpha^0 A^{(2)} C_0 \right], \end{aligned} \quad (57)$$

the coefficients  $M_L$ ,  $M_R$  being those of eq. (53) and the scalar point functions now evaluated with arguments

$$C_* = C_* (p, p', M_\alpha^0, m_{\tilde{t}_a}, m_{\tilde{b}_b}) . \quad (58)$$

- Diagram  $(V_{S3})$ : For this diagram –which in contrast to the previous ones is finite– we will need

$$A_\pm \equiv A_{\pm ai}^{(b)} \quad \text{and} \quad A_\pm^{(0)} \equiv A_{\pm a\alpha}^{(b)} , \quad (59)$$

and again omitting indices we shall use

$$\begin{aligned} A^{(3)} &= \cos \beta A_+^{(0)*} Q^L A_- , & E^{(3)} &= \cos \beta A_-^{(0)*} Q^L A_- , \\ B^{(3)} &= \cos \beta A_+^{(0)*} Q^L A_+ , & F^{(3)} &= \cos \beta A_-^{(0)*} Q^L A_+ , \\ C^{(3)} &= \sin \beta A_+^{(0)*} Q^R A_- , & G^{(3)} &= \sin \beta A_-^{(0)*} Q^R A_- , \\ D^{(3)} &= \sin \beta A_+^{(0)*} Q^R A_+ , & H^{(3)} &= \sin \beta A_-^{(0)*} Q^R A_+ . \end{aligned} \quad (60)$$

From this definitions the contribution of diagram  $(V_{S3})$  to the form factors can be obtained performing the following changes in that of diagram  $(V_{S1})$ , eq. (52):

- Everywhere in eqs. (52) and (54) replace  $M_i \leftrightarrow M_\alpha^0$  and  $m_{\tilde{t}_a} \leftrightarrow m_{\tilde{b}_a}$ .
- Replace in eq. (52) couplings from (51) by those of (60).

- Include a global minus sign.

## 4.2 Higgs vertex diagrams

Now we consider contributions arising from the exchange of virtual Higgs particles and Goldstone bosons in the Feynman gauge [36], as shown in Fig.3. We follow each vertex expression of the form factors by the value of the coefficient  $N$  and by the arguments of the corresponding 3-point functions.

- Diagram ( $V_{H1}$ ):

$$\begin{aligned}
F_L &= N [m_b^2(C_{12} - C_0) + m_t^2 \cot^2 \beta (C_{11} - C_{12})] \\
F_R &= N m_b^2 [C_{12} - C_0 + \tan^2 \beta (C_{11} - C_{12})] \\
N &= \mp \frac{ig^2}{2} \left( 1 - \frac{\{M_{H^0}^2, M_{h^0}^2\}}{2M_W^2} \right) \frac{\{\cos \alpha, \sin \alpha\}}{\cos \beta} \{\cos(\beta - \alpha), \sin(\beta - \alpha)\} \\
C_* &= C_* (p, p', m_b, M_{H^\pm}, \{M_{H^0}, M_{h^0}\}) .
\end{aligned}$$

- Diagram ( $V_{H2}$ ):

$$\begin{aligned}
F_L &= N \cot \beta [m_t^2(C_{11} - C_{12}) + m_b^2(C_0 - C_{12})] \\
F_R &= N m_b^2 \tan \beta (2C_{12} - C_{11} - C_0) \\
N &= \frac{ig^2}{4} \frac{\{\cos \alpha, \sin \alpha\}}{\cos \beta} \{\sin(\beta - \alpha), \cos(\beta - \alpha)\} \left( \frac{M_{H^\pm}^2}{M_W^2} - \frac{\{M_{H^0}^2, M_{h^0}^2\}}{M_W^2} \right) \\
C_* &= C_* (p, p', m_b, M_W, \{M_{H^0}, M_{h^0}\}) .
\end{aligned}$$

- Diagram ( $V_{H3}$ ):

$$\begin{aligned}
F_L &= N m_t^2 [\cot^2 \beta C_{12} + C_{11} - C_{12} - C_0] \\
F_R &= N [m_b^2 \tan^2 \beta C_{12} + m_t^2 (C_{11} - C_{12} - C_0)] \\
N &= -\frac{ig^2}{2} \frac{\{\sin \alpha, \cos \alpha\}}{\sin \beta} \{\cos(\beta - \alpha), \sin(\beta - \alpha)\} \left( 1 - \frac{\{M_{H^0}^2, M_{h^0}^2\}}{2M_W^2} \right) \\
C_* &= C_* (p, p', m_t, \{M_{H^0}, M_{h^0}\}, M_{H^\pm}) .
\end{aligned}$$

- Diagram ( $V_{H4}$ ):

$$\begin{aligned}
F_L &= N m_t^2 (2C_{12} - C_{11} + C_0) \cot \beta \\
F_R &= N [-m_b^2 C_{12} + m_t^2 (C_{11} - C_{12} - C_0)] \tan \beta \\
N &= \mp \frac{ig^2}{4} \frac{\{\sin \alpha, \cos \alpha\}}{\sin \beta} \{\sin(\beta - \alpha), \cos(\beta - \alpha)\} \left( \frac{M_{H^\pm}^2}{M_W^2} - \frac{\{M_{H^0}^2, M_{h^0}^2\}}{M_W^2} \right) \\
C_* &= C_* (p, p', m_t, \{M_{H^0}, M_{h^0}\}, M_W) .
\end{aligned}$$

- Diagram  $(V_{H5})$ :

$$\begin{aligned}
F_L &= N [m_b^2(C_{12} + C_0) + m_t^2(C_{11} - C_{12})] \\
F_R &= N m_b^2 \tan^2 \beta (C_{11} + C_0) \\
N &= -\frac{ig^2}{4} \left( \frac{M_{H^\pm}^2}{M_W^2} - \frac{M_{A^0}^2}{M_W^2} \right) \\
C_* &= C_*(p, p', m_b, M_W, M_{A^0}) .
\end{aligned}$$

- Diagram  $(V_{H6})$ :

$$\begin{aligned}
F_L &= N m_t^2 \cot^2 \beta (C_{11} + C_0) \\
F_R &= N [m_b^2 C_{12} + m_t^2 (C_{11} - C_{12} + C_0)] \\
N &= -\frac{ig^2}{4} \left( \frac{M_{H^\pm}^2}{M_W^2} - \frac{M_{A^0}^2}{M_W^2} \right) \\
C_* &= C_*(p, p', m_t, M_{A^0}, M_W) .
\end{aligned}$$

- Diagram  $(V_{H7})$ :

$$\begin{aligned}
F_L &= N [(2m_b^2 C_{11} + \tilde{C}_0 + 2(m_t^2 - m_b^2)(C_{11} - C_{12})) \cot^2 \beta + 2m_b^2 (C_{11} + 2C_0)] m_t^2 \\
F_R &= N [(2m_b^2 C_{11} + \tilde{C}_0 + 2(m_t^2 - m_b^2)(C_{11} - C_{12})) \tan^2 \beta + 2m_t^2 (C_{11} + 2C_0)] m_b^2 \\
N &= \pm \frac{ig^2}{4M_W^2} \frac{\sin \alpha \cos \alpha}{\sin \beta \cos \beta} \\
C_* &= C_*(p, p', \{M_{H^0}, M_{h^0}\}, m_t, m_b) .
\end{aligned}$$

- Diagram  $(V_{H8})$ :

$$\begin{aligned}
F_L &= N m_t^2 \cot^2 \beta \tilde{C}_0 \\
F_R &= N m_b^2 \tan^2 \beta \tilde{C}_0 \\
N &= \mp \frac{ig^2}{4M_W^2} \\
C_* &= C_*(p, p', \{M_{A^0}, M_Z\}, m_t, m_b) .
\end{aligned}$$

In the equations above, it is understood that the CP-even mixing angle,  $\alpha$ , is renormalized into  $\alpha_{\text{eff}}$  by the one-loop Higgs mass relations [23].

As for the SUSY and Higgs contributions to the counterterms, they are much simpler since they just involve 2-point functions. Thus we shall present the full electroweak results by adding up the various sparticle and Higgs effects:

### 4.3 Counterterms

- Counterterms  $\delta m_f, \delta Z_L, \delta Z_R$ : For a given down-like fermion  $b$ , being  $t$  its isospin partner, the fermionic scalar selfenergies turn out to be

$$\begin{aligned}
\Sigma_{\{L,R\}}^b(p^2) &= \Sigma_{\{L,R\}}^b(p^2) \Big|_{(C_{b1})+(C_{b2})} \\
&= -ig^2 \left[ \left| A_{\pm ai}^{(t)} \right|^2 B_1(p, M_i, m_{\tilde{t}_a}) + \frac{1}{2} \left| A_{\pm a\alpha}^{(b)} \right|^2 B_1(p, M_\alpha^0, m_{\tilde{b}_a}) \right], \\
m_b \Sigma_S^b(p^2) &= m_b \Sigma_S^b(p^2) \Big|_{(C_{b1})+(C_{b2})} \\
&= ig^2 \left[ M_i \text{Re} \left( A_{+ai}^{(t)*} A_{-ai}^{(t)} \right) B_0(p, M_i, m_{\tilde{t}_a}) \right. \\
&\quad \left. + \frac{1}{2} M_\alpha^0 \text{Re} \left( A_{-a\alpha}^{(b)*} A_{+a\alpha}^{(b)} \right) B_0(p, M_\alpha^0, m_{\tilde{b}_a}) \right], \tag{61}
\end{aligned}$$

in the SUSY case, and

$$\begin{aligned}
\Sigma_{\{L,R\}}^b(p^2) &= \Sigma_{\{L,R\}}^b(p^2) \Big|_{(C_{b3})+(C_{b4})} \\
&= \frac{g^2}{2iM_W^2} \left\{ m_{t,b}^2 \left[ \left\{ \cot^2 \beta, \tan^2 \beta \right\} B_1(p, m_t, M_{H^\pm}) + B_1(p, m_t, M_W) \right] \right. \\
&\quad + \frac{m_b^2}{2 \cos^2 \beta} \left[ \cos^2 \alpha B_1(p, m_b, M_{H^0}) + \sin^2 \alpha B_1(p, m_b, M_{h^0}) \right. \\
&\quad \left. \left. + \sin^2 \beta B_1(p, m_b, M_{A^0}) + \cos^2 \beta B_1(p, m_b, M_Z) \right] \right\}, \\
\Sigma_S^b(p^2) &= \Sigma_S^b(p^2) \Big|_{(C_{b3})+(C_{b4})} \\
&= -\frac{g^2}{2iM_W^2} \left\{ m_t^2 \left[ B_0(p, m_t, M_{H^\pm}) - B_0(p, m_t, M_W) \right] \right. \\
&\quad + \frac{m_b^2}{2 \cos^2 \beta} \left[ \cos^2 \alpha B_0(p, m_b, M_{H^0}) + \sin^2 \alpha B_0(p, m_b, M_{h^0}) \right. \\
&\quad \left. \left. - \sin^2 \beta B_0(p, m_b, M_{A^0}) - \cos^2 \beta B_0(p, m_b, M_Z) \right] \right\}, \tag{62}
\end{aligned}$$

for the higgs contributions. To obtain the corresponding expressions for an up-like fermion simply substitute wherever in (61) and (62) the labels  $b \leftrightarrow t$ . In addition, in eq. (62) replace  $\sin \alpha \leftrightarrow \cos \alpha$  and  $\sin \beta \leftrightarrow \cos \beta$  (which also implies replacing  $\tan \beta \leftrightarrow \cot \beta$ ).

Introducing the above expressions into eqs. (19), (20) one immediately obtains the SUSY contribution to the counterterms  $\delta m_f, \delta Z_{(L,R)}$ .

- Counterterm  $\delta Z_{H^+}$

$$\begin{aligned}
\delta Z_{H^\pm} &= \delta Z_{H^\pm} \Big|_{(C_{H1})+(C_{H2})} = \text{Re} \Sigma'_{H^\pm}(M_{H^\pm}^2) \\
&= -\frac{ig^2 N_C}{M_W^2} \left[ (m_b^2 \tan^2 \beta + m_t^2 \cot^2 \beta) (B_1 + M_{H^\pm}^2 B'_1 + m_b^2 B'_0) \right. \\
&\quad \left. + 2m_b^2 m_t^2 B'_0 \right] (M_{H^\pm}, m_b, m_t) \\
&\quad \frac{ig^2}{2M_W^2} N_C \sum_{ab} |G_{ba}|^2 B'_0(M_{H^\pm}, m_{\tilde{b}_b}, m_{\tilde{t}_a}). \tag{63}
\end{aligned}$$

- Counterterm  $\delta Z_{HW}$

$$\begin{aligned}
\delta Z_{HW} &= \delta Z_{HW}|_{(C_{M1})+(C_{M2})} = \frac{\Sigma_{HW}(M_{H^\pm}^2)}{M_W^2} \\
&= -\frac{ig^2 N_C}{M_W^2} \left[ m_b^2 \tan \beta (B_0 + B_1) + m_t^2 \cot \beta B_1 \right] (M_{H^\pm}, m_b, m_t) \\
&\quad - \frac{ig^2 N_C}{2M_W^2} \sum_{ab} G_{ba} R_{1a}^{(t)} R_{1b}^{(b)*} [2B_1 + B_0] (M_{H^\pm}, m_{\tilde{b}_b}, m_{\tilde{t}_a}),
\end{aligned} \tag{64}$$

and similar expressions for the other generations.

Finally, the computation of  $\Delta_\tau$  on eq.(44) yields similar bulky analytical formulae, which follow after computing diagrams akin to those in Figs.2-6 for the MSSM corrections to  $H^+ \rightarrow \tau^+ \bar{\nu}_\tau$ . We refrain from quoting them explicitly here. The numerical effect, though, will be explicitly given in Section 5.

We are now ready to furnish the corrected width of  $t \rightarrow H^+ b$  in the MSSM. It just follows after computing the interference between the tree-level amplitude and the one-loop amplitude. It is convenient to express the result as a “relative MSSM correction” with respect to the tree-level width both in the  $\alpha$ -scheme and in the  $G_F$ -scheme. In the former we obtain the relative correction

$$\begin{aligned}
\delta_\alpha^{MSSM} &= \frac{\Gamma - \Gamma_\alpha^{(0)}}{\Gamma_\alpha^{(0)}} \\
&= \frac{N_L}{D} [2 \operatorname{Re}(\Lambda_L)] + \frac{N_R}{D} [2 \operatorname{Re}(\Lambda_R)] + \frac{N_{LR}}{D} [2 \operatorname{Re}(\Lambda_L + \Lambda_R)],
\end{aligned} \tag{65}$$

where the corresponding lowest-order width is

$$\Gamma_\alpha^{(0)} = \left( \frac{\alpha}{s_W^2} \right) \frac{D}{16 M_W^2 m_t} \lambda^{1/2}(1, \frac{m_b^2}{m_t^2}, \frac{M_{H^\pm}^2}{m_t^2}), \tag{66}$$

with

$$\begin{aligned}
D &= (m_t^2 + m_b^2 - M_{H^\pm}^2) (m_t^2 \cot^2 \beta + m_b^2 \tan^2 \beta) + 4m_t^2 m_b^2, \\
N_L &= (m_t^2 + m_b^2 - M_{H^\pm}^2) m_b^2 \tan^2 \beta, \\
N_R &= (m_t^2 + m_b^2 - M_{H^\pm}^2) m_t^2 \cot^2 \beta, \\
N_{LR} &= 2m_t^2 m_b^2.
\end{aligned} \tag{67}$$

From eq.(17) it is obvious that the relative MSSM correction in the  $G_F$ -parametrization reads

$$\delta_{G_F}^{MSSM} = \frac{\Gamma - \Gamma_{G_F}^{(0)}}{\Gamma_{G_F}^{(0)}} = \delta_\alpha^{MSSM} - \Delta r^{MSSM}, \tag{68}$$

where the tree-level width in the  $G_F$ -scheme,  $\Gamma_{G_F}^{(0)}$ , is given by eq.(8) and is related to eq.(66) through

$$\Gamma_\alpha^{(0)} = \Gamma_{G_F}^{(0)} (1 - \Delta r^{MSSM}). \tag{69}$$

where  $\Delta r^{MSSM}$  has been evaluated in Ref.[38].

## 5. Numerical Analysis and Discussion

As stated in Section 2, quantum effects should be able to discriminate whether the charged Higgs emerging from the decay  $t \rightarrow H^+ b$  is supersymmetric or not, for the MSSM provides a very definite prediction of the typical size of these effects using the present bounds on sparticle masses. Some work on radiative corrections to the width of  $t \rightarrow H^+ b$  has already appeared in the literature. In particular, the conventional QCD corrections have been evaluated [11] and found to significantly reduce the partial width. The SUSY-QCD corrections are also substantial and have been analyzed, only in part in Refs.[44, 45], and in more detail in Ref.[12]. Nevertheless, the electroweak corrections produced by (R-odd) sparticles have not been considered at all yet. As for the virtual effects mediated by the Higgs bosons, a first treatment is given in Refs.[46] and [47]. However, these references disagree in several parts of the calculation, and moreover they are both incomplete calculations on their own, for they fully ignore the Higgs effects associated to the bottom quark Yukawa coupling, which could be very significant in the large  $\tan \beta$  region. On the other hand, even though the latter kind of Higgs effects have been addressed in the literature in other renormalization schemes based on alternative definitions of  $\tan \beta$  [39, 48], a detailed analysis including the genuine (R-odd) SUSY effects themselves has never been attempted. Thus, if only for completeness, we are providing here not only a dedicated treatment of the genuine supersymmetric contributions mediated by the plethora of sparticles of the MSSM, but also the fully-fledged pay-off of the supersymmetric Higgs effects in our scheme.

The bulk of the high  $\tan \beta$  corrections to the decay rate of  $t \rightarrow H^+ b$  in the MSSM is expected to come from SUSY-QCD, and specifically from the the enhanced Yukawa couplings of the form (2). In fact, it is known [10] that in the presence of non-vanishing sbottom mixing (which we do assume in the present analysis) an important source of SUSY-QCD quantum effects stems from the bottom mass corrections proportional to the mixing parameter  $M_{LR}^b = A_b - \mu \tan \beta$ . In our case these contributions are fed into the counterterm  $\delta m_b/m_b$  on eq.(49)<sup>7</sup>. These corrections, when viewed in terms of diagrams

---

<sup>7</sup>In the alternative framework of Ref.[12], the SUSY-QCD corrections have been computed assuming no mixing in the sbottom mass matrix. Nonetheless, the typical size of the SUSY-QCD corrections does not change as compared to the present approach (in which we do assume a non-diagonal sbottom matrix) the reason being that in the absence of sbottom mixing, i.e.  $M_{LR}^b = 0$ , the contribution to  $\delta m_b/m_b$  is no longer increasing with  $\mu \tan \beta$ , but in contrast the vertex correction does precisely inherits this dependence and compensates for it. The drawback of an scenario based on  $M_{LR}^b = 0$ , however, is that when it is combined with a large value of  $\tan \beta$  it may lead to a value of  $A_b$  which overshoots the natural range expected for this parameter.

of the electroweak eigenstate basis [10], appear as finite contributions generated from squark-gluino loops:

$$\left(\frac{\delta m_b}{m_b}\right)_{\text{SUSY-QCD}} = \frac{2\alpha_s(m_t)}{3\pi} m_{\tilde{g}} \mu \tan \beta I(m_{\tilde{b}_1}^2, m_{\tilde{b}_2}^2, m_{\tilde{g}}^2), \quad (70)$$

with

$$I(m_1^2, m_2^2, m_3^2) = \frac{m_1^2 m_2^2 \ln \frac{m_2^2}{m_1^2} + m_2^2 m_3^2 \ln \frac{m_3^2}{m_2^2} + m_1^2 m_3^2 \ln \frac{m_1^2}{m_3^2}}{(m_1^2 - m_2^2)(m_2^2 - m_3^2)(m_1^2 - m_3^2)}. \quad (71)$$

As for the  $\tan \beta$ -enhanced Yukawa couplings involved in  $\delta m_b/m_b$ , their contribution is smaller than the SUSY-QCD case. Although they have already been included in the calculation of Section 3 in the mass-eigenstate basis, it is illustrative of the origin of the kind of effects to be expected to write down the leading – and finite – corrections emerging in the electroweak-eigenstate basis:

$$\left(\frac{\delta m_b}{m_b}\right)_{\text{SUSY-Yukawa}} = \frac{h_t^2}{16\pi^2} \mu \tan \beta A_t I(m_{\tilde{t}_1}^2, m_{\tilde{t}_2}^2, \mu^2). \quad (72)$$

Notice that, at variance with eq.(70), the Yukawa coupling correction (72) dies away with increasing  $\mu$ . Setting  $h_t \simeq 1$  at high  $\tan \beta$ , and assuming that there is no large hierarchy between the sparticle masses, the ratio between (70) and (72) is given, in good approximation, by  $4 m_{\tilde{g}}/A_t$  times a slowly varying function of the masses of order 1, where the (approximate) proportionality to the gluino mass reflects the very slow decoupling rate of the latter, as we have already mentioned above. In view of the present bounds on the gluino mass, and since  $A_t$  (as well as  $A_b$ ) cannot increase arbitrarily – as also noted above – we expect that the SUSY-QCD effects can be dominant, and even overwhelming for sufficiently heavy gluinos. Now, in contradistinction to the SUSY-QCD case, there are also plenty of additional vertex contributions both from the Higgs sector and from the stop-sbottom/gaugino-higgsino sector where those Yukawa couplings do enter the game. And, in order to trace the origin of the leading contributions in the electroweak-eigenstate basis, a similar though somewhat more involved analysis can be done for vertex functions. Of course, all of these effects are included in our calculation of Section 3 within the framework of the mass-eigenstate basis<sup>8</sup>.

Before presenting our numerical results, we wish to point out that they have been thoroughly checked. Scale independence and cancellation of UV-divergences have been explicitly verified. Most of the analytical and numerical calculations have been doubled. In particular, we have constructed two independent numerical codes and checked that

---

<sup>8</sup>The mass-eigenstate basis is extremely convenient to carry out the numerical analysis, but it does not immediately provide a “physical interpretation” of the results. The electroweak-eigenstate basis, in contrast, is a better bookkeeping device to trace the origin of the most relevant effects, but as a drawback the intricacies of the full analytical calculation can be abhorrent.

the two approaches perfectly agree at different stages. After explicit computation of the various loop diagrams, the results are conveniently cast in terms of the relative correction with respect to the corresponding tree-level width:

$$\delta \equiv \frac{\Gamma_H - \Gamma_H^{(0)}}{\Gamma_H^{(0)}} = \frac{\Gamma(t \rightarrow H^+ b) - \Gamma^{(0)}(t \rightarrow H^+ b)}{\Gamma^{(0)}(t \rightarrow H^+ b)}. \quad (73)$$

In what follows we understand that  $\delta$  defined on eq.(73) is  $\delta_\alpha^{MSSM}$  – Cf. eq.(65) – i.e. we shall always give our corrections with respect to the tree-level width  $\Gamma_\alpha^0$  in the  $\alpha$ -scheme. The corresponding correction with respect to the tree-level width in the  $G_F$ -scheme is simply given by eq.(69), where  $\Delta r^{MSSM}$  was object of a particular study [38] and therefore it can be easily incorporated, if necessary. Notice, however, that  $\Delta r^{MSSM}$  is already tightly bound by the experimental data on  $M_Z = 91.1884 \pm 0.0022 \text{ GeV}$  at LEP [49] and the ratio  $M_W/M_Z$  in  $p\bar{p}$  [50], which lead to  $M_W^{\text{exp}} = 80.26 \pm 0.16 \text{ GeV}$ . Therefore, even without doing the exact theoretical calculation of  $\Delta r$  within the MSSM, we already know from

$$\Delta r = 1 - \frac{\pi\alpha}{\sqrt{2}G_F} \frac{1}{M_W^2 (1 - M_W^2/M_Z^2)}, \quad (74)$$

that  $\Delta r^{MSSM}$  must lie in the experimental interval  $\Delta r^{\text{exp}} \simeq 0.042 \pm 0.010$ . Now, since the corrections computed in Section 3 can typically be about one order of magnitude larger than  $\Delta r$ , the bulk of the quantum effects on  $t \rightarrow H^+ b$  is already comprised in the relative correction (73) in the  $\alpha$ -scheme<sup>9</sup>. Furthermore, in the conditions under study only a small fraction of  $\Delta r^{MSSM}$  is supersymmetric [38], and we should not be dependent on isolating this universal  $\mathcal{O}(g^2)$  part of the total SUSY correction to  $\delta$ . To put in a nutshell: if there is to be any hope to measure supersymmetric quantum effects on the charged Higgs decay of the top quark, they should better come from the potentially large, non-oblique, corrections computed in Section 3. The SUSY effects contained in  $\Delta r^{MSSM}$  [38], instead, will be measured in a much more efficient way from a high precision ( $\delta M_W^{\text{exp}} = \pm 40 \text{ MeV}$ ) determination of  $M_W$  at LEP 200.

Another useful quantity is the branching ratio

$$B_H \equiv BR(t \rightarrow H^+ b) = \frac{\Gamma_H}{\Gamma_W + \Gamma_H + \Gamma_{SUSY}}, \quad (75)$$

where  $\Gamma_W \equiv \Gamma(t \rightarrow W^+ b)$  and  $\Gamma_{SUSY}$  stands for decays of the top quark into SUSY particles. In particular, the potentially important SUSY-QCD mode  $t \rightarrow \tilde{t}_1 \tilde{g}$  is kinematically forbidden in most part of our analysis where we usually assume  $m_{\tilde{g}} = \mathcal{O}(300) \text{ GeV}$ . There

---

<sup>9</sup>For the standard decay  $t \rightarrow W^+ b$ , the situation is quite different since the SM electroweak corrections [51] and the maximal SUSY electroweak corrections [14] in the  $\alpha$ -scheme are much smaller than for the decay  $t \rightarrow H^+ b$ , namely they are of the order of  $\Delta r$ . Therefore, for the standard decay  $t \rightarrow W^+ b$  there is a subtle cancellation between the corrections in the  $\alpha$ -scheme and  $\Delta r$  which results in a much smaller correction in the  $G_F$ -scheme.

may also be the competing electroweak SUSY decays  $t \rightarrow \tilde{t}_1 \chi_\alpha^0$  and  $t \rightarrow \tilde{b}_1 \chi_i^+$  for some  $\alpha = 1, \dots, 4$  and some  $i = 1, 2$ . The latter, however, is also phase space obstructed in most of our explored parameter space, since we typically assume  $m_{\tilde{b}_1} = \mathcal{O}(200) \text{ GeV}$ . The decay  $t \rightarrow \tilde{t}_1 \chi_\alpha^0$ , instead, is almost always open. However, when studying the branching ratio (75) as a function of the squark and gluino masses, we do include the effects from all these supersymmetric channels whenever they are kinematically open. Thus in general  $\Gamma_{SUSY}$  on eq.(75) is given by

$$\Gamma_{SUSY} = \Gamma(t \rightarrow \tilde{t}_1 \tilde{g}) + \sum_{\alpha} \Gamma(t \rightarrow \tilde{t}_1 \chi_\alpha^0) + \sum_i \Gamma(t \rightarrow \tilde{b}_1 \chi_i^+). \quad (76)$$

The various terms contributing to this equation are computed at the tree-level. Recently, the SUSY-QCD corrections to some of these supersymmetric modes have been evaluated and, in contradistinction to our decay  $t \rightarrow H^+ b$ , they were found to be rather small [52]. Similarly, we treat the computation of the partial width of the standard mode  $t \rightarrow W^+ b$  at the tree-level. This is justified since, as shown in Ref.[14, 16, 53], this decay cannot in general develop large supersymmetric radiative corrections, or at least as large as to be comparable to those affecting the charged Higgs mode, for the same value of the input parameters. The reason for it stems from the very different structure of the counterterms for both decays; in particular, the standard decay mode of the top quark does not involve the mass renormalization counterterms for the external fermion lines, and as a consequence the aforementioned large quantum effects associated to the bottom quark self-energy at high  $\tan \beta$  are not possible.

We may now pass on to the numerical analysis of the over-all quantum effects. Figures 7-21 display a clear-cut resumé of our results. In all our numerical evaluations we are imposing the following restriction on the non-SM contributions to the  $\rho$ -parameter [9]:

$$\delta\rho < 0.003. \quad (77)$$

To start with, we concentrate on the case  $\mu < 0$ , which we study in Figs 7-19. (The case  $\mu > 0$  is studied apart in Figs. 20-21 and will be commented later on.) Notice that, for negative  $\mu$ , the leading SUSY-QCD effects on  $\delta$ , eq.(73), are positive. This means that in these circumstances the potentially large strong supersymmetric effects are in frank competition with the conventional QCD corrections, which are also very large and stay always negative (see below). Needless to say, a crucial parameter to be investigated is  $\tan \beta$ . In Fig. 7 we plot the tree-level width,  $\Gamma_0(t \rightarrow H^+ b)$ , and the total partial width,  $\Gamma_{MSSM}(t \rightarrow H^+ b)$  comprising all the MSSM effects, as a function of  $\tan \beta$ . Also shown is the (tree-level) partial width of the standard top quark decay  $t \rightarrow W^+ b$ , which is far less sensitive to quantum corrections [14].

For convenience, we have included in Fig.7 the corrected width that would be obtained in the absence of SUSY effects; we call it  $\Gamma_{\text{QCD+tb}}(t \rightarrow H^+ b)$  since the leading order non-SUSY effects involve only the standard strong corrections mediated by gluons (i.e. the QCD correction) plus all the non-supersymmetric electroweak top-bottom corrections. It is easy to see from eqs.(49) and (65) that the sum of the leading (oblique) top-bottom contributions – contained on the terms  $\delta v^2/v^2$ ,  $\delta Z_{H^+}$  and  $\delta Z_{HW}$  – gives a correction to  $\delta$  which is only relevant (at the level of a few percent) in the low  $\tan\beta$  region. In fact, at high  $\tan\beta$  the relevant form factor containing the oblique top-bottom contribution ( $\Lambda_R$ ) is killed by the vanishingly small coefficient  $N_R/D \lesssim \cot^2\beta$  from eq.(65). The non-oblique effects originated from Higgs-top-bottom interactions turn out to be very small (as will be discussed below). We have numerically checked that for  $\tan\beta \gtrsim 10$ ,  $\Gamma_{\text{QCD+tb}}(t \rightarrow H^+ b)$  is essentially given by just the pure QCD contribution  $\Gamma_{\text{QCD}}(t \rightarrow H^+ b)$ .

To appraise the relative importance of the various types of MSSM effects on  $t \rightarrow H^+ b$ , in Fig.8a we provide plots for the correction  $\delta$ , eq.(73), to the partial width and to the branching ratio, eq.(75), reflecting the individual contributions. Specifically, we show in Fig.8a:

- (i) The individual contribution from supersymmetric Higgs particles and Goldstone bosons (collectively called “Higgs” contribution, and denoted  $\delta_{\text{Higgs}}$ );
- (ii) The individual electroweak supersymmetric contribution (christened  $\delta_{\text{SUSY-EW}}$ ) from sfermions (squarks and sleptons), charginos and neutralinos;
- (iii) The individual strong supersymmetric contribution (denoted by  $\delta_{\text{SUSY-QCD}}$ ) from squarks and gluinos;
- (iv) The individual strong contribution from conventional quarks and gluons (labelled  $\delta_{\text{QCD}}$ ); and
- (v) The total MSSM contribution,  $\delta_{\text{MSSM}}$ , namely, the net sum of all the previous contributions.

In Fig.8b we reflect the effect on the branching ratio from the total MSSM correction and the non-supersymmetric  $QCD + tb$  correction as compared to the tree-level branching ratio. A typical set of inputs (well within standard expectations) has been chosen in Figs. 8a-8b such that the supersymmetric electroweak corrections turn out to reinforce the strong supersymmetric effects. For this set of inputs, the total MSSM correction on the partial width of  $t \rightarrow H^+ b$  is positive. Despite the huge negative effects induced by the gluon loops (QCD), we see that they are overridden by the SUSY loops provided  $\tan\beta$  is large enough; in fact, this takes place for  $\tan\beta \gtrsim 20$ . Beyond this value, the SUSY

output becomes overwhelming; e.g. at the representative value  $\tan\beta = m_t/m_b = 35$  we find  $\delta_{\text{MSSM}} \simeq +27\%$ . And, at  $\tan\beta \simeq 50$ , which is the preferred value claimed by  $SO(10)$  Yukawa coupling unification models [10], the correction is already  $\delta_{\text{MSSM}} \simeq +55\%$ ; in contrast, at that  $\tan\beta$  one would expect, in the absence of SUSY effects, a (QCD) correction of about  $-57\%$ , i.e. virtually of the same size but opposite in sign!. In Fig. 7 we see that, after including the SUSY effects, the partial width of  $t \rightarrow H^+ b$  exactly equals the partial width of the standard decay  $t \rightarrow W^+ b$  at the “ $SO(10)$ ” point  $\tan\beta = 50$ . Now, for the set of parameter values shown in Fig. 7, it turns out that  $\Gamma_{\text{SUSY}}$ , as computed from eq.(76), is small; hence in these conditions the branching ratio of the charged Higgs mode is remarkably high:  $BR(t \rightarrow H^+ b) \simeq 50\%$ . Notice that the corrected width without SUSY effects (i.e. basically the QCD-corrected width) is far smaller; at the pinpoint  $\tan\beta = 50$  it yields a branching ratio of barely 20%. Clearly, if the SUSY quantum effects are there, they could hardly be missed!.

A quick inspection of Fig.8 reveals that the dominant MSSM effects are, by far, the SUSY-QCD ones. However, the supersymmetric electroweak corrections are non-negligible. As a matter of fact,  $\delta_{\text{SUSY-EW}} \gtrsim 20$  for  $\tan\beta \gtrsim 32$ . At this rendezvous point of the two strongly interacting dynamics, the conventional QCD loops are fully cancelled by the SUSY-QCD loops. Therefore, this leads to a funny situation, namely, that the total MSSM correction is given by just the subleading, albeit non-negligible, electroweak supersymmetric contribution:  $\delta_{\text{MSSM}} \simeq \delta_{\text{SUSY-EW}}$ , and, a fortiori, the net effect on the width appears to be opposite in sign to what might naively be “expected” (i.e. the QCD sign). Of course, this is not a general result since it depends on the actual values of the parameters. In the following we wish to explore the various parameter dependences and in particular to assess whether a situation as the one just described is likely to happen in an ample portion of the parameter space.

From Fig. 8a it is apparent that the Higgs effects result in a very tiny contribution in all but a small part of the  $\tan\beta$  segment (12). Specifically,  $\delta_{\text{Higgs}}$  is seen to be of some relevance only in the low  $\tan\beta$  ballpark, where e.g. it can reach  $-15\%$  at  $\tan\beta \simeq 0.5$ . In the very low  $\tan\beta$  segment,  $0.5 \lesssim \tan\beta \lesssim 1$ , it is the dominant MSSM contribution, being larger than QCD which stays at the level of  $-8\%$ , and larger than SUSY-QCD which is below  $+4\%$ , the electroweak correction being negligible ( $\delta_{\text{SUSY-EW}} \simeq -1\%$ ). We have treated in detail the very low  $\tan\beta$  segment by including the one-loop renormalization of the Higgs masses [23]. This is necessary in order to avoid that the lightest CP-even Higgs mass either vanishes at  $\tan\beta = 1$  or becomes lighter than the phenomenological bounds near that value. In passing we have checked that the one-loop shift of the masses and of the CP-even mixing angle,  $\alpha$ , has little impact on the partial width of  $t \rightarrow H^+ b$ .

in the entire range of the parameter  $\tan\beta$ , eq.(12)<sup>10</sup> Although the one-loop Higgs mass relations are permanently “on” in our calculation, they entail at most an additional 5% negative shift of  $\delta$  in the very low  $\tan\beta$  region. It is precisely in this region where the Higgs effects are sizeable, and thus where the renormalization of the CP-even mixing angle may introduce some noticeable change in the neutral Higgs couplings. Quite on the contrary, at high  $\tan\beta$  the corresponding effect on  $\delta$  is found to be of order one per mil and is thus negligibly small. Now, a simple inspection of Figs. 7 and 8b shows that even in the very low  $\tan\beta$  ballpark, where there may be some ten percent effect from the Higgs sector, the rising of the tree-level width is so fast that it becomes very hard to isolate these corrections. We conclude that, despite the rather large number of diagrams involved, the over-all practical yield from the Higgs sector of the MSSM on  $t \rightarrow H^+ b$  is rather meagre in the whole  $\tan\beta$  range (12). This fact was not obvious a priori, due to the presence of enhanced Yukawa couplings (2) in most of the Higgs diagrams. The cancellations involved are reminiscent of the scanty SUSY Higgs effects obtained for the standard top quark decay  $t \rightarrow W^+ b$  [16].

As it is obvious from Figs. 7-8, the conventional QCD corrections [11] are negative and very important in the high  $\tan\beta \gtrsim 10$  region. Therefore, they need to be considered in order to isolate the virtual SUSY signature [11]. The leading behaviour of the standard QCD component in the relative correction (73) can be easily assessed by considering the following asymptotic formula

$$\delta_{QCD} = -\frac{2\alpha_S}{3\pi} \frac{\frac{8\pi^2-15}{12}(m_b^2 \tan^2 \beta + m_t^2 \cot^2 \beta) + 3(4 + \tan^2 \beta - 2\frac{M_{H^+}^2}{m_t^2} \cot^2 \beta)m_b^2 \ln\left(\frac{m_t^2}{m_b^2}\right)}{m_b^2 \tan^2 \beta + m_t^2 \cot^2 \beta}, \quad (78)$$

which we have obtained by expanding up to  $\mathcal{O}(m_b^2/m_t^2, M_{H^+}^2/m_t^2)$  the exact one-loop formula. The big log factor  $\ln(m_t^2/m_b^2)$  originates from the running b-quark mass at the top quark scale. The correction is seen to be always negative. We point out that while we have used the exact formula for the numerical evaluation, the approximate expression given above is accurate to within 10% for  $M_{H^+} \lesssim 120 \text{ GeV}$  and  $1 \lesssim \tan\beta \lesssim 30$ , and most importantly, it immediately conveys the general behaviour to be expected both at low and at high  $\tan\beta$ . In particular, for  $m_b \neq 0$  and large  $\tan\beta$ , the QCD correction becomes very large and saturates at the value

$$\delta_{QCD} = -\frac{2\alpha_S}{\pi} \left( \frac{8\pi^2 - 15}{36} + \ln \frac{m_t^2}{m_b^2} \right) \quad (\tan\beta \gg \sqrt{m_t/m_b} \simeq 6). \quad (79)$$

We remark that for  $m_b = 0$  the dependence on  $\tan\beta$  totally disappears from the correction

---

<sup>10</sup> To perform that check, we have included both the stop and sbottom contributions to the one-loop Higgs mass relations. A set of 7 independent parameters have been used to fully characterize these effects, viz.  $(M_{A^0}, \mu, \tan\beta, m_{\tilde{b}_1}, m_{\tilde{t}_1}, A_b, A_t)$ . We refrain from writing out the cumbersome formulae [23].

(78), so that one would never be able to suspect the large contribution (79) in the high  $\tan\beta$  regime. In spite of this fact, the limit  $m_b = 0$  has been considered for the standard QCD corrections in some places of the literature [54, 55] but, as we have seen, it is untenable unless one concentrates on values of  $\tan\beta$  of order 1, in which case the relevance of the decay is doomed to oblivion. This situation is similar to the one mentioned above concerning the SUSY-QCD corrections in the limit  $m_b = 0$ , which leads to an scenario totally blind to the outstanding supersymmetric quantum effects obtained for  $m_b \neq 0$  at high  $\tan\beta$ ; in fact, most likely the leading quantum effects on  $t \rightarrow H^+ b$  in the MSSM [12]. In spite of the respectable size of the standard QCD effects, they become fast stuck at the saturation value (79), which is independent of  $\tan\beta$ . On the contrary, the SUSY-QCD effects grow endlessly with  $\tan\beta$  and thus rapidly overtake standard QCD.

Worth noticing is the evolution of the corrections (73), (75) as a function of the gluino mass (Cf. Figs.9a-9b). Of course, only the SUSY-QCD component is sensitive to  $m_{\tilde{g}}$ . Although the SUSY-QCD effects have been object of a particular study in Ref.[12], we find it convenient, to ease comparison, to display the corresponding results in the very same conditions in which the electroweak supersymmetric corrections are presented. The steep falls in Fig.9a are associated to the presence of threshold effects occurring at points satisfying  $m_{\tilde{g}} + m_{\tilde{t}_1} \simeq m_t$ . An analogous situation was observed in Ref.[14] for the SUSY corrections to the standard top-quark decay. Away from the threshold points, the behaviour of  $\delta_{SUSY-QCD}$  is smooth and perfectly consistent with perturbation theory. In Fig.9b, where the branching ratio (75) is plotted, the steep falls at the threshold points are no longer present since they are compensated for by the simultaneous opening of the two-body supersymmetric mode  $t \rightarrow \tilde{t}_1 \tilde{g}$ , for  $m_{\tilde{g}} < m_t - m_{\tilde{t}_1}$ . Remarkably, the relevant gluino mass region for the decay  $t \rightarrow H^+ b$  is not the light gluino region, but the heavy one, the reason being that the important self-energy correction mentioned above, eq. (70), involves a gluino mass insertion. As a consequence, virtually for any set of MSSM parameters, there is a well sustained SUSY correction for any gluino mass above a certain value, in our case  $m_{\tilde{g}} \gtrsim 250 - 300 \text{ GeV}$ . The correction raises with the gluino mass up to a long flat maximum before bending –very gently – into the decoupling regime (far beyond  $1 \text{ TeV}$ ). The fact that the decoupling rate of the gluinos appears to be so slow has an obvious phenomenological interest.

Next we consider in detail the sensitivity of our decay on the higgsino-gaugino parameters  $(\mu, M)$  characterizing the chargino-neutralino mass matrices (Cf. Appendix A). We start with the supersymmetric Higgs mixing mass,  $\mu$ . As already stated above, we will largely concentrate on the  $\mu < 0$  case. The individual contributions, together with the total MSSM yield, are given in Figs.10a-10b, for given values of the other parameters. In particular, the value  $\tan\beta = m_t/m_b = 35$  is chosen. This value is used in all our plots

where that parameter must be fixed. We consider it as representative of the low end of the so-called “large  $\tan \beta$  segment”, viz.  $35 \lesssim \tan \beta \lesssim 60$ . Thus  $\tan \beta = m_t/m_b = 35$  behaves as a crossover point beyond which the total quantum effect on  $t \rightarrow H^+ b$  takes off very fast and it thus becomes very substantial, namely, entailing branching ratio corrections above 20%.

From Figs.10a-10b we immediately gather that the SUSY-QCD correction is extremely sensitive to  $\mu$ . In fact,  $\delta_{\text{SUSY-QCD}}$  grows rather fast with  $|\mu|$ . This is already patent at the level of the leading contribution given by eq.(70). In all figures where a definite  $\mu < 0$  is to be chosen, we have taken the moderate value  $\mu = -150 \text{ GeV}$ . In this way, for  $M \simeq |\mu| = 150 \text{ GeV}$ , we guarantee that the lightest chargino mass is above the LEP 1.5 phenomenological bound:  $m_{\chi^\pm} \gtrsim 65 \text{ GeV}$  [56]. Concerning the electroweak contribution, we noted above that the electroweak component (72) actually decreases with  $\mu$ . However, the  $\mu$  dependences in the full  $\delta_{\text{SUSY-EW}}$  are more complicated than in  $\delta_{\text{SUSY-QCD}}$  and cannot just be read off eq. (72). The upshot (see Fig.10a) is that  $\delta_{\text{SUSY-EW}}$  is fairly insensitive to  $\mu$ . The full  $\delta_{\text{MSSM}}$ , therefore, inherites its  $\mu$ -dependence basically from that of the  $\delta_{\text{SUSY-QCD}}$  component. As for the sensitivity of the corrections on the  $SU(2)_L$ -gaugino soft SUSY-breaking parameter,  $M$ , Fig.11 shows that it is virtually non-existent.

There is some slight evolution of the corrections with  $A_b$  (Fig.12a), especially the SUSY-QCD component. We realize that  $\delta_{\text{SUSY-QCD}}$  is not symmetric with respect to the sign of  $A_b$ . Once the sign  $\mu < 0$  is chosen, the correction is larger for negative values of  $A_b$  than for positive values. We have erred on the conservative side by choosing  $A_b = +300 \text{ GeV}$  wherever this parameter is fixed. As far as  $A_t$  is concerned,  $\delta_{\text{SUSY-QCD}}$  can only evolve as a function of that parameter through vertex corrections, which are proportional to  $A_t \cot \beta$ ; however, at large  $\tan \beta$  these are very depressed. The electroweak correction  $\delta_{\text{SUSY-EW}}$ , in contrast, is very much dependent on  $A_t$ . A typical contribution – raising with  $\tan \beta$  – induced by a nonvanishing value of this parameter in the electroweak-eigenstate basis is seen from eq.(72), which is linear in  $A_t$ . The full dependence, however, is not linear and is shown in Fig.12b. We see that  $\delta_{\text{SUSY-EW}}$  and  $\delta_{\text{MSSM}}$  change sign with  $A_t$ . The shaded vertical band in Fig.12b is excluded by our choice of the parameters in Fig.7.

Another very crucial parameter to be investigated is the value of  $m_{\tilde{b}_1}$ . This is because the SUSY-QCD correction hinges a great deal on the value of the sbottom masses, as it is plain from eq.(70). As a matter of fact, a too large a value of  $m_{\tilde{b}_1}$  may upside down the leadership of the SUSY-QCD effects. As a phenomenological lower bound for all the squark masses we take  $m_{\tilde{q}} \geq 65 \text{ GeV}$  [56]. However, as a typical value for all squarks other than the stop we use  $m_{\tilde{q}} \geq 150 - 200 \text{ GeV} (\tilde{q} \neq \tilde{t})$ . From Fig.13a we see that for  $m_{\tilde{b}_1} \lesssim 300 \text{ GeV}$  the SUSY-QCD effects remain dominant, but the latters steadily go

down the larger is  $m_{\tilde{b}_1}$ . The electroweak correction  $\delta_{\text{SUSY-}EW}$ , instead, slowly goes up with  $m_{\tilde{b}_1}$ . At some point beyond  $400\text{ GeV}$  the latter correction catches up the former. However, at the meeting point the total MSSM correction becomes negative and is of order  $\delta_{\text{MSSM}} \simeq -20\%$ . This is still three times smaller (in absolute value) than the ordinary QCD correction, which remains at about  $-60\%$ . Therefore, the SUSY effect should be observable even for rather obese sbottom masses. The corresponding behaviour of the branching ratio is plotted in Fig. 13b.

Needless to say, the evolution of the large SUSY-QCD corrections with the stop masses is basically flat (Fig.14) since the leading effect is independent of  $m_{\tilde{t}_1}$ . Therefore, it is of little help to use the strict lower mass bound  $m_{\tilde{t}_1} \simeq 65\text{ GeV}$  in our calculation, instead of say the more conservative  $m_{\tilde{t}_1} \simeq 100\text{ GeV}$ . However, we cannot go too far with  $m_{\tilde{t}_1}$ , for the electroweak correction is seen to decrease with  $m_{\tilde{t}_1}$ . Indeed, whereas for  $m_{\tilde{t}_1} = 65 - 100\text{ GeV}$  one has  $\delta_{\text{SUSY-}EW} \gtrsim 20\%$ , for  $m_{\tilde{t}_1} \gtrsim 250\text{ GeV}$  one finds  $\delta_{\text{SUSY-}EW} \lesssim 10\%$ .

The incidence from the sleptons and the other squarks is practically irrelevant (Cf. Figs. 15a-15b). They enter the correction through universal  $\mathcal{O}(g^2)$  effects. The only exception are the  $\tau$ -sleptons (“staus”), since they are involved in the process-dependent (non-oblique) contribution (44), where the  $\tau$ -lepton Yukawa coupling is slightly enhanced at large  $\tan\beta$ . For this reason,  $\delta_{\text{SUSY-}EW}$  in Fig.15b is somewhat larger the smaller is the  $\tau$ -sneutrino mass (assumed to be degenerate with the other sneutrinos). In all our calculation we have fixed the common sneutrino mass at  $200\text{ GeV}$ .

We have also tested the variation of our results as a function of the external particle masses, namely the top quark, bottom quark and charged Higgs boson masses within the corresponding narrow intervals. As for the external fermion masses, the corrections themselves are not very sensitive (see Figs.16a and 17a). The most sensitive one on  $m_t$  (respectively on  $m_b$ ) is  $\delta_{\text{SUSY-}EW}$  (resp.  $\delta_{\text{SUSY-}QCD}$ ). The branching ratios, on the other hand, do indeed show a sensitivity (Figs.16b and 17b) but it is mainly due to the variation of the tree-level partial widths as a function of  $m_t$  and  $m_b$ . As for the charged Higgs mass,  $M_{H^+}$ , up to now it was fixed at  $M_{H^+} = 120\text{ GeV}$ . We see in Fig. 18a that there is nothing special in the chosen value for that parameter since the sensitivity is in general low enough, except near the uninteresting boundary of the phase space where the branching ratio (Fig. 18b) becomes, at any rate, very small.

We close our study of the corrections in the  $\mu < 0$  case by displaying  $\delta_\tau$  (see Fig.19), i.e. the SUSY-electroweak and Higgs contributions to  $\delta$  from the process-dependent term  $\Delta_\tau$ , eq.(44), as a function of  $\tan\beta$ . This piece of information is relevant enough. In fact, it should be clear that the quantum corrections displayed in the previous figures are scheme dependent and in particular they rely on our definition of  $\tan\beta$  given on eq.(41). What is *not* scheme dependent, of course, is the predicted value of the width and branching

ratio (Figs. 7 and 8b) after including all the radiative corrections. Now, from Fig.19 it is clear that the process-dependence corrections are not negligible, and so there is a process-dependence in our definition of  $\tan \beta$ . At first sight, the  $\delta_\tau$  effects are not dramatic since they are negligible as compared to  $\delta_{\text{SUSY-QCD}}$ , but since the latter is cancelled by QCD it turns out that  $\delta_\tau$  is of the order (roughly half the size) of the total electroweak correction,  $\delta_{\text{SUSY-EW}}$ . As long as the “physical” value of  $\tan \beta$  turns out to be high, the process  $H^+ \rightarrow \tau^+ \bar{\nu}_\tau$ , is suited enough for a good determination of  $\tan \beta$  after including the corrections displayed in Fig.19.

Finally, the corrections corresponding to the case where  $\mu > 0$  are given in Fig.20a and the branching ratio is shown in Fig.20b. The problem with  $\mu > 0$  is that the large SUSY-QCD corrections have the same (negative) sign as the conventional QCD effects, and as a consequence the total MSSM correction can easily be larger than 100%, the branching ratio becoming negative!. To avoid this disaster, we force the SUSY-QCD correction to be small by choosing a sufficiently large value for the sbottom mass ( $m_{\tilde{b}_1} = 600 \text{ GeV}$ ) and the gluino mass ( $m_{\tilde{g}} = 1000 \text{ GeV}$ ). In Fig.21 we may see the effect on the total partial width. In that case, the physical signature would be to observe that the partial width is smaller than it is predicted after incorporating the QCD corrections. Needless to say, the  $\mu > 0$  scenario is not as appealing as the  $\mu < 0$  one.

In the end, from the explicit numerical analysis, we have confirmed our expectations that the SUSY-QCD contribution is generally dominant, unless the bottom squark is very heavy, irrespective of the mass of the gluino. In particular, by restricting ourselves to the case  $\mu < 0$  (in many respects the preferred sign for the  $\mu$  parameter in the literature), we confirm that for typical values of the parameters the total (standard plus supersymmetric) QCD correction largely cancels out, with a remainder on the SUSY side (Figs. 7-8). In this window of parameter space, therefore, where the net outcome from the higgses is very small, one is left with at least the electroweak supersymmetric contribution,  $\delta_{\text{SUSY-EW}}$ , which can be sizeable enough to be pinned down by experiment even in the unfavourable circumstance that the total strong correction exactly cancels out:  $\delta_{\text{SUSY-QCD}} + \delta_{\text{QCD}} = 0$ . However, in general there is a remainder  $\delta_{\text{SUSY-QCD}} + \delta_{\text{QCD}}$  (of the same sign as the  $\delta_{\text{SUSY-EW}}$ ) which grows very fast with  $\tan \beta$  and that adds up to  $\delta_{\text{SUSY-EW}}$ . In this favourable scenario, the virtual SUSY effects could not be missed. This is true not only because in the relevant window of parameter space the SUSY quantum corrections to the tree-level width are by themselves rather large, but also because they push into the opposite direction than the “expected” (non-SUSY) quantum corrections. As a result, the relative departure between the MSSM prediction and the “expected” prediction effectively “doubles” the size of the effect to be measured, a fact which is definitely welcome from the experimental point of view.

From the experimental point of view, one should expect that, if the decay  $t \rightarrow H^+ b$  is indeed possible at a branching ratio of order 10% or above, a rich event statistics will be collected at the Tevatron and especially at the LHC e.g. by means of the identification methods described in Section 2. Therefore, if in addition it turns out that the dynamics underlying that decay is truly supersymmetric, then the very valuable quantum effects that we have been able to unveil over an ample portion of the MSSM parameter space should eventually become patent and we could not miss them. Basically, our statistics would rely on our experimental ability to recognize the top quark decays originating from standard patterns (angular distribution, energy spectrum, etc.) associated to the usual Drell-Yan production mechanism. Notwithstanding, we wish to point out that it should also be possible to clutch at the supersymmetric virtual corrections through an accurate measurement of the various inclusive top quark and Higgs boson production cross sections. In fact, in Fig. 22 we sketch a few alternative mechanisms which would generate different top quark production patterns heavily hinging on the properties of the interaction  $t H^\pm b$ -vertex. This vertex can be substantially enhanced with respect to the usual SM vertex. While the former could be responsible in part for the decay of the top quark, once it is produced, it might as well be at the root of the production process itself at LHC energies, where the fusion mechanisms may take over from Drell-Yan production [24, 57, 58]. In some of these mechanisms a Higgs boson (charged or neutral) is produced in association, but in some others the Higgs boson enters as a virtual particle. Among the latters, there are final states involving  $t\bar{t}$  or single top production. Now, however different are these production processes, all of them are sensitive to the effective structure of the  $t H^\pm b$ -vertex. Needless to say, similar mechanisms can be depicted involving the neutral Higgs bosons of the MSSM interacting with  $t\bar{t}$  and  $b\bar{b}$  via enhanced Yukawa couplings. While it goes beyond the scope of this paper to compute the SUSY corrections to the production processes themselves, we have at least addressed a detailed analysis of a partial decay width involving one of the presumably relevant production vertices. In this way, a definite prediction is made on the properties of a physical observable, and moreover this should suffice both to exhibit the relevance of the SUSY quantum effects and to demonstrate the necessity to incorporate these corrections in a future, truly comprehensive, analysis of the cross-sections, namely, an analysis where one would include the quantum effects on all the relevant production mechanisms within the framework of the MSSM. For this reason we think that in the future a precise measurement of the various (single and double) top quark production cross-sections should be able to detect or to exclude the  $t b H^\pm$ -vertex as well as the vertices  $q\bar{q} A^0(h^0, H^0)$  involving the neutral Higgs particles of the MSSM and the third generation quarks  $q = t, b$ .

While, on the one hand, the top quark partial widths might be measured at a precision

of 10% at (Di)Tevatron and perhaps better than 10% at LHC [24], on the other hand from the point of view of an *inclusive* model-independent measurement of the *total* top-quark width,  $\Gamma_t$ , the future  $e^+ e^-$  supercollider should be a better suited machine. In an inclusive measurement, all possible non-SM effects would appear on top of the corresponding SM effects already computed in the literature [51]. As shown in Ref.[59], one expects to be able to measure the total top-quark width in  $e^+ e^-$  supercolliders at a level of  $\sim 4\%$  on the basis of a detailed analysis of both the top momentum distribution and the resonance contributions to the forward-backward asymmetry in the  $t\bar{t}$  threshold region. Under the assumption that the SUSY effects on the total top quark width,  $\Gamma_t$ , are purely virtual effects, it follows that a typical 50% SUSY correction to  $t \rightarrow H^+ b$  translates into (approximately) a 20% correction to  $\Gamma_t$ . This effect should, therefore, be perfectly visible.

Thus, the combined information from a future  $e^+ e^-$  supercollider and from present and medium term hadron machines should be extremely useful to pin down the nature of the observed effects. Our general conclusion is clearcut: in view of the potentially large size and large variety of manifestations, quantum corrections on top quark (and Higgs boson) physics may be the clue to “virtual” Supersymmetry.

### **Acknowledgements:**

One of us (JS) is thankful to W. Hollik for useful discussions on the renormalization framework used in our work and its relation to other schemes based on alternative definitions of  $\tan\beta$ . He is also grateful to G.L. Kane and H. Baer for remarks on SUSY phenomenology at the Tevatron, and to F. Matorras and D.P. Roy for helpful conversations on  $\tau$  physics at the LHC. He is also indebted to A. Heinson and to the experimental colleagues in our Institute, especially to M. Bosman, M. Cavalli-Sforza and M. Martínez for useful conversations on the experimental aspects of present and future top quark physics at Tevatron and at the LHC. This work has been partially supported by CICYT under project No. AEN93-0474. The work of DG and JG has also been financed by a grant of the Comissionat per a Universitats i Recerca, Generalitat de Catalunya.

## **Appendix A. Interaction Lagrangian of the MSSM in the mass-eigenstate basis**

In this appendix we single out the specific pieces of the MSSM Interaction Lagrangian involved in the decay rate of the process  $t \rightarrow H^+ b$ . Although the Lagrangian of the MSSM is well-known [8], it is always useful to project explicitly the relevant pieces and to cast them in a most suitable form for specific purposes. As a matter of fact, we have produced a complete set of Feynman rules for the MSSM using an algebraic computer

code based on MATHEMATICA [60]<sup>11</sup>. Here we limit ourselves to quote the Lagrangian interactions affecting the process-dependent parts of our decay and omit the interaction pieces needed to compute the universal counterterm structures, whose SM parts are well-known [36] and the corresponding SUSY contributions are also available in the literature since long time ago [42]. All our interactions are expressed in the mass-eigenstate basis.

Within the context of the MSSM we need two Higgs superfield doublets

$$\hat{H}_1 = \begin{pmatrix} \hat{H}_1^0 \\ \hat{H}_1^- \end{pmatrix} \quad , \quad \hat{H}_2 = \begin{pmatrix} \hat{H}_2^+ \\ \hat{H}_2^0 \end{pmatrix} , \quad (\text{A.1})$$

with weak hypercharges  $Y_{1,2} = \mp 1$ . The (neutral components of the) corresponding scalar Higgs doublets give mass to the down (up) -like quarks through the VEV  $\langle H_1^0 \rangle = v_1$  ( $\langle H_2^0 \rangle = v_2$ ). This is seen from the structure of the MSSM superpotential [8]

$$\hat{W} = \epsilon_{ij} [h_b \hat{H}_1^i \hat{Q}^j \hat{D} + h_t \hat{H}_2^j \hat{Q}^i \hat{U} - \mu \hat{H}_1^i \hat{H}_2^j] , \quad (\text{A.2})$$

where we have singled out only the Yukawa couplings of the third quark generation,  $(t, b)$ , as a generical fermion-sfermion generation of chiral matter superfields  $\hat{Q}$ ,  $\hat{U}$  and  $\hat{D}$ . Their respective scalar (squark) components are:

$$\tilde{Q} = \begin{pmatrix} \tilde{t}'_L \\ \tilde{b}'_L \end{pmatrix} \quad , \quad \tilde{U} = \tilde{t}'_R^* \quad , \quad \tilde{D} = \tilde{b}'_R^* , \quad (\text{A.3})$$

with weak hypercharges  $Y_Q = +1/3$ ,  $Y_U = -4/3$  and  $Y_D = +2/3$ . The primes in (A.3) denote the fact that  $\tilde{q}'_a = \{\tilde{q}'_L, \tilde{q}'_R\}$  are weak-eigenstates, not mass-eigenstates. The ratio

$$\tan \beta = \frac{v_2}{v_1} , \quad (\text{A.4})$$

is a most relevant parameter throughout our analysis.

We briefly describe the necessary SUSY partners formalism entering our computations:

- The fermionic partners of the weak-eigenstate gauge bosons and Higgs bosons, called gauginos,  $\tilde{B}$ ,  $\tilde{W}$ , and higgsinos,  $\tilde{H}$ , respectively. From them we construct the fermionic mass-eigenstates, the so-called charginos and neutralinos, by, first, forming the following three sets of two-component Weyl spinors:

$$\Gamma_i^+ = \{-i\tilde{W}^+, \tilde{H}_2^+\} , \quad \Gamma_i^- = \{-i\tilde{W}^-, \tilde{H}_1^-\} , \quad (\text{A.5})$$

$$\Gamma_\alpha^0 = \{-i\tilde{B}^0, -i\tilde{W}_3^0, \tilde{H}_2^0, \tilde{H}_1^0\} , \quad (\text{A.6})$$

---

<sup>11</sup>We have corrected several mistakes in the subset of rules presented in Ref.[22] involving sparticles and Higgses.

which get mixed up when the neutral Higgs fields acquire nonvanishing VEV's and then diagonalizing the resulting "ino" mass Lagrangian

$$\begin{aligned}\mathcal{L}_M = & - \langle \Gamma^+ | \begin{pmatrix} M & \sqrt{2}M_W c_\beta \\ \sqrt{2}M_W s_\beta & \mu \end{pmatrix} | \Gamma^- \rangle \\ & - \frac{1}{2} \langle \Gamma^0 | \begin{pmatrix} M' & 0 & M_Z s_\beta s_W & -M_Z c_\beta s_W \\ 0 & M & -M_Z s_\beta c_W & M_Z c_\beta c_W \\ M_Z s_\beta s_W & -M_Z s_\beta c_W & 0 & -\mu \\ -M_Z c_\beta s_W & M_Z c_\beta c_W & -\mu & 0 \end{pmatrix} | \Gamma^0 \rangle \\ & + h.c. ,\end{aligned}\quad (\text{A.7})$$

where we remark the presence of the parameter  $\mu$  introduced above and of the soft SUSY-breaking Majorana masses  $M$  and  $M'$ , usually related as  $M'/M = (5/3) \tan^2 \theta_W$ , and where  $c_\beta = \cos \beta$  and  $s_\beta = \sin \beta$ . The corresponding mass-eigenstates<sup>12</sup> (charginos and neutralinos) are the following:

$$\Psi_i^+ = \begin{pmatrix} U_{ij} \Gamma_j^+ \\ V_{ij}^* \bar{\Gamma}_j^- \end{pmatrix} \quad , \quad \Psi_i^- = C \bar{\Psi}_i^{-T} = \begin{pmatrix} V_{ij} \Gamma_j^- \\ U_{ij}^* \bar{\Gamma}_j^+ \end{pmatrix} , \quad (\text{A.8})$$

and

$$\Psi_\alpha^0 = \begin{pmatrix} N_{\alpha\beta} \Gamma_\beta^0 \\ N_{\alpha\beta}^* \bar{\Gamma}_\beta^0 \end{pmatrix} = C \bar{\Psi}_\alpha^{0T} , \quad (\text{A.9})$$

where the matrices  $U, V, N$  are defined through

$$U^* \mathcal{M} V^\dagger = \text{diag}\{M_1, M_2\} \quad , \quad N^* \mathcal{M}^0 N^\dagger = \text{diag}\{M_1^0, \dots, M_4^0\} . \quad (\text{A.10})$$

In practice, we have performed the calculation with real matrices  $U, V$  and  $N$ , so we have been using unphysical mass-eigenstates (corresponding to non-positively definite chargino-neutralino masses). The transition from our unphysical mass-eigenstate basis  $\{\Psi\} \equiv \{\Psi_i^\pm, \Psi_\alpha^0\}$  into the physical mass-eigenstate basis  $\{\chi\} \equiv \{\chi_i^\pm, \chi_\alpha^0\}$  can be done by introducing a set of  $\epsilon$  parameters: thus, for every chargino-neutralino  $\Psi$  associated to a mass eigenvalue  $\tilde{M} = M_i, M_\alpha$ , we set  $\tilde{M} = \epsilon |\tilde{M}|$ , so that the corresponding physical state  $\chi$  is given by

$$\chi = \begin{cases} \Psi & \text{if } \epsilon = 1 \\ \pm \gamma_5 \Psi & \text{if } \epsilon = -1 \end{cases} . \quad (\text{A.11})$$

This procedure is entirely equivalent [61] to use complex diagonalization matrices insuring that physical states are characterized by a set of positively definite mass eigenvalues; and for this reason we have maintained the complex notation in all our formulae in Section 4. Whereas for computations with real sparticles the distinction matters [21], for virtual sparticles the  $\epsilon$  parameters cancel out, and so either basis

---

<sup>12</sup>We use the following notation: first Latin indices  $a, b, \dots = 1, 2$  are reserved for sfermions, middle Latin indices  $i, j, \dots = 1, 2$  for charginos, and first Greek indices  $\alpha, \beta, \dots = 1, \dots, 4$  for neutralinos.

$\{\Psi\}$  or  $\{\chi\}$  can be used without the inclusion of the  $\epsilon$  factors. We have distinguished here between the two bases just to make clear what are the physical chargino-neutralino states, when they are referred to in the text.

Among the gauginos we also have the strongly interacting gluinos,  $\tilde{g}^r$  ( $r = 1, \dots, 8$ ), which are the fermionic partners of the gluons.

- As for the scalar partners of quarks and leptons, they are called squarks,  $\tilde{q}$ , and sleptons,  $\tilde{l}$ , respectively. The squark mass-eigenstates,  $\tilde{q}_a = \{\tilde{q}_1, \tilde{q}_2\}$ , if we neglect intergenerational mixing, are obtained from the weak-eigenstate ones  $\tilde{q}'_a = \{\tilde{q}'_1 \equiv \tilde{q}_L, \tilde{q}'_2 \equiv \tilde{q}_R\}$ , through

$$\begin{aligned} \tilde{q}'_a &= \sum_b R_{ab}^{(q)} \tilde{q}_b, \\ R^{(q)} &= \begin{pmatrix} \cos \theta_q & \sin \theta_q \\ -\sin \theta_q & \cos \theta_q \end{pmatrix} \quad (q = t, b), \end{aligned} \quad (\text{A.12})$$

where again we use the third quark generation,  $(t, b)$ , as a generical fermion-sfermion generation, and the rotation matrices in (A.12) diagonalize the corresponding stop and sbottom mass matrices:

$$\begin{aligned} \mathcal{M}_{\tilde{q}}^2 &= \begin{pmatrix} M_{\tilde{q}_L}^2 + m_q^2 + \cos 2\beta (T_3^{qL} - Q_q s_W^2) M_Z^2 & m_q M_{\tilde{q}_R}^q \\ m_q M_{\tilde{q}_L}^q & M_{\tilde{q}_R}^2 + m_q^2 + Q_q \cos 2\beta s_W^2 M_Z^2 \end{pmatrix}, \\ R^{(q)\dagger} \mathcal{M}_{\tilde{q}}^2 R^{(q)} &= \text{diag}\{m_{\tilde{q}_1^2}, m_{\tilde{q}_2^2}\} \end{aligned} \quad (\text{A.13})$$

with  $T_3^{qL}$  the third component of the weak isospin,  $Q$  the electric charge, and  $M_{\tilde{q}_{L,R}}$  the soft SUSY-breaking squark masses [8] (By  $SU(2)_L$ -gauge invariance, we must have  $M_{\tilde{t}_L} = M_{\tilde{b}_L}$ , whereas  $M_{\tilde{t}_R}, M_{\tilde{b}_R}$  are in general independent parameters.). Furthermore,

$$M_{LR}^t = A_t - \mu \cot \beta, \quad M_{LR}^b = A_b - \mu \tan \beta, \quad (\text{A.14})$$

are, respectively, the stop and the sbottom off-diagonal mixing terms,  $\mu$  the SUSY Higgs mass parameter in the superpotential, and  $A_{t,b}$  the trilinear soft SUSY-breaking parameters. We shall assume that  $|A_{t,b}| < 3M_{\tilde{Q}}$ , where  $M_{\tilde{Q}}$  is the average soft SUSY-breaking mass appearing in the mass matrix (A.13); this relation roughly corresponds to the necessary, though not sufficient, condition for the absence of colour-breaking minima [62].

The charged slepton mass-eigenstates can be obtained in a similar way after straightforward substitutions in the mass matrices, with the only proviso that there is no  $\tilde{\nu}_R$ , so that  $\tilde{\nu}_L$  is itself the sneutrino mass-eigenstate, hence  $R_{ab}^{(\tilde{\nu})} = 0$  unless  $a = b = 1$ .

### fermion-sfermion-(chargino or neutralino)

Here we again single out the third quark generation,  $(t, b)$ , as a generical fermion-sfermion generation. After translating the stop-sbottom-higgsino and stop-sbottom-gaugino interactions into the mass-eigenstate basis, one finds

$$\begin{aligned}\mathcal{L}_{\Psi q\bar{q}} = & g \sum_{a=1,2} \sum_{i=1,2} \left( -\tilde{t}_a^* \bar{\Psi}_i^- \left( A_{+ai}^{(t)} P_L + A_{-ai}^{(t)} P_R \right) b - \tilde{b}_a^* \bar{\Psi}_i^+ \left( A_{+ai}^{(b)} P_L + A_{-ai}^{(b)} P_R \right) t \right) \\ & + \frac{g}{\sqrt{2}} \sum_{a=1,2} \sum_{\alpha=1,\dots,4} \left( -\tilde{t}_a^* \bar{\Psi}_\alpha^0 \left( A_{+aa}^{(t)} P_L + A_{-aa}^{(t)} P_R \right) t + \tilde{b}_a^* \bar{\Psi}_\alpha^0 \left( A_{+aa}^{(b)} P_L + A_{-aa}^{(b)} P_R \right) b \right) \\ & + \text{h.c.}\end{aligned}\quad (\text{A.15})$$

where  $A_{\pm ai}^{(t)}$ ,  $A_{\pm ai}^{(b)}$ ,  $A_{\pm a\alpha}^{(t)}$ ,  $A_{\pm a\alpha}^{(b)}$  are

$$\begin{aligned}A_{+ai}^{(t)} &= R_{1a}^{(t)*} U_{i1}^* - \lambda_t R_{2a}^{(t)*} U_{i2}^*, \\ A_{-ai}^{(t)} &= -\lambda_b R_{1a}^{(t)*} V_{i2}, \\ A_{+aa}^{(t)} &= R_{1a}^{(t)*} (N_{\alpha 2}^* + Y_L \tan \theta_W N_{\alpha 1}^*) + \sqrt{2} \lambda_t R_{2a}^{(t)*} N_{\alpha 3}^*, \\ A_{-aa}^{(t)} &= \sqrt{2} \lambda_t R_{1a}^{(t)*} N_{\alpha 3} - Y_R^t \tan \theta_W R_{2a}^{(t)*} N_{\alpha 1}, \\ A_{+ai}^{(b)} &= R_{1a}^{(b)*} V_{i1}^* - \lambda_b R_{2a}^{(b)*} V_{i2}^*, \\ A_{-ai}^{(b)} &= -\lambda_t R_{1a}^{(b)*} U_{i2}, \\ A_{+aa}^{(b)} &= R_{1a}^{(b)*} (N_{\alpha 2}^* - Y_L \tan \theta_W N_{\alpha 1}^*) - \sqrt{2} \lambda_b R_{2a}^{(b)*} N_{\alpha 4}^*, \\ A_{-aa}^{(b)} &= -\sqrt{2} \lambda_b R_{1a}^{(b)*} N_{\alpha 4} + Y_R^b \tan \theta_W R_{2a}^{(b)*} N_{\alpha 1}.\end{aligned}\quad (\text{A.16})$$

with  $Y_L$  and  $Y_R^{t,b}$  the weak hypercharges of the left-handed  $SU(2)_L$  doublet and right-handed singlet fermion, and  $\lambda_t$  and  $\lambda_b$  are – Cf. eq.(2) – the potentially significant Yukawa couplings normalized to the  $SU(2)_L$  gauge coupling constant  $g$ .

### quark–squark–gluino

$$\mathcal{L}_{\tilde{q}q\bar{q}} = -\frac{g_s}{\sqrt{2}} \tilde{q}_{a,k}^* \bar{\tilde{q}}_r (\lambda^r)_{kl} \left( R_{1a}^{(q)*} P_L - R_{2a}^{(q)*} P_R \right) q_l + \text{h.c.}\quad (\text{A.17})$$

where  $\lambda^r$  are the Gell-Mann matrices. This is just the SUSY-QCD Lagrangian written in the squark mass-eigenstate basis.

### squark–squark–Higgs

$$\mathcal{L}_{H^\pm \tilde{q}\bar{q}} = -\frac{g}{\sqrt{2} M_W} H^- \tilde{b}_a^* G_{ab} \tilde{t}_b + \text{h.c.}\quad (\text{A.18})$$

where we have introduced the coupling matrix

$$G_{ab} = R_{cb}^{(t)} R_{da}^{*(b)} g_{cd}\quad (\text{A.19})$$

$$g_{cd} = \begin{pmatrix} M_W^2 \sin 2\beta - (m_b^2 \tan \beta + m_t^2 \cot \beta) & -m_b (\mu + A_b \tan \beta) \\ -m_t (\mu + A_t \cot \beta) & -m_t m_b (\tan \beta + \cot \beta) \end{pmatrix}.\quad (\text{A.20})$$

### chargino–neutralino–charged Higgs

$$\mathcal{L}_{H^\pm \Psi^\mp \Psi^0} = -g H^- \bar{\Psi}_\alpha^0 \left( \cos \beta Q_{\alpha i}^L P_L + \sin \beta Q_{\alpha i}^R P_R \right) \Psi_i^+ + \text{h.c.}\quad (\text{A.21})$$

with

$$\begin{cases} Q_{\alpha i}^L &= U_{i1}^* N_{\alpha 3}^* + \frac{1}{\sqrt{2}} (N_{\alpha 2}^* + \tan \theta_W N_{\alpha 1}^*) U_{i2}^* \\ Q_{\alpha i}^R &= V_{i1} N_{\alpha 4} - \frac{1}{\sqrt{2}} (N_{\alpha 2} + \tan \theta_W N_{\alpha 1}) V_{i2}. \end{cases} \quad (\text{A.22})$$

### Gauge interactions

In our calculation we only need the sparticle interactions with the  $W^\pm$ :

- quarks

$$\mathcal{L}_{W^\pm qq} = \frac{g}{\sqrt{2}} \bar{t} \gamma^\mu P_L b W_\mu^\pm + \text{h.c.} \quad (\text{A.23})$$

- squarks

$$\mathcal{L}_{W^\pm \tilde{q} \tilde{q}} = i \frac{g}{\sqrt{2}} R_{1a}^{(t)*} R_{1b}^{(b)} W_\mu^+ \tilde{t}_a^* \overset{\leftrightarrow}{\partial}^\mu \tilde{b}_b + \text{h.c.} \quad (\text{A.24})$$

- charginos and neutralinos

$$\mathcal{L}_{W^\pm \Psi^\mp \Psi^0} = g \bar{\Psi}_\alpha^0 \gamma^\mu \left( C_{\alpha i}^L \epsilon_\alpha \epsilon_i P_L + C_{\alpha i}^R P_R \right) \Psi_i^+ W_\mu^- + \text{h.c.} \quad (\text{A.25})$$

$$\begin{cases} C_{\alpha i}^L &= \frac{1}{\sqrt{2}} N_{\alpha 3} U_{i2}^* - N_{\alpha 2} U_{i1}^* \\ C_{\alpha i}^R &= -\frac{1}{\sqrt{2}} N_{\alpha 4}^* V_{i2} - N_{\alpha 2}^* V_{i1}. \end{cases} \quad (\text{A.26})$$

## Appendix B. The Counterterm $\delta Z_{WH}$

We briefly discuss the structure of  $\delta Z_{WH}$  (Cf. Fig.23) both in the unitary gauge and in the Feynman gauge [36]. In order to renormalize the mixed self-energy  $\Sigma^{HW}(k^2)$ , a mixing counterterm must be introduced in the wave function of  $W_\mu^\pm$ :

$$W_\mu^\pm \rightarrow \left( Z_2^W \right)^{1/2} W_\mu^\pm \pm i \frac{\delta Z_{HW}}{M_W} \partial_\mu H^\pm. \quad (\text{B.1})$$

### B.1 Unitary gauge

If one chooses to work in the unitary gauge, then the renormalization is straightforward:

$$L_{UG} = -\frac{1}{4} F_{\mu\nu} F^{\mu\nu} + M_W^2 W_\mu^+ W^{-\mu} \rightarrow L_{ct} = i M_W \delta Z_{HW} (W_\mu^- \partial^\mu H^+ - W_\mu^+ \partial^\mu H^-). \quad (\text{B.2})$$

In this gauge the corresponding renormalized 2-point Green function reads (Fig.23a):

$$\frac{i}{k^2 - M_{H^\pm}^2} \left[ -i \frac{k^\mu}{M_W} \Sigma^{HW} (k^2) + i k^\mu M_W^2 \frac{\delta Z_{HW}}{M_W} \right] \frac{-i \left( g_{\mu\nu} - \frac{k_\mu k_\nu}{M_W^2} \right)}{k^2 - M_W^2}. \quad (\text{B.3})$$

Thus, a renormalized self-energy can be defined as follows:

$$\hat{\Sigma}_{HW}(k^2) = \Sigma_{HW}(k^2) - M_W^2 \delta Z_{HW} \quad (\text{B.4})$$

Now we must impose a renormalization condition on  $\hat{\Sigma}^{HW}(k^2)$ ; and we choose it in a way that the physical Higgs does not mix with the physical  $W^\pm$ :

$$\hat{\Sigma}_{HW}(M_{H^\pm}^2) = 0 \implies \delta Z_{HW} = \frac{\Sigma_{HW}(M_{H^\pm}^2)}{M_W^2}. \quad (\text{B.5})$$

## B.2 Feynman gauge

As we carry out our calculation in the Feynman gauge, we would also like to perform the renormalization of the Higgs sector in that gauge. The lagrangian is sketched as follows [36]:

$$L = L_{Cl} + L_{fix} + L_{gh}. \quad (\text{B.6})$$

We are interested in the charged Gauge-Goldstone sector, whose kinematical term is written as

$$L_{Cl} = L_{UG} + \partial_\mu G^+ \partial^\mu G^- + iM_W (W_\mu^- \partial^\mu G^+ - W_\mu^+ \partial^\mu G^-). \quad (\text{B.7})$$

The complete set of counterterms is formed by those of the Standard Model, (B.1) and <sup>13</sup>

$$G^\pm \rightarrow Z_G^{\frac{1}{2}} G^\pm. \quad (\text{B.8})$$

On substituting the counterterm expressions into the Lagrangian (B.7) one obtains the mixing term that comes from the kinetic lagrangian:

$$L_{Mix} = \delta Z_{HW} \left[ iM_W (W_\mu^- \partial^\mu H^+ - W_\mu^+ \partial^\mu H^-) + (\partial_\mu H^- \partial^\mu G^+ + \partial_\mu H^+ \partial^\mu G^-) \right]. \quad (\text{B.9})$$

In addition to that, there is another mixing term between  $H^+$  and  $G^+$  originating from the mass matrix of the higgs sector [63]. This one loop mixture reads:

$$V^b = \begin{pmatrix} H^{+b} G^{+b} \end{pmatrix} \begin{pmatrix} M_{H^\pm}^{b2} & \frac{t_0^b}{\sqrt{2}v^b} \\ \frac{t_0^b}{\sqrt{2}v^b} & \frac{t_1^b}{\sqrt{2}v^b} \end{pmatrix} \begin{pmatrix} H^{-b} \\ G^{-b} \end{pmatrix}, \quad (\text{B.10})$$

where we have attached a superscript b to bare quantities, and  $t_i$  are the tadpole counterterms

$$\begin{aligned} t_0 &= -\sin(\beta - \alpha) t_{H^0} + \cos(\beta - \alpha) t_{h^0} \\ t_1 &= \sin(\beta - \alpha) t_{h^0} + \cos(\beta - \alpha) t_{H^0}. \end{aligned} \quad (\text{B.11})$$

We are now ready to find an expression for the mixed 2-point Green functions (Figs.23a and b). As the mixing lagrangian between  $H^+$  and  $W^+$  on eq. (B.9) is the same than eq. (B.2), the Green function will have the same expression (B.3) but with the  $W^\pm$  propagator in the Feynman gauge, namely:

$$\frac{i}{k^2 - M_{H^\pm}^2} \left[ -i \frac{k^\mu}{M_W} \Sigma^{HW}(k^2) + ik^\mu M_W^2 \frac{\delta Z_{HW}}{M_W} \right] \frac{-ig_{\mu\nu}}{k^2 - M_W^2}. \quad (\text{B.12})$$

<sup>13</sup>In fact,  $Z_{G^\pm} = 1 + \delta Z_{G^\pm}$  is not an independent parameter but a combination of the other ones,

$$\delta Z_{G^\pm} = \cos^2 \beta \delta Z_{H_1} + \sin^2 \beta \delta Z_{H_2}.$$

Next we impose  $\hat{\Sigma}_{HW}(M_{H^\pm}^2) = 0$  as before, thus leading to the same formal expression for  $\delta Z_{HW}$ . However, as a new ingredient we now have the mixed  $H^+ - G^+$  self-energy:

$$\frac{i}{k^2 - M_{H^\pm}^2} \left( -i\Sigma^{HG}(k^2) + ik^2\delta Z_{HW} - i\frac{t_0}{\sqrt{2}v^b} \right) \frac{i}{k^2 - M_W^2}. \quad (\text{B.13})$$

This allows us to define renormalized self-energies, (B.4) and

$$\hat{\Sigma}^{HG}(k^2) = \Sigma^{HG}(k^2) - k^2\delta Z_{HW} + \frac{t_0}{\sqrt{2}v^b}. \quad (\text{B.14})$$

Notice that the choice  $\hat{\Sigma}_{HW}(M_{H^\pm}^2) = 0$  in the Feynman gauge is also consistent with the requirement of having no mixing among the physical  $H^+$  and  $W^+$  fields. This is so thanks to the following Slavnov-Taylor identity:

$$k^2\hat{\Sigma}_{HW} - M_W^2\hat{\Sigma}_{HG} = 0. \quad (\text{B.15})$$

This identity also ensures that  $\hat{\Sigma}^{HG}$  is finite, and that it vanishes at  $k^2 = M_{H^\pm}^2$ . Thus we have proven that the expression for  $\delta Z_{HW}$  is formally the same in both (unitary and Feynman) gauges, but in the latter one must take into account the additional renormalization of the mixed self-energy  $\Sigma_{HG}$ .

## Appendix C. Vertex functions

In this appendix we briefly collect, for notational convenience, the basic vertex functions frequently referred to in the text. Dimensional regularization is used throughout. The given formulas are exact for arbitrary internal masses and external on-shell momenta. Most of them are an adaptation to the  $g_{\mu\nu} = \{+ - - -\}$  metric of the standard formulae of ref.[64]. The basic one, two and three-point scalar functions are:

$$A_0(m) = \int d^n \tilde{q} \frac{1}{[q^2 - m^2]}, \quad (\text{C.1})$$

$$B_0(p, m_1, m_2) = \int d^n \tilde{q} \frac{1}{[q^2 - m_1^2][(q+p)^2 - m_2^2]}, \quad (\text{C.2})$$

$$C_0(p, k, m_1, m_2, m_3) = \int d^n \tilde{q} \frac{1}{[q^2 - m_1^2][(q+p)^2 - m_2^2][(q+p+k)^2 - m_3^2]}; \quad (\text{C.3})$$

using the integration measure

$$d^n \tilde{q} \equiv \mu^{(4-n)} \frac{d^n q}{(2\pi)^n}. \quad (\text{C.4})$$

The two and three-point tensor functions needed for our calculation are the following

$$[B_\mu, B_{\mu\nu}](p, m_1, m_2) = \int d^n \tilde{q} \frac{[q_\mu, q_\mu q_\nu]}{[q^2 - m_1^2][(q+p)^2 - m_2^2]}, \quad (\text{C.5})$$

$$[\tilde{C}_0, C_\mu, C_{\mu\nu}](p, k, m_1, m_2, m_3) = \int d^n \tilde{q} \frac{[q^2, q_\mu, q_\mu q_\nu]}{[q^2 - m_1^2] [(q + p)^2 - m_2^2] [(q + p + k)^2 - m_3^2]}. \quad (\text{C.6})$$

By Lorentz covariance, they can be decomposed in terms of the above basic scalar functions and the external momenta:

$$\begin{aligned} B_\mu(p, m_1, m_2) &= p_\mu B_1(p, m_1, m_2). \\ B_{\mu\nu}(p, m_1, m_2) &= p_\mu p_\nu B_{21}(p, m_1, m_2) + g_{\mu\nu} B_{22}(p, m_1, m_2). \\ \tilde{C}_0(p, k, m_1, m_2, m_3) &= B_0(k, m_2, m_3) + m_1^2 C_0(p, k, m_1, m_2, m_3). \\ C_{\mu\nu}(p, k, m_1, m_2, m_3) &= p_\mu p_\nu C_{21} + k_\mu k_\nu C_{22} + (p_\mu k_\nu + k_\mu p_\nu) C_{23} + g_{\mu\nu} C_{24}, \end{aligned} \quad (\text{C.7})$$

where we have defined the Lorentz invariant functions:

$$B_1(p, m_1, m_2) = \frac{1}{2p^2} [A_0(m_1) - A_0(m_2) - f_1 B_0(p, m_1, m_2)], \quad (\text{C.8})$$

$$\begin{aligned} B_{21}(p, m_1, m_2) &= \frac{1}{2p^2(n-1)} [(n-2)A_0(m_2) - 2m_1^2 B_0(p, m_1, m_2) \\ &\quad - n f_1 B_1(p, m_1, m_2)], \end{aligned} \quad (\text{C.9})$$

$$B_{22}(p, m_1, m_2) = \frac{1}{2(n-1)} [A_0(m_2) + 2m_1^2 B_0(p, m_1, m_2) + f_1 B_1(p, m_1, m_2)], \quad (\text{C.10})$$

$$\begin{pmatrix} C_{11} \\ C_{12} \end{pmatrix} = Y \begin{pmatrix} B_0(p+k, m_1, m_3) - B_0(k, m_2, m_3) - f_1 C_0 \\ B_0(p, m_1, m_2) - B_0(p+k, m_1, m_3) - f_2 C_0 \end{pmatrix}, \quad (\text{C.11})$$

$$\begin{pmatrix} C_{21} \\ C_{23} \end{pmatrix} = Y \begin{pmatrix} B_1(p+k, m_1, m_3) + B_0(k, m_2, m_3) - f_1 C_{11} - 2C_{24} \\ B_1(p, m_1, m_2) - B_1(p+k, m_1, m_3) - f_2 C_{11} \end{pmatrix}, \quad (\text{C.12})$$

$$\begin{aligned} C_{22} &= \frac{1}{2[p^2 k^2 - (pk)^2]} \{ -pk[B_1(p+k, m_1, m_3) - B_1(k, m_2, m_3) - f_1 C_{12}] \\ &\quad + p^2[-B_1(p+k, m_1, m_3) - f_2 C_{12} - 2C_{24}] \}, \end{aligned} \quad (\text{C.13})$$

$$C_{24} = \frac{1}{2(n-2)} [B_0(k, m_2, m_3) + 2m_1^2 C_0 + f_1 C_{11} + f_2 C_{12}], \quad (\text{C.14})$$

the factors  $f_{1,2}$  and the matrix  $Y$ ,

$$\begin{aligned} f_1 &= p^2 + m_1^2 - m_2^2, \\ f_2 &= k^2 + 2pk + m_2^2 - m_3^2, \\ Y &= \frac{1}{2[p^2 k^2 - (pk)^2]} \begin{pmatrix} k^2 & -pk \\ -pk & p^2 \end{pmatrix}. \end{aligned} \quad (\text{C.15})$$

The UV divergences for  $n \rightarrow 4$  can be parametrized as

$$\begin{aligned} \epsilon &= n - 4, \\ \Delta &= \frac{2}{\epsilon} + \gamma_E - \ln(4\pi), \end{aligned} \quad (\text{C.16})$$

being  $\gamma_E$  the Euler constant. In the end one is left with the evaluation of the scalar one-loop functions:

$$A_0(m) = \left( \frac{-i}{16\pi^2} \right) m^2 (\Delta - 1 + \ln \frac{m^2}{\mu^2}), \quad (\text{C.17})$$

$$\begin{aligned} B_0(p, m_1, m_2) &= \left( \frac{-i}{16\pi^2} \right) \left[ \Delta + \ln \frac{p^2}{\mu^2} - 2 + \ln[(x_1 - 1)(x_2 - 1)] \right. \\ &\quad \left. + x_1 \ln \frac{x_1}{x_1 - 1} + x_2 \ln \frac{x_2}{x_2 - 1} \right], \end{aligned} \quad (\text{C.18})$$

$$C_0(p, k, m_1, m_2, m_3) = \left( \frac{-i}{16\pi^2} \right) \frac{1}{2} \frac{1}{pk + p^2\xi} \Sigma \quad (\text{C.19})$$

with

$$\begin{aligned} x_{1,2} = x_{1,2}(p, m_1, m_2) &= \frac{1}{2} + \frac{m_1^2 - m_2^2}{2p^2} \pm \frac{1}{2p^2} \lambda^{1/2}(p^2, m_1^2, m_2^2), \\ \lambda(x, y, z) &= [x - (\sqrt{y} - \sqrt{z})^2][x - (\sqrt{y} + \sqrt{z})^2], \end{aligned} \quad (\text{C.20})$$

and where  $\Sigma$  is a bookkeeping device for the following alternate sum of twelve (complex) Spence functions:

$$\begin{aligned} \Sigma = Sp \left( \frac{y_1}{y_1 - z_1^i} \right) - Sp \left( \frac{y_1 - 1}{y_1 - z_1^i} \right) + Sp \left( \frac{y_1}{y_1 - z_2^i} \right) - Sp \left( \frac{y_1 - 1}{y_1 - z_2^i} \right) \\ - Sp \left( \frac{y_2}{y_2 - z_1^{ii}} \right) + Sp \left( \frac{y_2 - 1}{y_2 - z_1^{ii}} \right) - Sp \left( \frac{y_2}{y_2 - z_2^{ii}} \right) + Sp \left( \frac{y_2 - 1}{y_2 - z_2^{ii}} \right) \\ Sp \left( \frac{y_3}{y_3 - z_1^{iii}} \right) - Sp \left( \frac{y_3 - 1}{y_3 - z_1^{iii}} \right) + Sp \left( \frac{y_3}{y_3 - z_2^{iii}} \right) - Sp \left( \frac{y_3 - 1}{y_3 - z_2^{iii}} \right). \end{aligned} \quad (\text{C.21})$$

The Spence function is defined as

$$Sp(z) = - \int_0^1 \frac{\ln(1 - zt)}{t} dt, \quad (\text{C.22})$$

and we have set, on one hand:

$$\begin{aligned} z_{1,2}^i &= x_{1,2}(p, m_2, m_1), \\ z_{1,2}^{ii} &= x_{1,2}(p + k, m_3, m_1), \\ z_{1,2}^{iii} &= x_{1,2}(k, m_3, m_2); \end{aligned} \quad (\text{C.23})$$

and on the other:

$$y_1 = y_0 + \xi, \quad y_2 = \frac{y_0}{1 - \xi}, \quad y_3 = -\frac{y_0}{\xi}, \quad y_0 = -\frac{1}{2} \frac{g + h\xi}{pk + p^2\xi}, \quad (\text{C.24})$$

where

$$g = -k^2 + m_2^2 - m_3^2, \quad h = -p^2 - 2pk - m_2^2 + m_1^2, \quad (\text{C.25})$$

and  $\xi$  is a root (always real for external on-shell momenta) of

$$p^2\xi^2 + 2pk\xi + k^2 = 0. \quad (\text{C.26})$$

Derivatives of some 2-point functions are also needed in the calculation of selfenergies, and we use the following notation:

$$\frac{\partial}{\partial p^2} B_*(p, m_1, m_2) \equiv B'_*(p, m_1, m_2). \quad (\text{C.27})$$

We can obtain all the derivatives from the basic  $B'_0$ :

$$\begin{aligned} B'_0(p, m_1, m_2) = & \left( \frac{-i}{16\pi^2} \right) \left\{ \frac{1}{p^2} + \frac{1}{\lambda^{1/2}(p^2, m_1^2, m_2^2)} \right. \\ & \left. \cdot \left[ x_1(x_1 - 1) \ln \left( \frac{x_1 - 1}{x_1} \right) - x_2(x_2 - 1) \ln \left( \frac{x_2 - 1}{x_2} \right) \right] \right\}, \end{aligned} \quad (\text{C.28})$$

which has a threshold for  $|p| = m_1 + m_2$  and a pseudo-threshold for  $|p| = m_1 - m_2$ .

## References

- [1] F. Abe *et al.* (CDF Collab.), *Phys. Rev. Lett.* **74** (1995) 2626; S. Abachi *et al.* (D0 Collab.), *Phys. Rev. Lett.* **74** (1995) 2632.
- [2] G.F. Tartarelli, talk given at the XXXIst Rencontres de Moriond on Electroweak Interactions and Grand Unified Theories, Les Arcs, March 1996, to appear in the Proceedings (eds. Frontières).
- [3] D. Shaile, P.M. Zerwas, *Phys. Rev. D* **45** (1992) 3262.
- [4] W.A. Bardeen, C.T. Hill, M. Lindner, *Phys. Rev. D* **41** (1990) 1647; C.T. Hill, *Phys. Lett. B* **266** (1991) 419; *ibid. B* **345** (1995) 483.
- [5] R.S. Chikuvula, E.H. Simmons, J. Terning, *Phys. Lett. B* **331** (1994) 383.
- [6] H. Georgi, *Weak Interactions and Modern Particle Theory* (The Benjamin/Cummings Publishing Company, 1984).
- [7] R.D. Peccei, X. Zhang, *Nucl. Phys. B* **337** (1990) 269; C. Hill, X. Zhang *Phys. Rev. D* **51** (1995) 3563.
- [8] H. Nilles, *Phys. Rep.* **110** (1984) 1; H. Haber, G. Kane, *Phys. Rep.* **117** (1985) 75; A. Lahanas, D. Nanopoulos, *Phys. Rep.* **145** (1987) 1; See also the exhaustive reprint collection **Supersymmetry** (2 vols.), ed. S. Ferrara (North Holland/World Scientific, Singapore, 1987).

[9] P. Langacker, in: *Tests and status of the Standard Model*, talk given at the 4th International Workshop on Supersymmetry (SUSY 96), Univ. of Maryland, College Park, USA, May 29th-June 1st 1996; J. Ellis, G.L. Fogli, E. Lisi, *Phys. Lett.* **B 333** (1994) 118; P. Chankowski, S. Pokorski, preprint IFT-95/6 [hep-ph/9505308]; W.de Boer, A. Dabelstein, W. Hollik, W. Mösle, U. Schwickerath, preprint IEK-KA.96-07 [hep-ph/9607286].

[10] V. Barger, M.S. Berger, P. Ohmann *Phys. Rev.* **D 47** (1993) 1093; M. Carena, S. Pokorski, C.E.M. Wagner, *Nucl. Phys.* **B 426** (1994) 269; L.J. Hall, R. Rattazzi, U. Sarid, *Phys. Rev.* **D 50** (1994) 7048.

[11] A. Czarnecki, S. Davidson, *Phys. Rev.* **D 48** (1993) 4183; **D 47** (1993) 3063, and references therein.

[12] J. Guasch, R.A. Jiménez, J. Solà, *Phys. Lett.* **B 360** (1995) 47.

[13] J. Solà, *Supersymmetric effects on top quark and Higgs boson decay widths in the MSSM*, talk given at the XXXIst Rencontres de Moriond on Electroweak Interactions and Grand Unified Theories, Les Arcs, March 1996, and talk given at the the 4th International Workshop on Supersymmetry (SUSY 96), Univ. of Maryland, College Park, USA, May 29th-June 1st 1996.

[14] D. Garcia, W. Hollik, R.A. Jiménez, J. Solà, *Nucl. Phys.* **B 427** (1994) 53.

[15] A. Dabelstein, W. Hollik, R.A. Jiménez, C. Jünger, J. Solà, *Nucl. Phys.* **B 456** (1995) 75.

[16] B. Grzadkowski, W. Hollik, *Nucl. Phys.* **B 384** (1992) 101; A. Denner, A.H. Hoang, *Nucl. Phys.* **B 397** (1993) 483.

[17] D. Garcia, R.A. Jiménez, J. Solà, *Phys. Lett.* **B 347** (1995) 321; D. Garcia, J. Solà, *Phys. Lett.* **B 354** (1995) 335 and **B 357** (1995) 349.

[18] M. Boulware, D. Finnell, *Phys. Rev.* **D 44** (1991) 2054; A. Djouadi, G. Girardi, C. Verzegnassi, W. Hollik, F.M. Renard, *Nucl. Phys.* **B 349** (1991) 48; G. Altarelli, R. Barbieri, F. Caravaglios, *Phys. Lett.* **B 314** (1993) 357; *Nucl. Phys.* **B 405** (1993) 3.

[19] J.D. Wells, C. Kolda, G.L. Kane, *Phys. Lett.* **B 338** (1994) 219; J.E. Kim, G.T. Park, *Phys. Rev.* **D 50** (1994) 6686; X. Wang, J.L. Lopez, D.V. Nanopoulos, *Phys. Rev.* **D 52** (1995) 4116 and preprint CERN-TH.7553/95 [hep-ph/9501258]; A.

Dabelstein, W. Hollik, W. Mösl, preprint KA-THEP-5-1995 [hep-ph/9506251];  
 P. Chankowski, S. Pokorski, preprint IFT-96/6 [hep-ph/9603310].

[20] M. Martínez, private communication.

[21] J. Guasch, J. Solà, preprint UAB-FT-389 [hep-ph/9603441] (Z. Phys. C, to appear).

[22] J.F. Gunion, H.E. Haber, G.L. Kane, S. Dawson, *The Higgs Hunters' Guide* (Addison-Wesley, Menlo-Park, 1990).

[23] J. Ellis, G. Ridolfi, F. Zwirner, *Phys. Lett.* **B 262** (1991) 477; A. Brignole, J. Ellis, G. Ridolfi, F. Zwirner, *Phys. Lett.* **B 271** (1991) 123; H.E. Haber, R. Hempfling, *Phys. Rev. Lett.* **66** (1991) 1815; *Phys. Rev.* **D 48** (1993) 4280; H.E. Haber, in: *Perspectives on Higgs Physics*, Advanced Series on Directions in High Energy Physics, Vol.13, ed. by G.L. Kane (World Scientific, Singapore, 1993); P.H. Chankowski, S. Pokorski, J. Rosiek, *Nucl. Phys.* **B 423** (1994) 437; A. Dabelstein *Z. Phys.* **C67** (1995) 495.

[24] C.-P. Yuan, *Top Quark Physics*, preprint-MSUHEP-50228 [hep-ph/9503216].

[25] J. Kim, J.L. Lopez, D.V. Nanopoulos, R. Rangarajan, preprint ACT-05/96 [hep-ph/9605419]; J.M. Yang, C.S. Li, [hep-ph/9603442]; W. Beenakker, R.H. Höpker, [hep-ph/9606290 and 9607345].

[26] G.L. Kane, S. Mrenna, preprint ANL-HEP-PR-96-43 [hep-ph/9605351]; T. Kon, T. Nonaka, *Phys. Rev.* **D 50** (1994) 6005.

[27] F. Abe *et al.* (CDF Collab.), *Phys. Rev. Lett.* **72** (1994) 1977.

[28] F. Matorras, private communication.

[29] Atlas Collab., *Atlas technical proposal for a general-purpose pp experiment at the Large Hadron Collider at CERN*, preprint CERN/LHCC/94-43, December 1994.

[30] J. Conway, talk given at the 4th International Workshop on Supersymmetry, Univ. of Maryland, College Park, USA, May 29th-June 1st 1996.

[31] D.P. Roy, private communication.

[32] S. Raychaudhuri, D.P. Roy, *Phys. Rev.* **D 52** (1995) 1556, and *Phys. Rev.* **D 53** (1996) 4902.

[33] D.A. Ross, J.C. Taylor, *Nucl. Phys.* **B 51** (1973) 25.

- [34] A. Sirlin, *Phys. Rev.* **D 22** (1980) 971; W. Marciano, A. Sirlin, *Phys. Rev.* **D 22** (1980) 2695.
- [35] See e.g. M. Consoli, W. Hollik, G. Burgers, F. Jegerlehner, in: *Z physics at LEP 1*, eds. G. Altarelli, R. Kleiss, C. Verzegnassi, Yellow Report CERN 89-08 (1989).
- [36] M. Böhm, H. Spiesberger, W. Hollik, *Fortschr. Phys.* **34** (1986) 687; W. Hollik, *Fortschr. Phys.* **38** (1990) 165; W. Hollik, in: *Precision Tests of the Standard Electroweak Model*, Advanced Series in Directions in High Energy Physics, ed. by P. Langacker (World Scientific, Singapore, 1995).
- [37] F. Jegerlehner, *Renormalizing the Standard Model*, lectures given at the Theoretical Advanced Study Institute in Elementary Particle Physics, Boulder, Colorado, June 1990 (Boulder TASI 90, pp 476-590); A. Denner, *Fortschr. Phys.* **41** (1993) 307.
- [38] D. Garcia, J. Solà, *Mod. Phys. Lett.* **A 9** (1994) 211; P.H. Chankowski, A. Dabelstein, W. Hollik, W. Mösle, S. Pokorski, J. Rosiek, *Nucl. Phys.* **B 417** (1994) 101.
- [39] P.H. Chankowski, S. Pokorski, J. Rosiek, *Nucl. Phys.* **B 423** (1994) 437; A. Dabelstein, Karlsruhe preprints KA-THEP-5-1994 [hep-ph/9409375] and KA-THEP-4-1995 [hep-ph/9503443] and references therein.
- [40] R.M. Barnett, J.F. Gunion, H.E. Haber, I. Hinchliffe, B. Hubbard, H.J. Trost, preprint SDC-90-00141; R.M. Godbole, D.P. Roy, *Phys. Rev.* **D 43** (1991) 3640; J.F. Gunion, L.H. Orr, *Phys. Rev.* **D 46** (1992) 2052.
- [41] W. Hollik, private conversation; W. Hollik, talk given at the IFAE, Barcelona, February 1996.
- [42] J. Grifols and J. Solà, *Nucl. Phys.* **B 253** (1985) 47; *Phys. Lett.* **B 137** (1984) 257; For a detailed review, see: J. Solà, in: *Phenomenological Aspects of Supersymmetry*, ed. W. Hollik, R. Rückl and J. Wess (Springer -Verlag, Lecture Notes in Physics **405**, 1992).
- [43] S. Bertolini, *Nucl. Phys.* **B 272** (1986) 77.
- [44] H. König, *Phys. Rev.* **D 50** (1994) 3310.
- [45] C.S. Li, J.M. Yang, B.Q. Hu, *Phys. Rev.* **D 48** (1993) 5425.
- [46] A. Méndez, A. Pomarol, *Phys. Lett.* **B 265** (1991) 177.

- [47] C.S. Li, B.Q. Hu, J.M. Yang, *Phys. Rev. D* **47** (1993) 2865.
- [48] A. Yamada, *Phys. Lett. B* **263** (1991) 233; A. Brignole, *Phys. Lett. B* **281** (1992) 284; H.E. Haber, R. Hempfling, *Phys. Rev. D* **48** (1993) 4280; M.A. Diaz, H.E. Haber, *Phys. Rev. D* **45** (1992) 4246; M.A. Diaz, *Phys. Rev. D* **48** (1993) 2152.
- [49] The LEP Collaborations and the LEP Electroweak Working Group, CERN-PPE/95-172.
- [50] J. Alitti et al. (UA2 Collab.), *Phys. Lett. B* **276** (1992) 354; F. Abe et al. (CDF Collab.), *Phys. Rev. D* **43** (1991) 2070; *ibid* FERMILAB-PUB-95/033-E and FERMILAB-PUB-95/035-E (1995).
- [51] M. Jezabek and J.H. Kühn, *Nucl. Phys. B* **314** (1989) 1; *ibid* **B320** (1989) 20; C.S. Li, R.J. Oakes and T.C. Yuan, *Phys. Rev. D* **43** (1991) 3759; G. Eilam, R.R. Mendel, R. Migneron and A. Soni, *Phys. Rev. Lett.* **66** (1991) 3105; A. Denner and T. Sack, *Z. Phys. C* **46** (1990) 653; *Nucl. Phys. B* **358** (1991) 46; B.A. Irwin, B. Magnolis and H.D. Trottier, *Phys. Lett. B* **256** (1991) 533; T.C. Yuan and C.-P. Yuan, *Phys. Rev. D* **44** (1991) 3603.
- [52] A. Djouadi, W. Hollik, C. Jünger, preprint KA-TP-14-96 [hep-ph/9605340]; C.S. Li, R.J. Oakes, J.M. Yang, preprint NUHEP-TH-96-3 [hep-ph/9606385].
- [53] J.M. Yang, C.S. Li, *Phys. Lett. B* **320** (1994) 117.
- [54] C.S. Li, T.C. Yuan, *Phys. Rev. D* **42** (1990) 3088.
- [55] T. Mehen, preprint JHU-TIPAC-96004 [hep-ph/9602410].
- [56] J. Nachtman and P. Rebecchi, talks given at the XXXIst Rencontres de Moriond on Electroweak Interactions and Grand Unified Theories, Les Arcs, March 1996, to appear in the Proceedings (eds. Frontières).
- [57] S. Willenbrock, *Top Quark Physics at Fermilab*, talk presented at the International Symposium on Particle Theory and Phenomenology, Iowa State University, May 1995 [hep-ph/9508212], and talk presented in the XXXIst Rencontres de Moriond on Electroweak Interactions and Grand Unified Theories, Les Arcs, March 1996, to appear in the Proceedings (eds. Frontières); C. Quigg, preprint Fermilab-CONF-95/139-T [hep-ph/9507257].
- [58] A.P. Heinson, *Electroweak Top Quark Production at the Fermilab Tevatron*, Talk given at the Workshop on Physics of the Top Quark, Ames, Iowa, May 1995; A.P. Heinson, A.S. Belyaev, E.E. Boos, preprint UCR/95-17 [hep-ph/9509274].

- [59] K. Fujii, T. Matsui, *Phys. Rev.* **50** (1994) 4341.
- [60] S. Wolfram, *Mathematica- A System for doing Mathematics by Computer*, Addison-Wesley, Redwood City, CA, 1991).
- [61] J.F. Gunion, H. Haber, *Nucl. Phys.* **B 272** (1986) 1.
- [62] J.M. Frère, D.R.T. Jones and S. Raby, *Nucl. Phys.* **B 222** (1983) 11; M. Claudson, L. Hall and I. Hinchliffe, *Nucl. Phys.* **B 228** (1983) 501; J.F. Gunion, H.E. Haber and M. Sher, *Nucl. Phys.* **B 306** (1988) 1.
- [63] A. Yamada *Z. Phys.* **C 61** (1994) 247.
- [64] G. 't Hooft, M. Veltman, *Nucl. Phys.* **B 153** (1979) 365; G. Passarino, M. Veltman, *Nucl. Phys.* **B 160** (1979) 151; A. Axelrod, *Nucl. Phys.* **B 209** (1982) 349.

## Figure Captions

- **Fig.1** The lowest-order Feynman diagram for the charged Higgs decay of the top quark.
- **Fig.2** Feynman diagrams, up to one-loop order, for the electroweak SUSY vertex corrections to the decay process  $t \rightarrow H^+ b$ . Each one-loop diagram is summed over all possible values of the mass-eigenstate charginos ( $\Psi_i^\pm$ ;  $i = 1, 2$ ), neutralinos ( $\Psi_\alpha^0$ ;  $\alpha = 1, \dots, 4$ ), stop and sbottom squarks ( $\tilde{b}_a, \tilde{t}_b$ ;  $a, b = 1, 2$ ).
- **Fig.3** Feynman diagrams, up to one-loop order, for the Higgs and Goldstone boson vertex corrections to the decay process  $t \rightarrow H^+ b$ .
- **Fig.4** Electroweak self-energy corrections to the top and bottom quark external lines from the various supersymmetric particles, Higgs and Goldstone bosons.
- **Fig.5** Corrections to the charged Higgs self-energy from the various supersymmetric particles and matter fermions. Only the third quark-squark generation is illustrated.
- **Fig.6** Corrections to the mixed  $W^+ - H^+$  self-energy from the various supersymmetric particles and matter fermions. Only the third quark-squark generation is illustrated.

- **Fig.7** The total partial width,  $\Gamma_{MSSM}(t \rightarrow H^+ b)$ , including all MSSM effects, versus  $\tan \beta$ , as compared to the tree-level width and the non-SUSY (QCD + tb-corrected) width. Also plotted is the partial width of the standard top quark decay  $t \rightarrow W^+ b$ . The masses of the top and bottom quarks are  $m_t = 175 \text{ GeV}$  and  $m_b = 5 \text{ GeV}$ , respectively, and the rest of the inputs are explicitly exhibited. Unless explicitly stated otherwise, the inputs staying at fixed values in the remaining figures are common to the values stated here.
- **Fig.8** (a) The relative correction  $\delta$ , eq.(73), as a function of  $\tan \beta$ . Shown are the individual Higgs, SUSY-EW, SUSY-QCD, conventional QCD and total contributions. (b) The branching ratio (75), as a function of  $\tan \beta$ , for the same contributions as in Fig.7.
- **Fig.9** (a) The relative corrections  $\delta$ , eq.(73), as a function of the gluino mass,  $m_{\tilde{g}}$ , for the Higgs, SUSY-EW, SUSY-QCD, conventional QCD and total contributions; (b) As in (a), but for the respective branching ratios (75). The value  $\tan \beta = 35$  is also used for the rest of figures where  $\tan \beta$  needs to be fixed.
- **Fig.10** (a) The relative corrections  $\delta$ , eq.(73), as a function of the supersymmetric Higgs mixing parameter,  $\mu$ , for the Higgs, SUSY-EW, SUSY-QCD, conventional QCD and total contributions; (b) As in (a), but for the respective branching ratios (75). From the choice of the  $SU(2)_L$ -gaugino soft SUSY-breaking mass  $M$  as in Fig.7,  $\mu < 0$  is fixed in a range where the chargino masses are above  $65 \text{ GeV}$ .
- **Fig.11** Dependence of  $\delta$  on the  $SU(2)_L$ -gaugino soft SUSY-breaking mass,  $M$ , assuming that the  $U(1)_Y$  gaugino mass,  $M'$ , is related to  $M$  through  $M'/M = \frac{5}{3} \tan^2 \theta_W$ . The same individual and total contributions as in Fig.8a are shown.
- **Fig.12** (a) The relative corrections  $\delta$ , as a function of the trilinear soft SUSY-breaking parameter  $A_b$  in the bottom sector; (b) As in (a), but for the trilinear soft SUSY-breaking parameter  $A_t$  in the top sector. Shown are the same individual and total contributions as in Fig.8a.
- **Fig.13** (a) The relative corrections  $\delta$ , as a function of the lightest sbottom mass,  $m_{\tilde{b}_1}$ , for the Higgs, SUSY-EW, SUSY-QCD, conventional QCD and total contributions; (b) As in (a), but for the respective branching ratios (75).
- **Fig.14** The relative corrections  $\delta$ , as a function of the lightest stop mass,  $m_{\tilde{t}_1}$ , for the Higgs, SUSY-EW, SUSY-QCD, conventional QCD and total contributions.

- **Fig.15** (a) The relative corrections  $\delta$ , as a function of the up-squark masses  $m_{\tilde{u}} \equiv m_{\tilde{u}_1} = m_{\tilde{u}_2}$ . The c-squarks are assumed to be degenerate with the up-squarks; (b)  $\delta$  as a function of the sneutrino masses, assumed to be degenerate.
- **Fig.16** (a) The relative corrections  $\delta$ , as a function of the top quark mass within about  $2\sigma$  of the present experimental range at the Tevatron. (b) As in (a), but for the respective branching ratios (75).
- **Fig.17** (a) The relative correction  $\delta$ , eq.(73), as a function of the bottom quark mass. (b) As in (a), but for the respective branching ratios (75).
- **Fig.18** (a) The relative corrections  $\delta$ , as a function of the charged Higgs mass; (b) As in (a), but for the respective branching ratios (75).
- **Fig.19** The SUSY-EW and Higgs contributions to  $\delta$ , eq.(73), from the process-dependent term  $\Delta_\tau$ , eq.(44), as a function of  $\tan\beta$ .
- **Fig.20** (a) The relative corrections  $\delta$ , eq.(73), as a function of the sbottom quark mass, for positive  $\mu$  and given values of the other parameters; (b) As in (a), but for the respective branching ratios (75).
- **Fig.21** The total partial width,  $\Gamma(t \rightarrow H^+ b)$ , including all MSSM effects, versus  $\tan\beta$ , for the same inputs as in Fig.20, as compared to the tree-level width and the non-SUSY (QCD + tb-corrected) width. A large value of  $m_{\tilde{b}_1}$  is needed to damp down the total correction below 100%. Also plotted is the partial width of the standard top quark decay  $t \rightarrow W^+ b$ .
- **Fig.22** Typical fusion diagrams for top and charged Higgs production in hadron colliders.
- **Fig.23** The generic mixed blobs  $W^+ - H^+$  and  $G^+ - H^+$  at any order of perturbation theory.

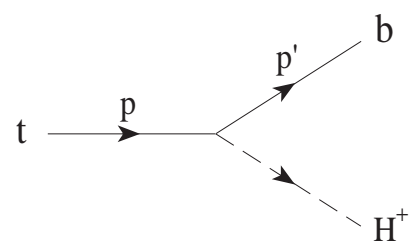
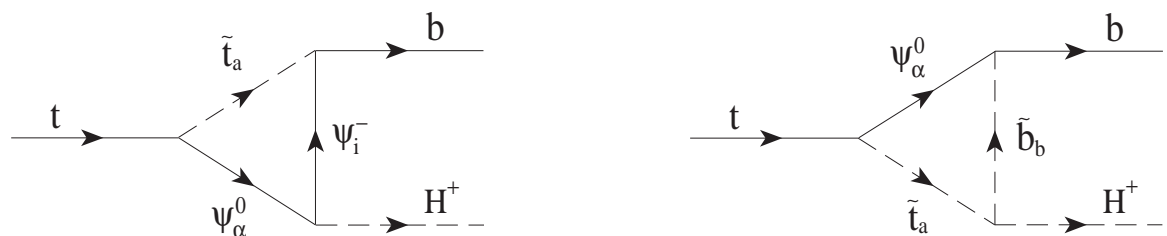
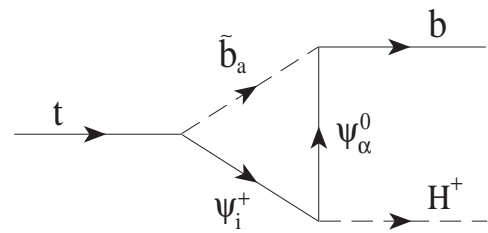


Fig.1



$(V_{S1})$

$(V_{S2})$



$(V_{S3})$

Fig.2

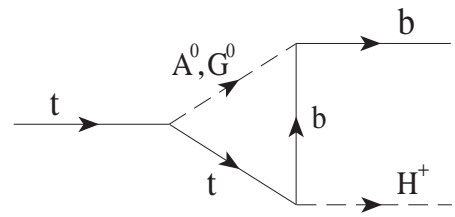
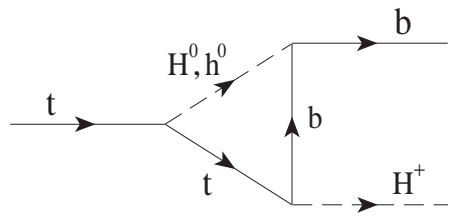
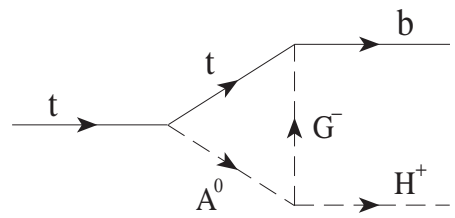
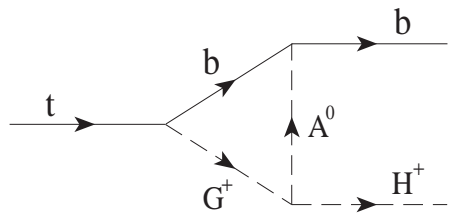
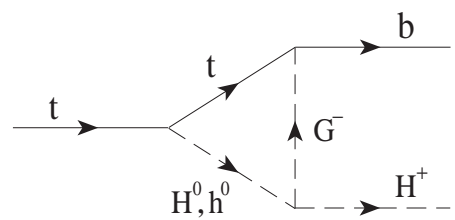
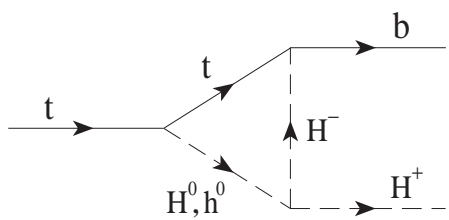
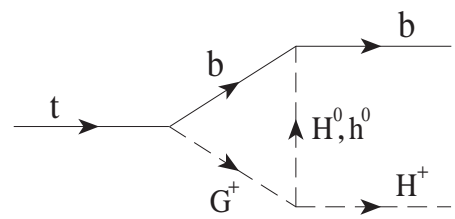
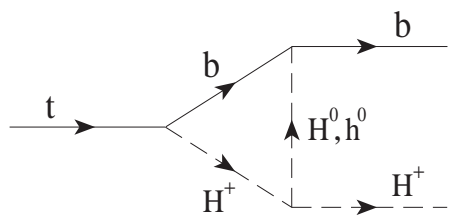


Fig.3

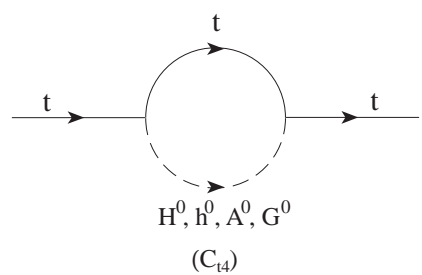
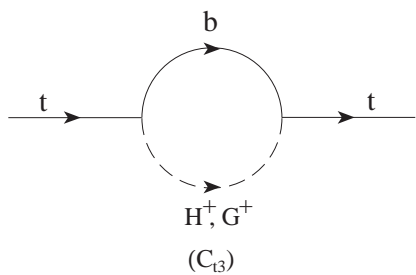
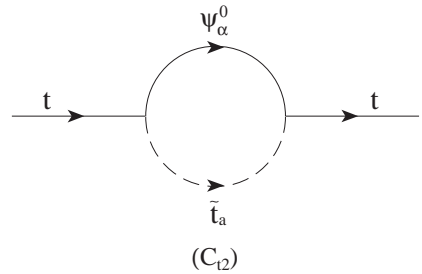
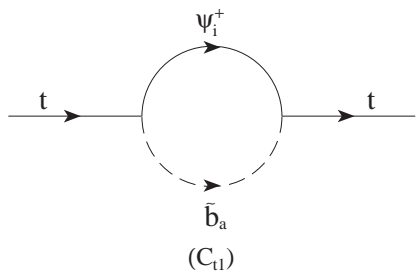
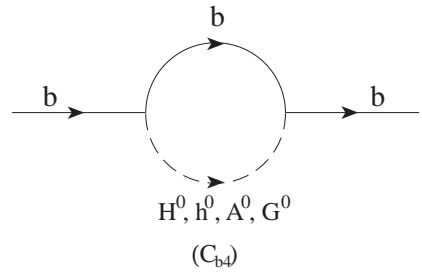
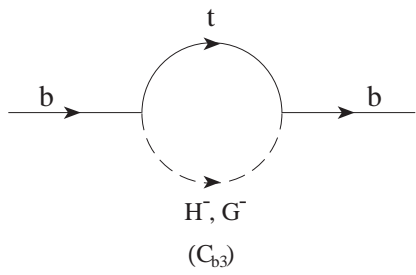
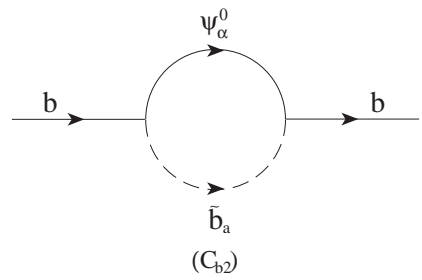
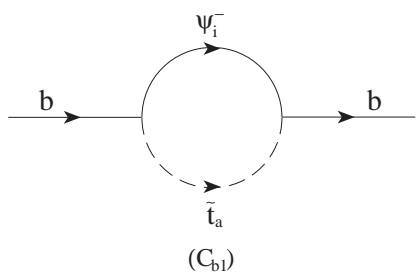


Fig.4

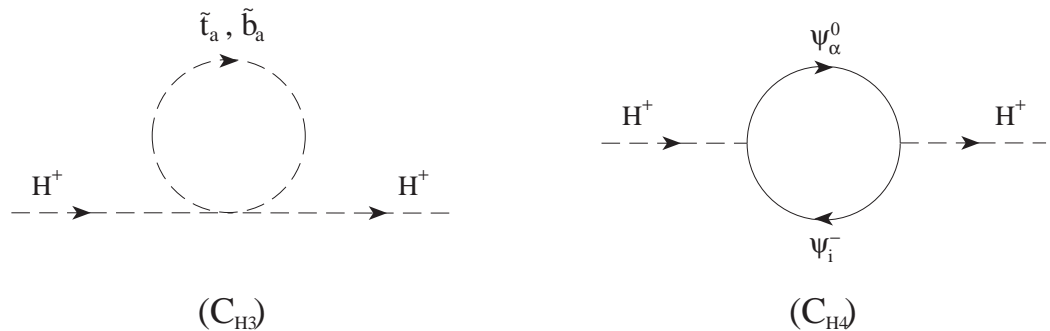
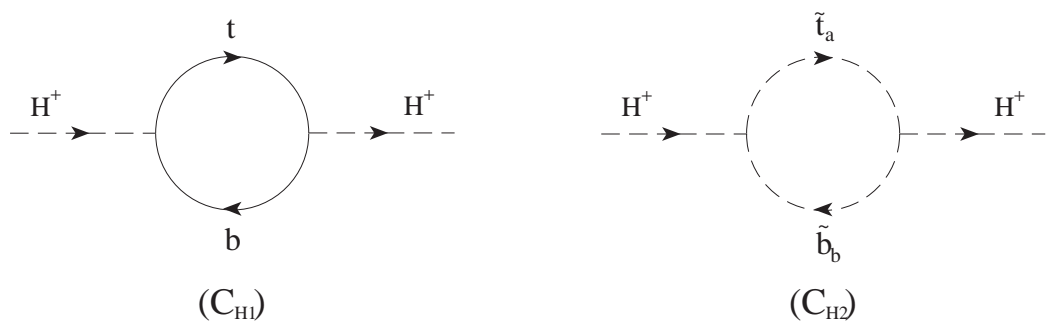


Fig.5

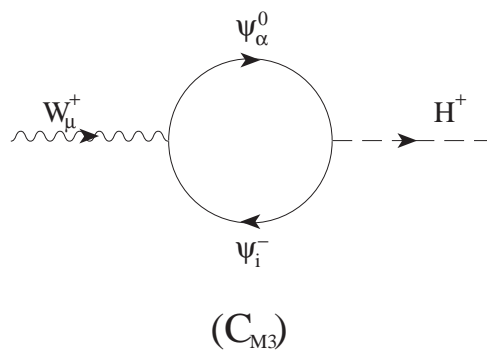
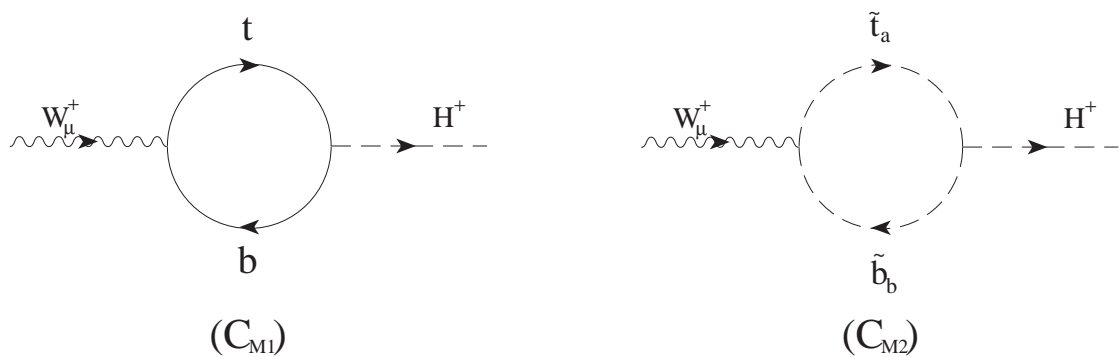


Fig.6

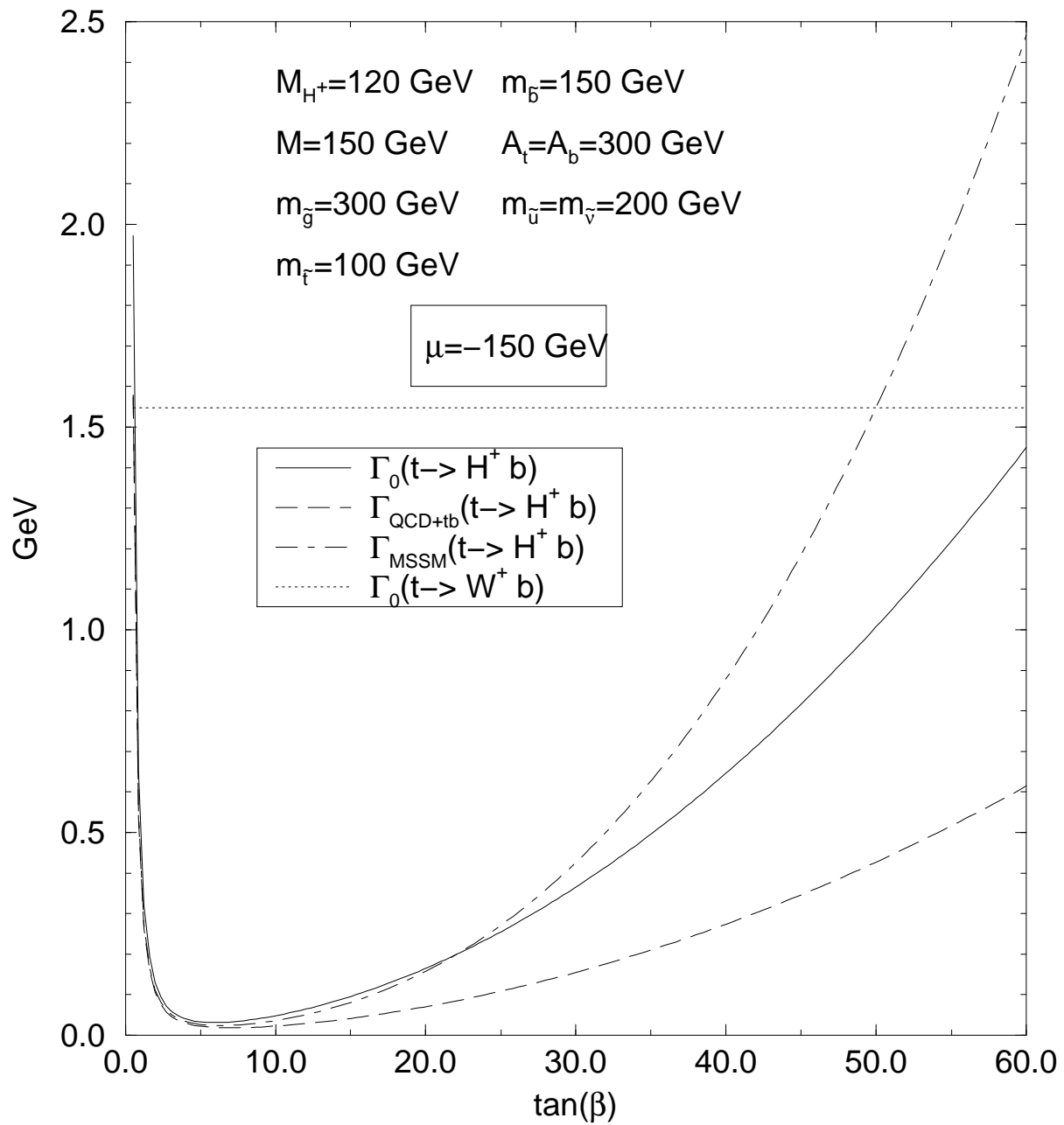


Fig.7

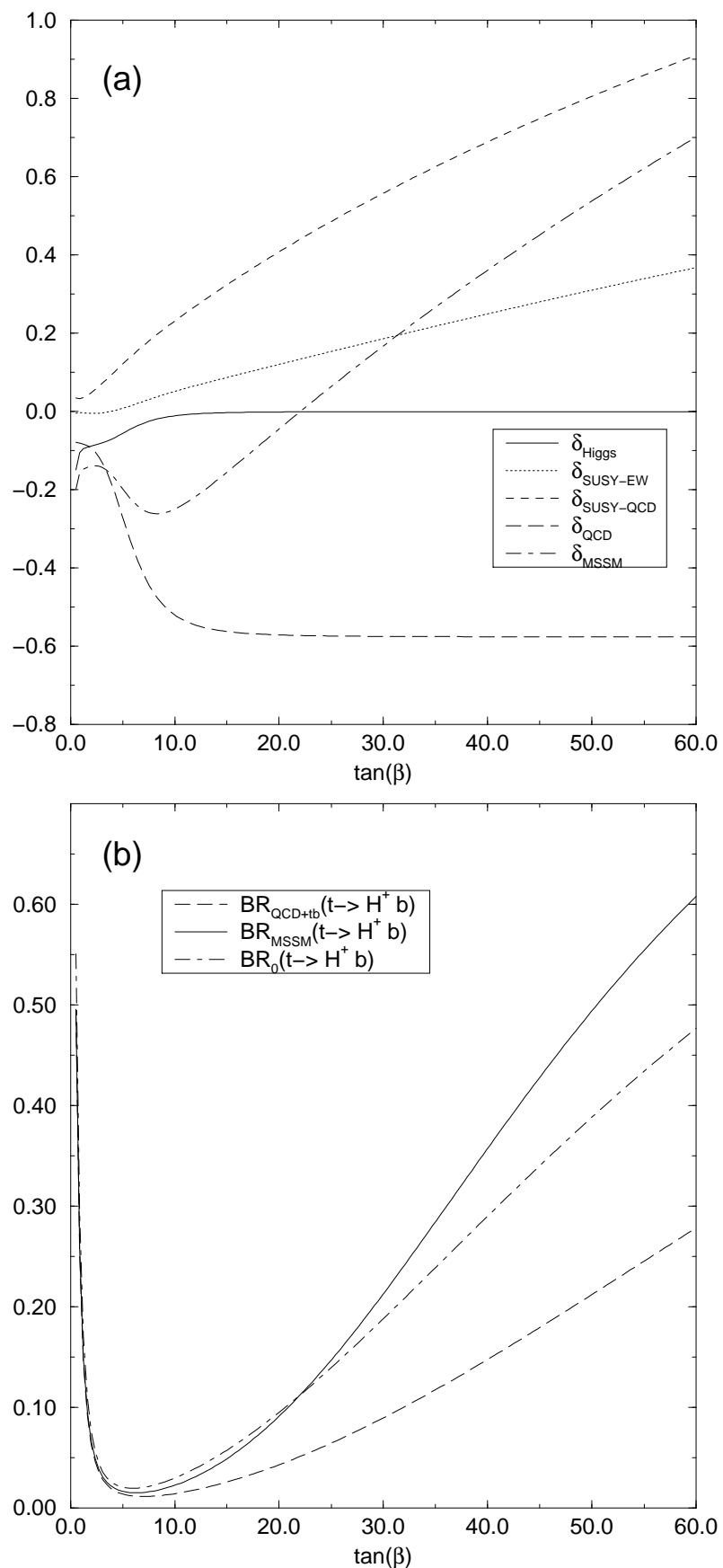


Fig.8

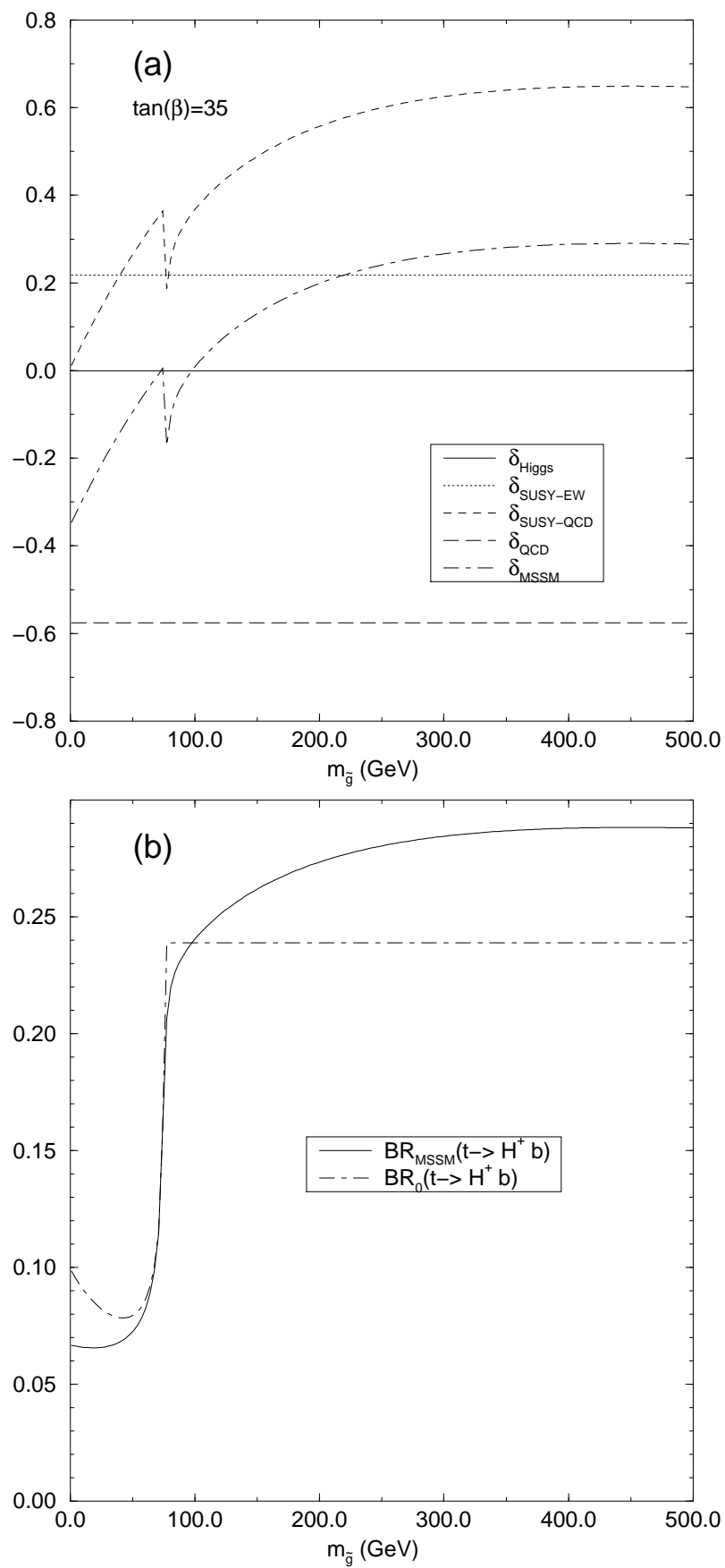


Fig.9

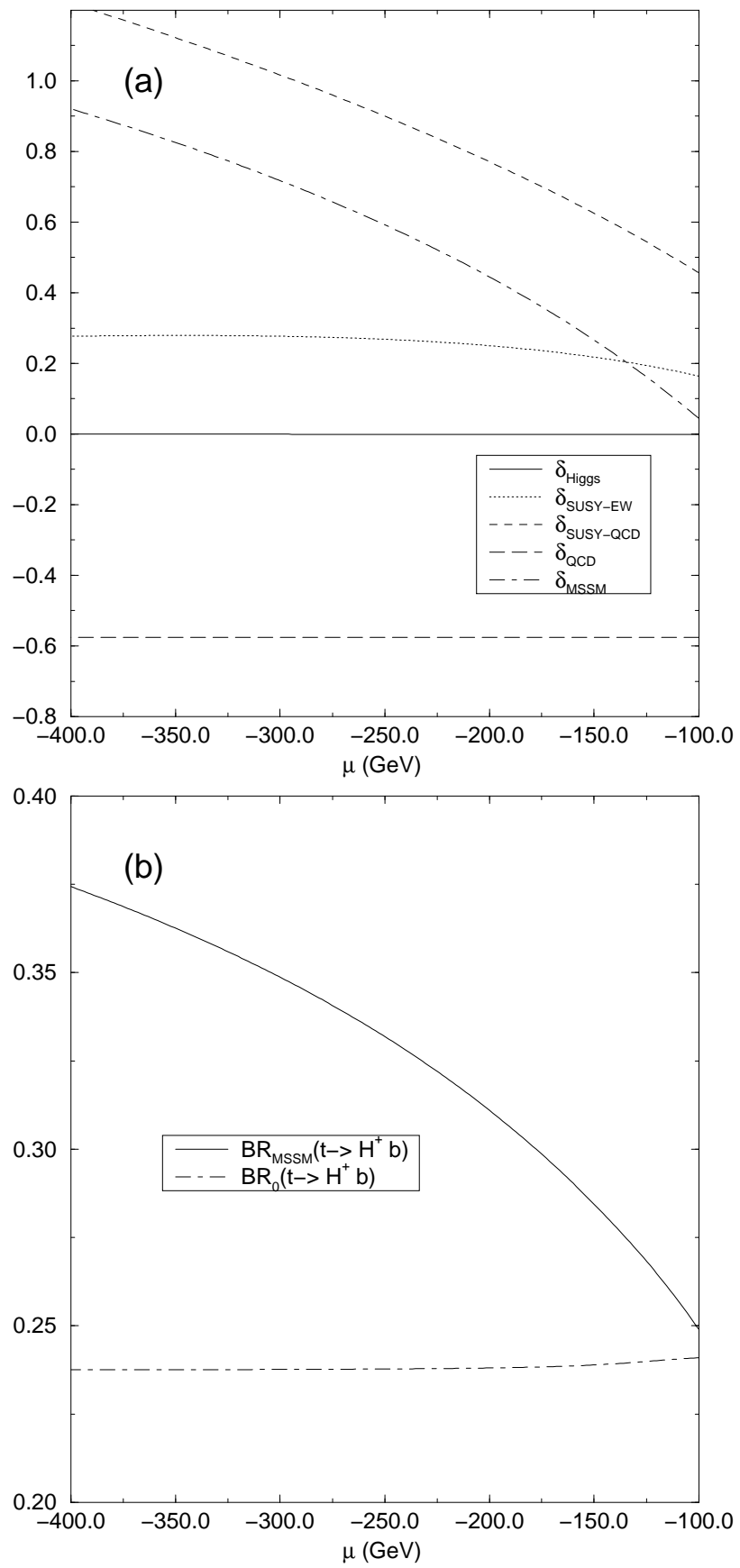


Fig.10

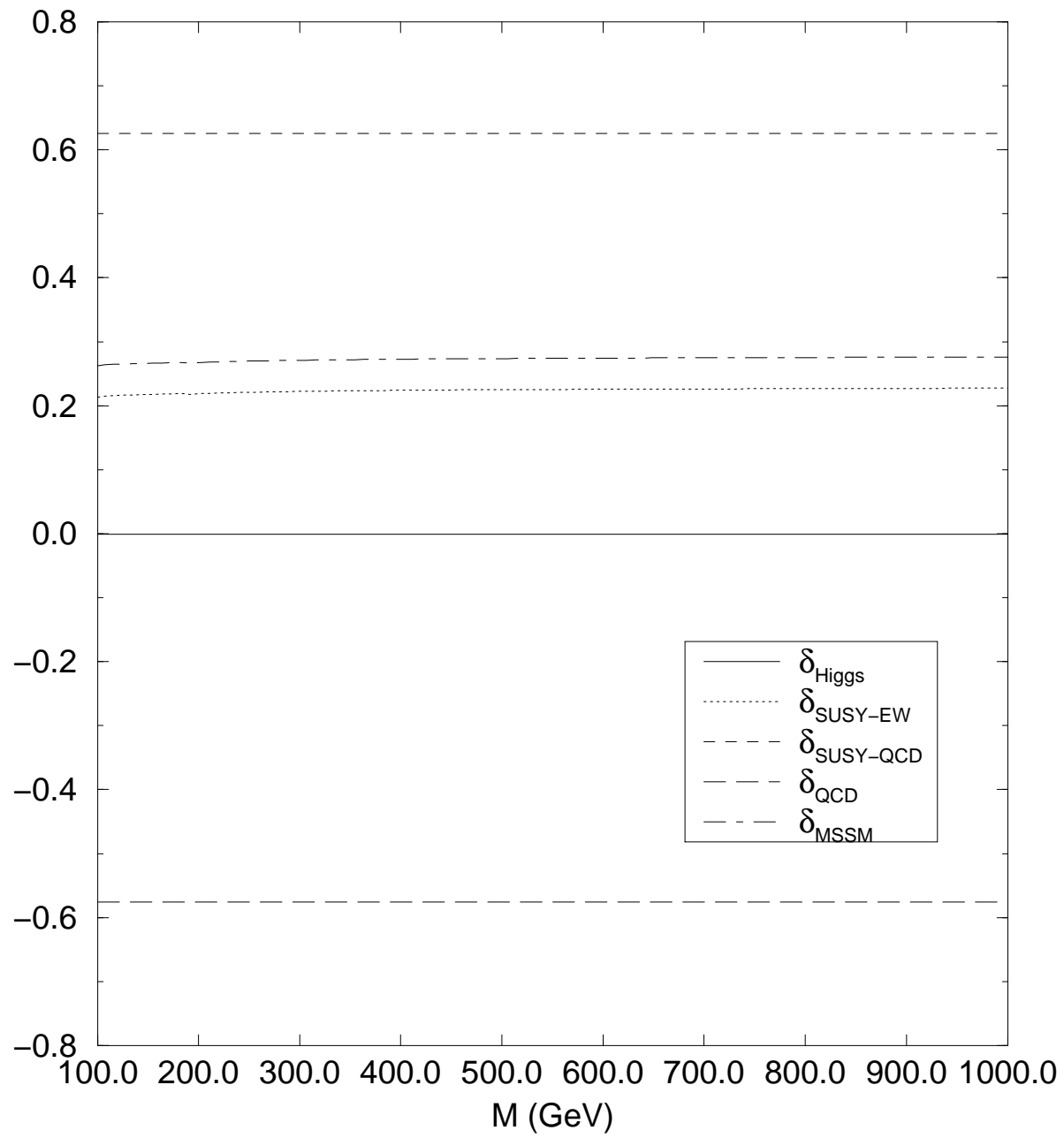


Fig.11

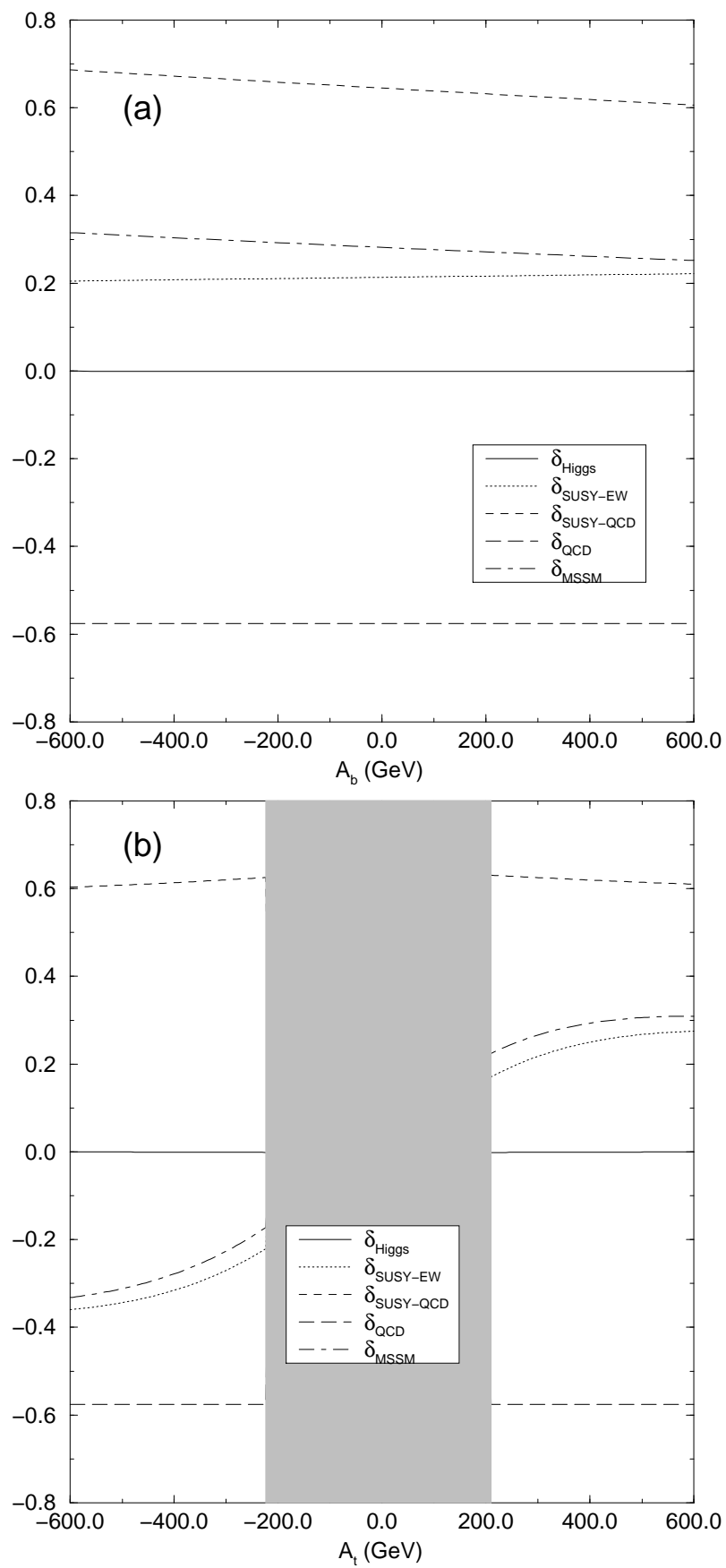


Fig.12

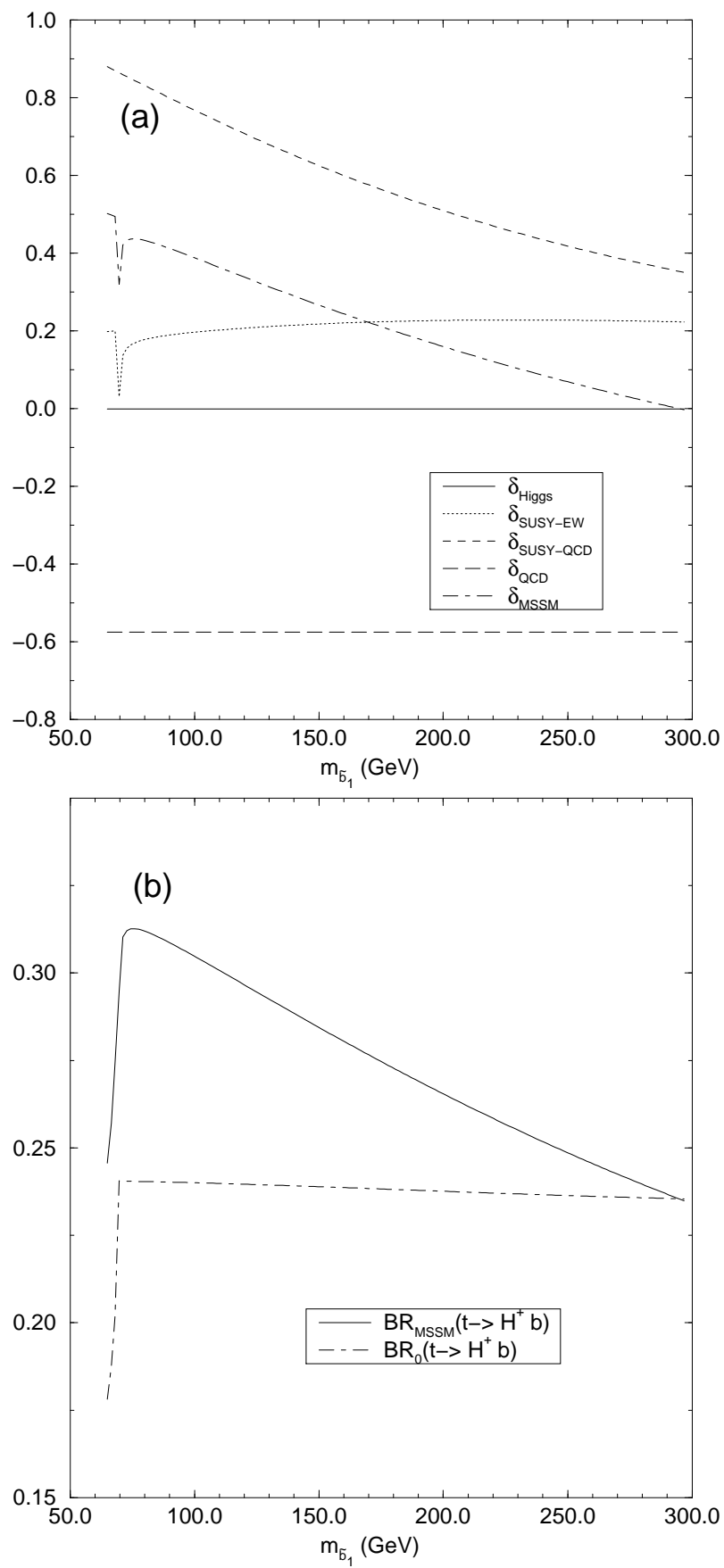


Fig.13

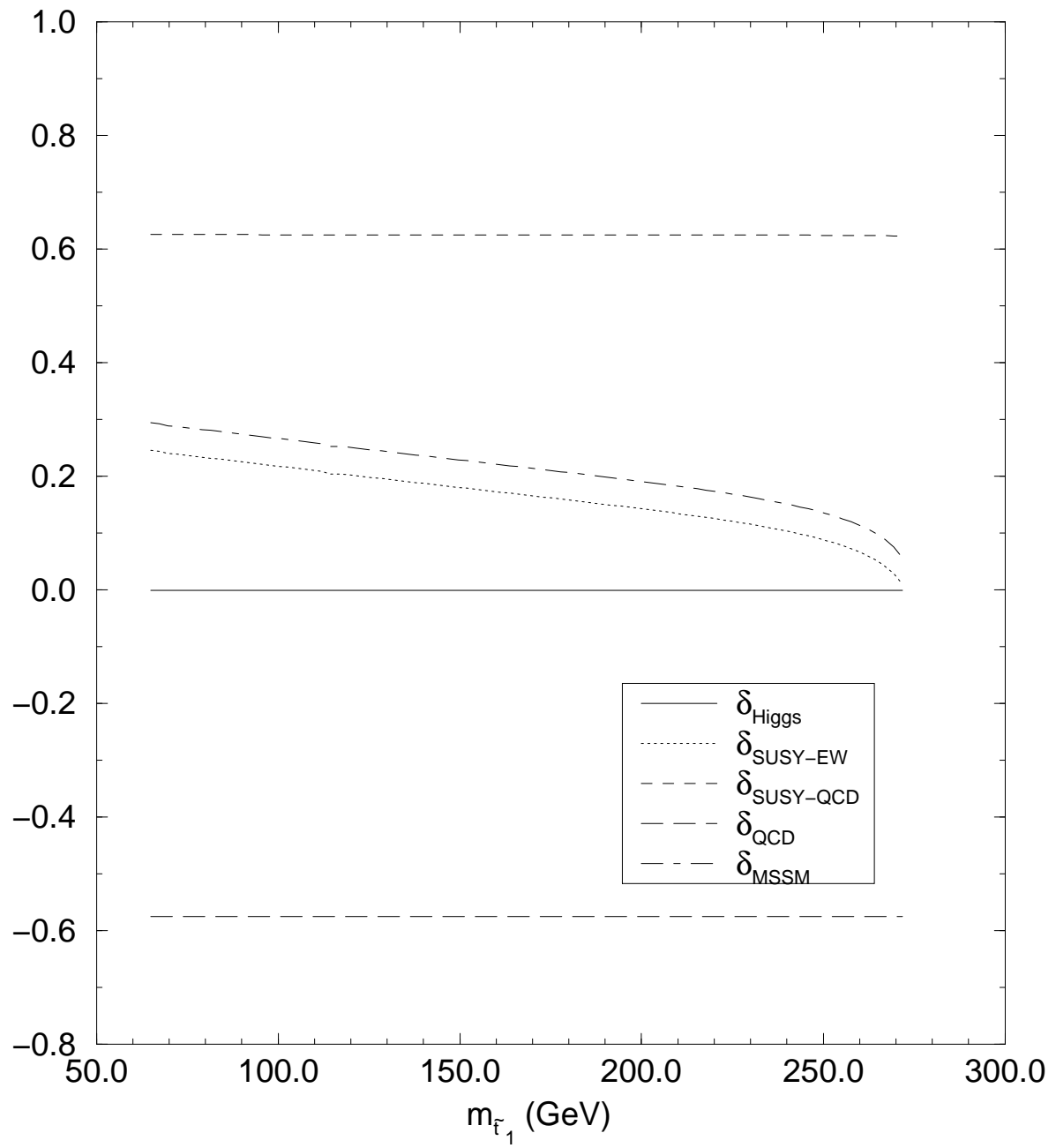


Fig.14

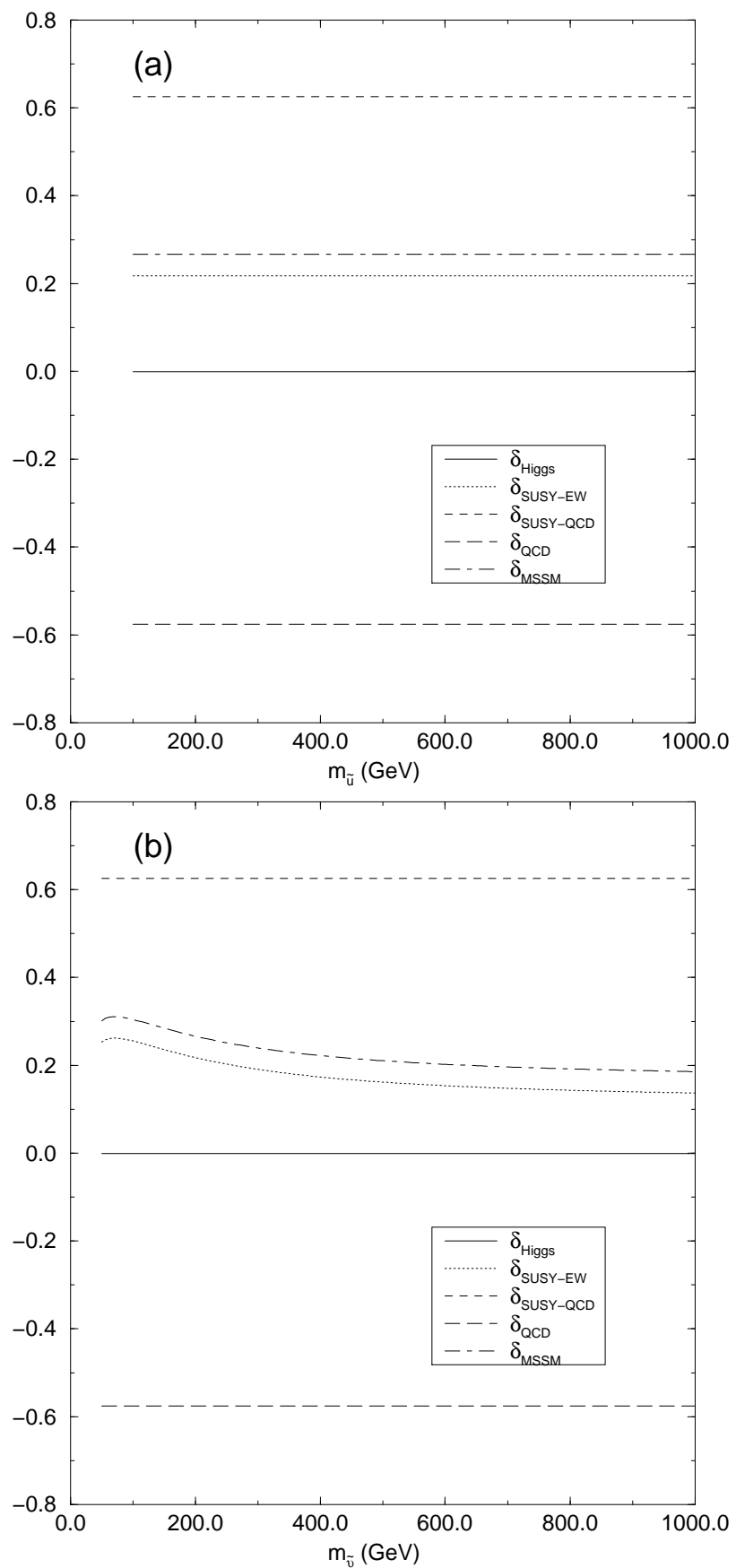


Fig.15

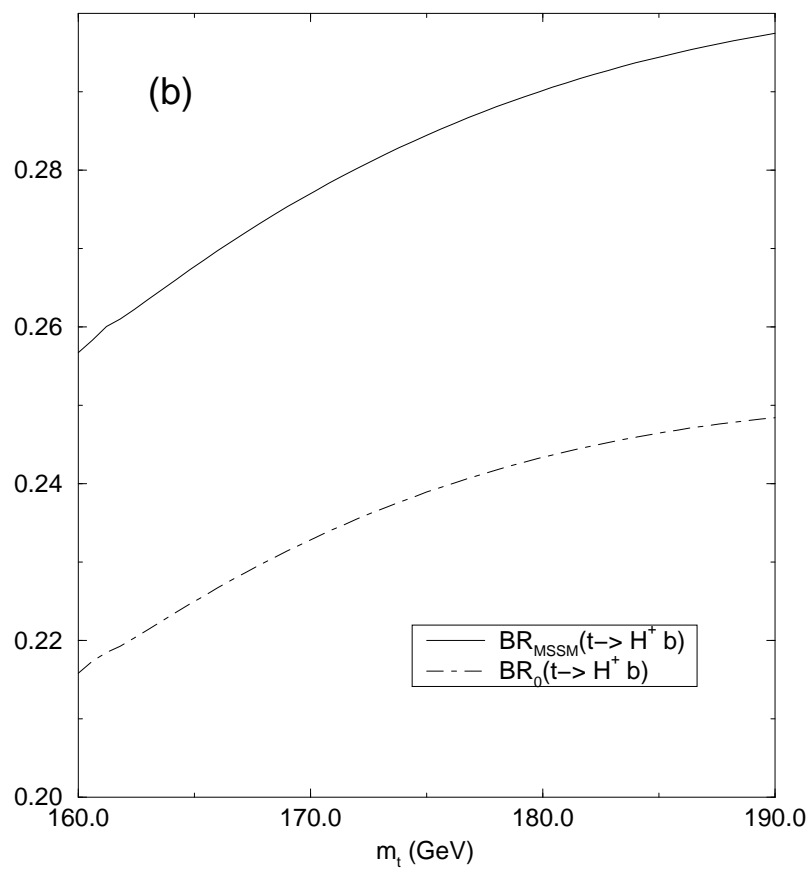
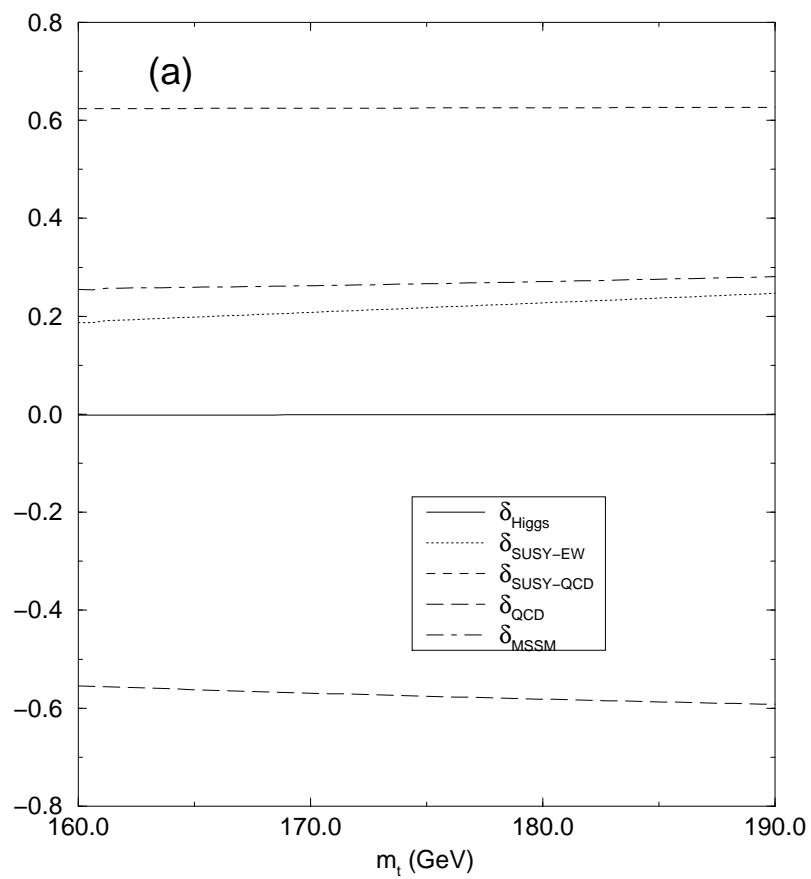


Fig.16

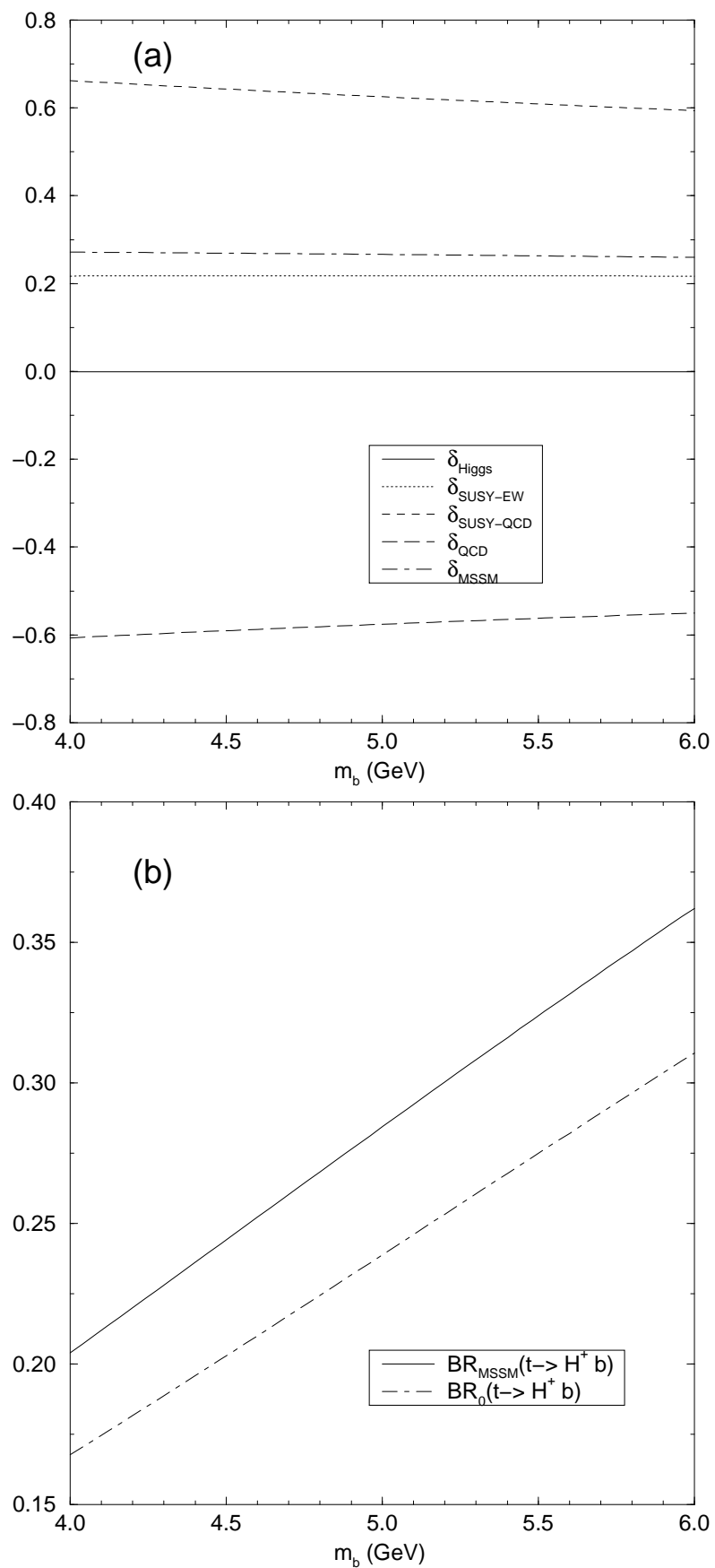


Fig.17

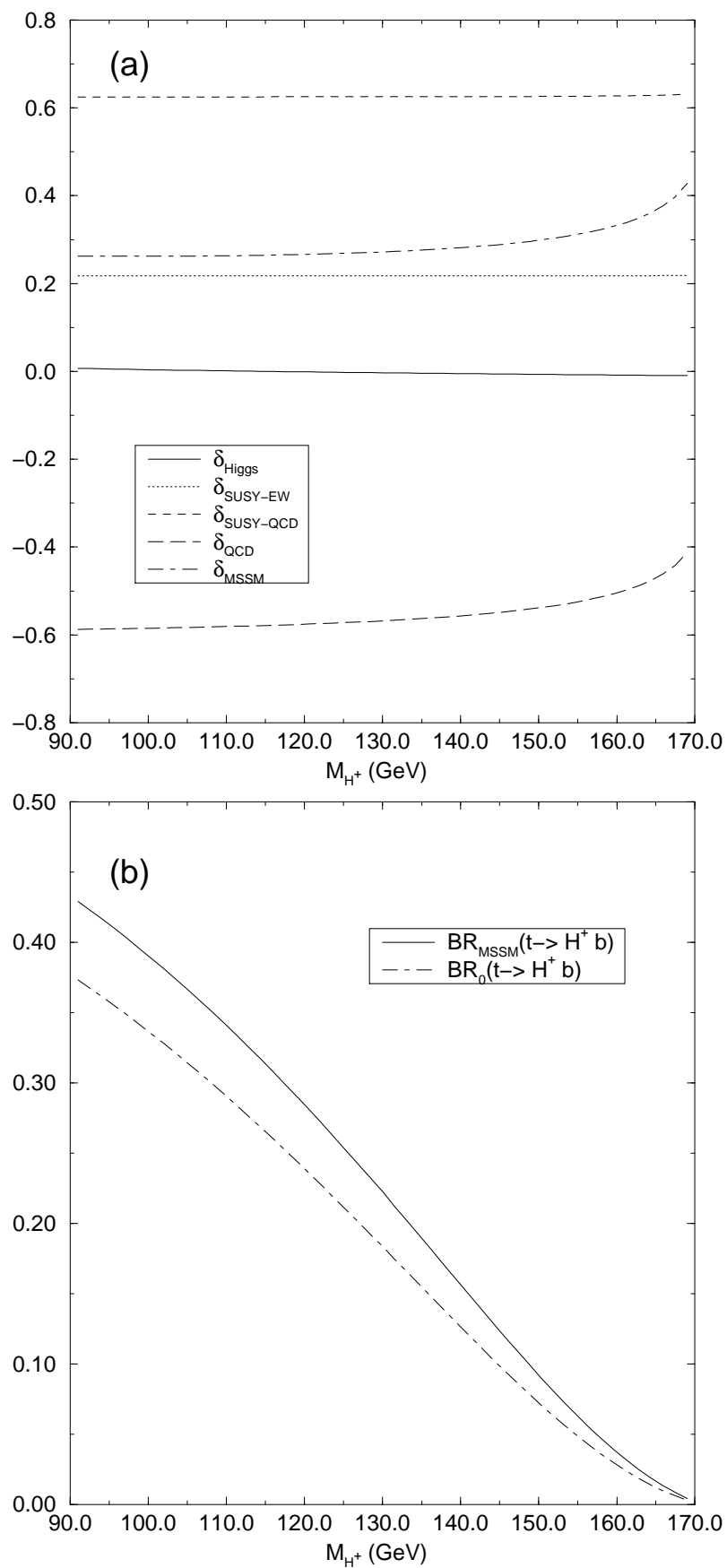


Fig.18

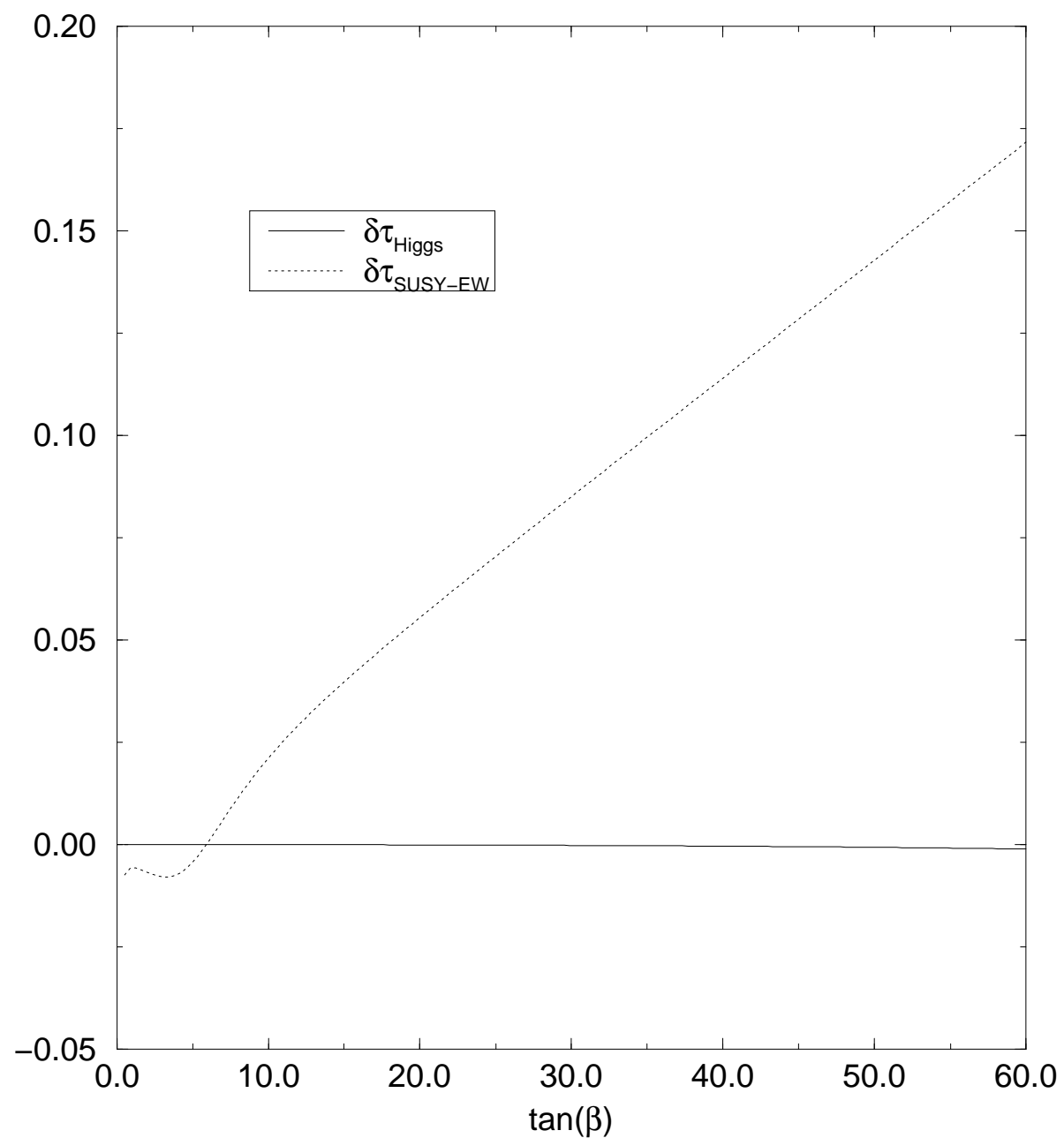


Fig.19

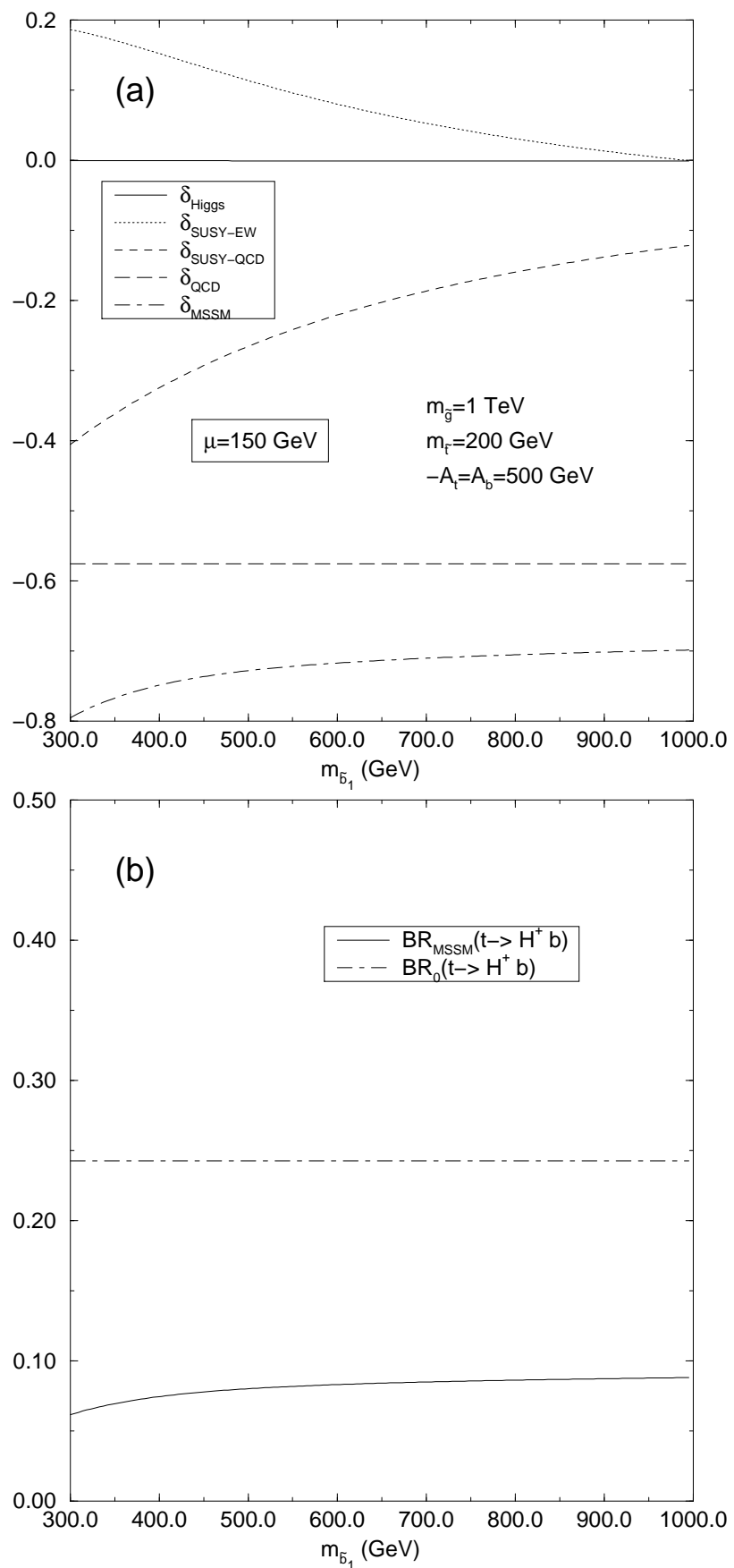


Fig.20

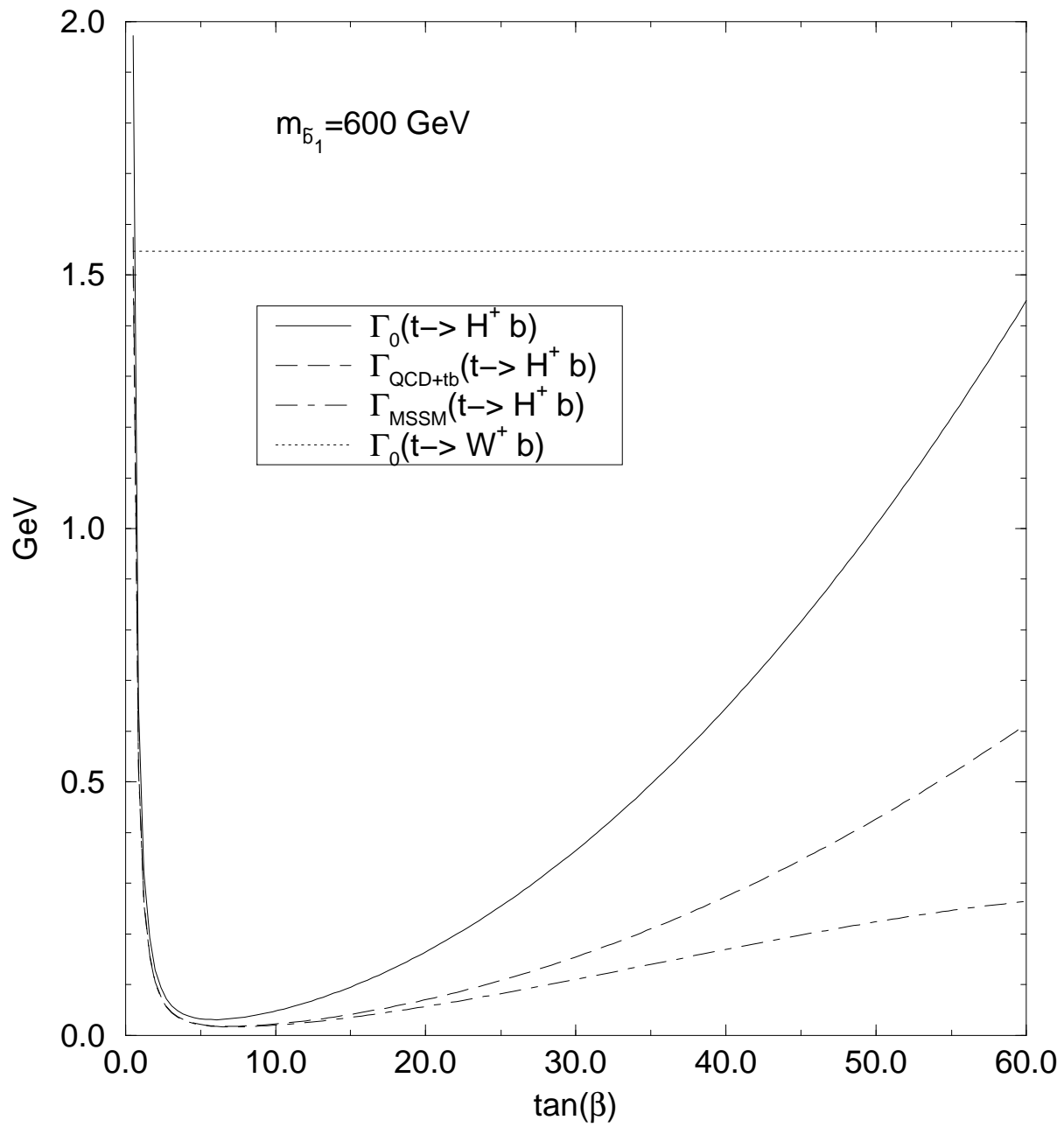


Fig.21

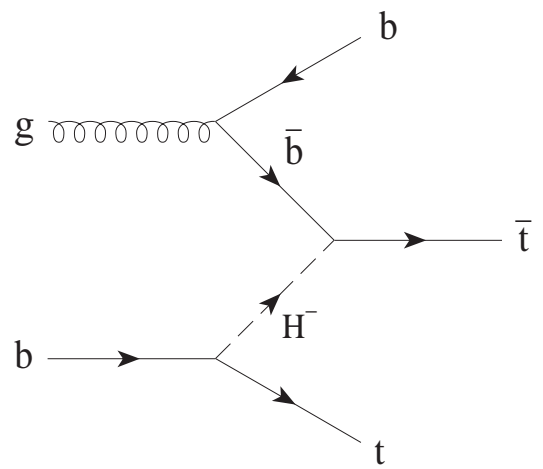
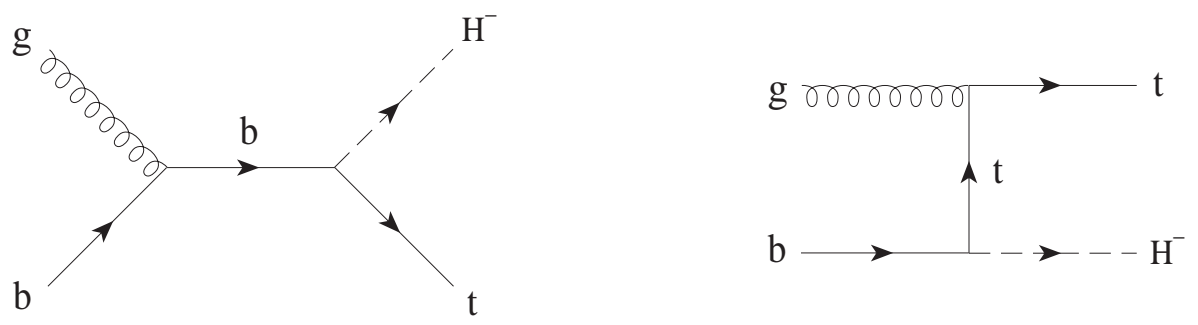


Fig.22

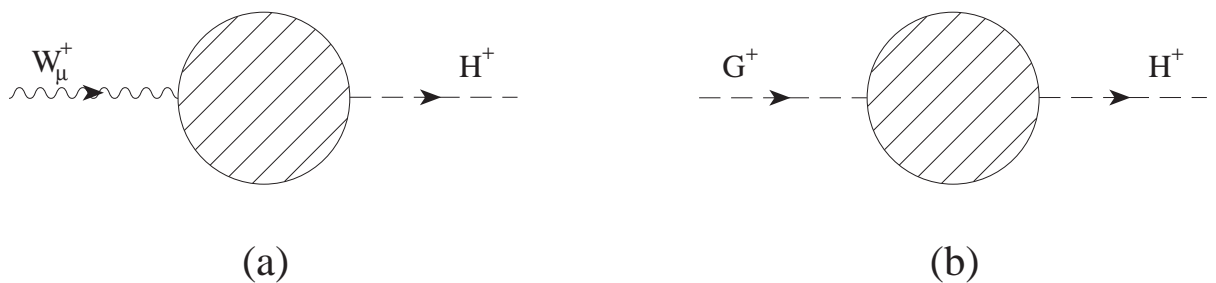


Fig.23